NUMERICAL AND EXPERIMENTAL STUDY OF SOLAR WATER HEATER IN HEATING A SPACE

A THESIS
SUBMITTED TO THE DEPARTMENT OF MECHANICAL
ENGINEERING TECHNIQUES OF POWER IN PARTIAL
FULFILLMENT OF THE REQUIREMENTS FOR MASTER OF
THERMAL TECHNOLOGIES DEGREE IN MECHANICAL
ENGINEERING TECHNIQUES OF POWER
(M. Tech.)

BY
MOHAMMED JASIM OBAID
(B. SC. MECH. ENG. 2003)

Supervisors
Asst. prof. Dr. Dhafer M. Hachim   Asst. prof.Dr. Asaad A. Alsahlanee

January 2020

بِسْمِ اللهِ الرَّحْمَنِ الرَّحِيمِ

قَالُوا سُبْحَانَكَ لَا عِلْمَ لَنَا إِلَّا مَا عَلَّمْتَنَا ۖ إِنَّكَ أَنتَ الْعَلِيمُ الْحَكِيمُ

صدق الله العلي العظيم

البقرة الآية (32)

الاهداء

الى ائمة الهدى ومصابيح الدجى . . اهل بيت النبوة (عليهم افضل الصلاة والسلام)

اجلالا لهـم جميعا

الى روح ابي . . إلى الذي وهبني كل ما يملك حتى أحقق له آماله، إلى من كان يدفعني قدما

نحو الأمام لنيل المبتغى، الى مدرستي الأولى في الحياة . .

إلى امي . . إلى التي صبرت على كل شيء، وكانت دعواها لي بالتوفيق، تتبعتني خطوة خطوة

في عملي جزاها الله عني خير الجزاء في الدارين . .

إلى إخي وأخواتي . . الذين تقاسموا معي عبء الحياة . .

الى اسرتي الصغيرة، زوجتي رفيقة دربي . .

الى اساتذتي وكل من علمني حرفاً فصرت له بعلمي عبداً . .

ACKNOWLEDGMENTS

Supervisor Certification

I/We certify that this thesis titled **Numerical and Experimental Study of Solar Water Heater in Heating a Space** which is being submitted by **Mohammed Jasim Obaid** was prepared under my/our supervision at the Mechanics of Power Department, Engineering Technical College-Najaf, AL-Furat Al-Awsat Technical University, as a partial fulfillment of the requirements for the degree of Master of Technical in Thermal Engineering.

Signature:

Name: **Dr. Dhafer Manea Hachim**

(Supervisor)

Date:15/ 9 / 2019

Signature:

Name: **Dr. Assaad Awad Alsahlani**

(Co-Supervisor)

Date:15/ 9/ 2019

In view of the available recommendation, I/we forward this thesis for debate by the examining committee.

Signature:

Name: **Dhafer Manea Hachim**

(Head of …... Tech. Eng. Dept.)

Date:15/ 9 / 2019

Committee Report
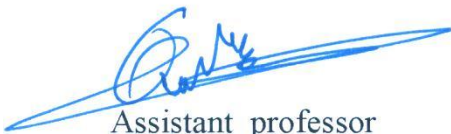
We certify that we have read this thesis entitled " Numerical and Experimental Study of Solar Water Heater in Heating a Space " submitted by Mohammed Jasim Obaid and as examining committee, examined the student in thesis contents. In our opinion, the thesis is fully adequate in scope and quality for a Master degree in Thermal Technologies Engineering.
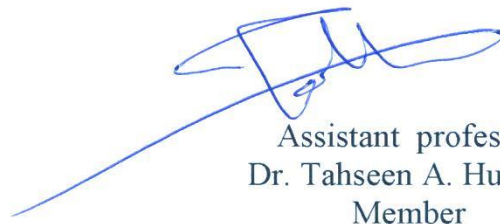
Assistant professor
Dr. Dhafer M. Hachim
Supervisor
Date: 29 / 1 /2020

Assistant professor
Dr. Asaad A. Abass
Co- Supervisor
Date: /   / 2020

Assistant professor
Dr. Qahtan adnan abed
Member
Date: 29 / 1 / 2020

Assistant professor
Dr. Tahseen A. Hussian
Member
Date: /   / 2020

Professor
Dr. Majid H. Majeed
Chairman
Date: 29 / 1 / 2020

Approval of the Engineering Technical College- Najaf:

Signature:
Name: Asst. prof. Dr. Hassanain Ghani Hameed
Dean of Engineering Technical College- Najaf
Date: /   / 2020

III

Abstract

In this work, solar water heaters were used to heat the space by passing a hot fluid from the solar collector to a radiator inside the room. This work aims to save electrical energy, and reduce environmental pollution. A numerical and experimental study was conducted to evaluate the thermal performance of the heating system. Experimental tests were conducted to heating a room with a 10 m^2 area by using flat plate collector (FPC) solar water heater at The Engineering Technical College in the Alternative and Renewable Energy Research unit Najaf / Iraq (31.59^o N Lat., 44.19^o E Long.) within three months (January, February, March) in 2019. The factors whose impact has been studied are (weather conditions, working fluid type, and economic analysis of the system). The numerical studies were obtained by COMSOL 5.3 multiphysics software to analysis the thermal performance of a flat plate collector, where the effect of (volume flow rate, working fluid type, and weather conditions) were studied. Numerical results showed the optimum volume flow rate was 40 L/hr. Also, the ethylene-glycol-water mixture achieved the highest amount of useful heat and efficiency than other fluids at the same flow rate. The experimental results showed that the use of engine oil grade (10w-30) as a working fluid gave the highest amount of useful heat and efficiency at the high volume of flow rate compared to other fluids. So the solar heating system has contributed to save electric power at a rate of 34% of the total energy required for room heating at days test in January. Whereas in February and March were 39.5% and 86% respectively. The economic analysis of the use of heating systems showed that the average cost saved was 38000 IQD/month, while the payback period was 5.2 years. In the present work, the maximum error between theoretical and experimental results does not exceed (8%).

Contents

Nomenclatures

Symbol	Definition	Unit
A	Area	m^2
ACH	Number of air changes per hour	-
cp	Specific heat	$J/kg.\,K$
d_i	Inner diameter of the tube in solar collector	m
G	Heat flux of solar radiation	W/m^2
gr	gravitational constant	m^2/s
h_c	Convection heat transfer coefficient	$W/(m^2.K)$
h_r	Radiation heat transfer coefficient	$W/(m^2.K)$
h_{r1}	Radiation heat transfer coefficient between the glass cover and ambient air	$W/(m^2.K)$
h_{r2}	Radiation heat transfer coefficient between the glass cover and absorber plate	$W/(m^2.K)$
h_{r3}	Radiation heat transfer coefficient between the absorber plate and glass cover	$W/(m^2.K)$
h_{r4}	Radiation heat transfer coefficient between the tube and air of room	$W/(m^2.K)$
h_{r5}	Radiation heat transfer coefficient between the fin and air room	$W/(m^2.K)$
h_{fg}	latent heat of vaporization of water	KJ/kg
I_B	Beam radiation	W/m^2
I_D	Diffuse radiation	W/m^2
K	Thermal conductivity	$W/(m.K)$

L	geographic latitude	Degree
l	Air gap space thickness between absorber and glass cover	m
$m^{\cdot}$	Mass flow rate	kg/s
$m_f^{\cdot}$	Mass flow rate inlet to the solar collector	kg/s
$m_t^{\cdot}$	Mass flow rate inlet to single tube of collector	kg/s
n	Number of tubes	-
Nu	Nusselt number	-
Pr	Prandtl number	-
p_o	Gage pressure	N/m^2
p	Width of control volume of solar collector	m
Q_l	Latent heat transfer	W
Q_L	Heat losses from collector	W
Q_s	Sensible heat transfer	W
$Q_{l,total}$	Total latent heat transfer	W
$Q_{s,total}$	Total sensible heat transfer	W
$Q_h^{\cdot}$	Heating load of space	W
$Q_{in}^{\cdot}$	Heat transfer in the system	W
$Q_{out}^{\cdot}$	Heat transfer out the system	W
$Q_v^{\cdot}$	Heat generation in the system	W
Q_u	Useful heat	W
R_a	Rayleigh number	-
R	Thermal resistance	k/W
R_B	Beam radiation tilt factor	-
R_L	Total thermal resistance	k/W

$SHGF_{max}$	Maximum solar heat gain factor	W/m^2
SC	Shading Coefficient	-
S	Absorbed Solar Radiation	(W)
T	Temperature	^{o}C
U	Overall heat transfer coefficient	$W/(m^2.K)$
U_L	Overall heat losses coefficient of the solar collector	$W/(m^2.K)$
U_s	Internal energy of the system	W
V	Volume	m^3
$V^{\cdot}$	Infiltration volume flow rate	m^3/s
V_{out}	Wind speed	m/s
v	Fluid velocity at y-direction	m/s
u	Fluid velocity at x-direction	m/s
w	Fluid velocity at z-direction	m/s
W_i	Indoor humidity ratio	-
W_o	Outdoor humidity ratio	-

Greek Symbols		
α	Absorptivity coefficient	-
β	Tilt angle of solar collector	degree
$\acute{\beta}$	volumetric coefficient of expansion	$1/°C$
δ	Thickness	m
Δ	Change in Variable	-
ε	Emissivity coefficient	-
η	Thermal efficiency	-
ν	Kinetic viscosity	m^2/s
τ	Transitivity coefficient	-
σ	Boltzmann constant	$W/(m^2 . K^4)$

Abbreviations	
Symbol	**Description**
CPC	Compound parabolic collector
COP	Coefficient of performance
CWSC	Concentrating water solar collector
DHW	Domestic hot water
ETC	Evacuated tube collector
FPC	Flat plate collector
HTF	Heat transfer fluid
ICS	integrated collector storage
PCM	Phase change material
SWH	Solar water heaters
PIV	Particle Image Velocimetry

Subscripts	
Symbols	**Definition**
a	Air gap
ab	Absorber plate
am	Ambient air
f	Working fluid
fin	The fin
g	Glass cover of collector
ins	Insulation of collector
inf	Infiltration
M	Moist air
c	collector
f	Floor
r	Roof
t	Tube
w	Wall
out	Outlet fluid of solar collector
in	Inlet fluid of solar collector
e	Outlet fluid of the radiator
i	Inlet fluid of the radiator
r	Room air
o	Outdoor

CHAPTER ONE

INTRODUCTION

CHAPTER ONE

INTRODUCTION

1.1 General:

The process of heating buildings consume a large amount of energy, which makes them very economically expensive. Heating of buildings facing many challenges to using traditional energy sources, including the lack of supplying of electric power and high costs and pollution of the environment due to the use of fossil fuels. The increase in population leads to increased demand for energy consumption and thus the problem of pollution is constantly increasing, which affects human health and lead to global warming. Many countries have resorted to the use of alternative energy sources to meet some of their energy needs, the most important of these alternative energy source is solar energy. Solar energy is used to heating buildings by solar heating systems. Solar energy is a sustainable, clean and free source that contributes to solving the problem of electricity shortage, reducing environmental pollution, saving high costs of energy consumption and investing in these systems to achieve economic feasibility.

1.2 Solar Energy

Solar radiation is radiant light and heat emitted by the sun, which is a huge source of energy. Solar radiation travels in the form of electromagnetic waves that travel across space uniformly in all directions to reach Earth and other plant. Solar radiation loses approximately half of its energy as a result of its reflection in the atmosphere and clouds (Dickinson 1983)[1]. When sunlight passes through the atmosphere, it is devalued as a part of it which is absorbed as it passes through

different layers of the atmosphere. Very short wavelengths such as X-rays and gamma rays are absorbed in the ionosphere at very high altitudes. The Ozone layer absorbs relatively longer waves in the ultraviolet region at the height of 15 to 40 km above the Earth's surface (Torres et al. 1998)[2]. In the closest atmosphere some of the infrared beams are absorbed by water vapor and carbon dioxide. Solar radiation reaching the Earth's surface lies primarily in the wavelength range from 0.29 to 2.5 µm (Reach et al. 2009)[3]. Furthermore, part of the radiation is dispersed and intercepted from dry air, water vapor, and suspended dust particles. As a result of the absorption of the atmosphere of part of the radiation and the dispersion of the other part, the energy loaded in the radiation decreases its value before reaching the earth surface as shown in Figure.1.1. Also it depends on the degree of shortness of radiation along the path in the atmosphere and the nature of the atmosphere in this path(Wald 2018)[4].
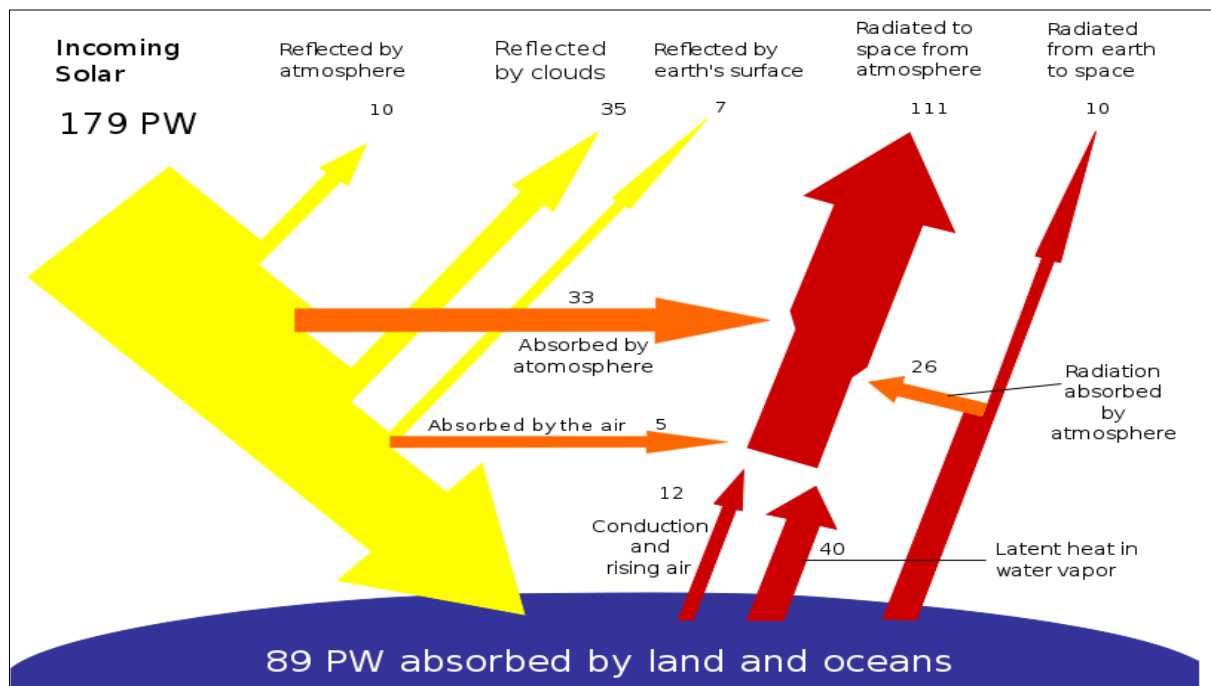
Fig 1.1: Shows the loss of solar radiation as it reaches the Earth's surface (Kim 2018)[5]

Solar radiation consists of direct and diffuse radiation. Direct radiation reaches the surface directly without contraindications. Diffuse radiation is radiation that reaches the Earth's surface indirectly from the sun as a result of reflections occurring as it passes through the atmosphere and clouds.

Iraq is located in the Middle East region, which is characterized by high rates of solar radiation in most months of the year, as shown in Figure1.2. This feature makes Iraq distinguished from many countries to take advantage of solar energy in various fields, in fields of generation of electric power and the use of solar water heaters, especially Iraq suffers from a constant shortage of electricity.
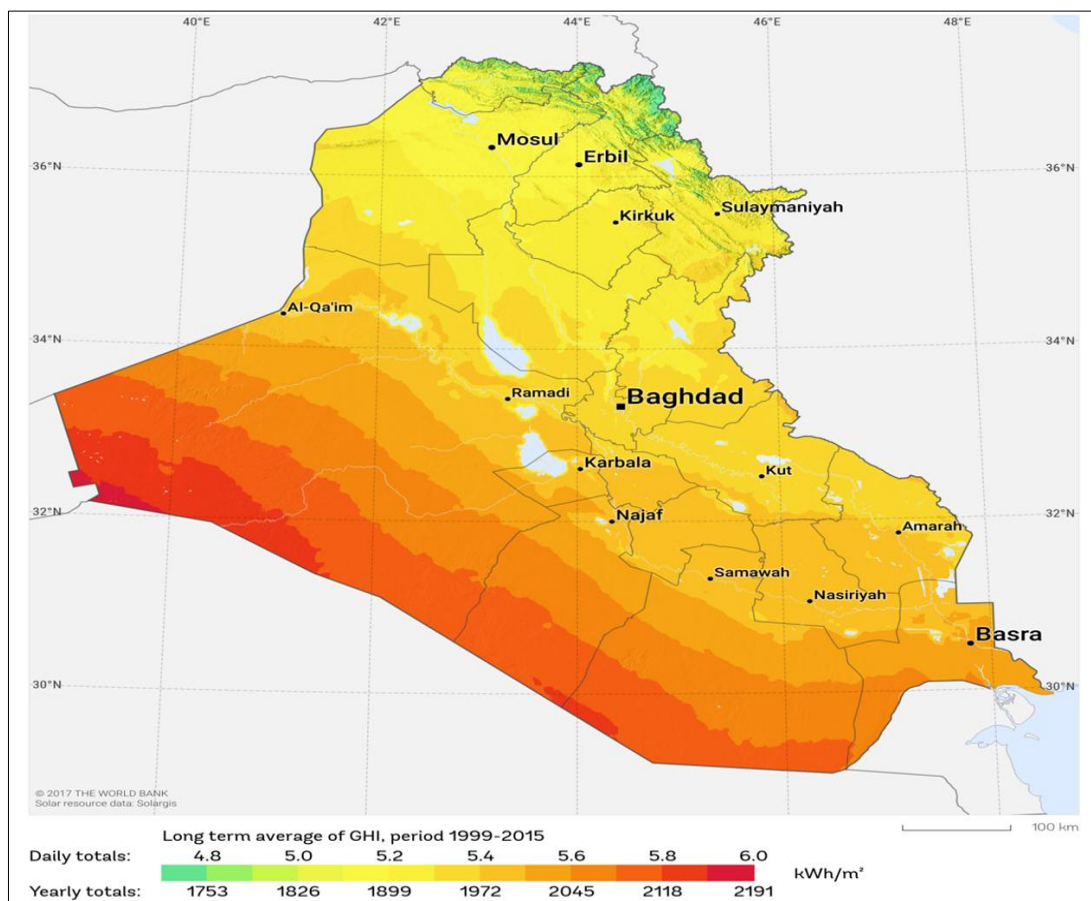
Fig. 1.2: Shows the rates of solar radiation distribution in Iraq (Al-kayiem 2019)[6]

1.3 Application of Solar Energy

The sun is the most important source of energy in the earth. It is considered a cause of the presence of other sources of energy. It cannot be dispensed in any way. (Kalogirou, 2008)[7]. At the last nineteenth century, humans began to use fossil and nuclear energy sources, ignoring solar energy and developing methods to avoid many of the problems and complications of the current era of depletion of fossil fuels, high prices, and environmental pollution. Scientific development and technologies have opened up broad prospects for increasing energy demand in all commercial, industrial, and social fields. There is a growing need for renewable energy sources, which differ in form and combine in their sources.(Deceased and Beckman n.d.)[8]. Applications of solar energy for electrical and thermal energy remain the most important and most accessible sources of energy for easy design, ease of maintenance and achieved high economic feasibility in long-term use. The widespread applications of solar energy are [9, 10, 11, 12 and 13]:

1. **Solar heaters**: Solar heaters have several uses: household usage, heating of buildings, drying ,and industrial applications.
2. **Solar distillation**: Solar energy is used to convert salt water into potable water by solar distillers in desert and semi-arid areas where well water is available.
3. **Solar panels for electricity generation**: Photovoltaics convert sunlight falling into electrical energy and can be used directly or stored.
4. **Solar Thermal Production**: In thermal plants, electrical energy can be produced depending on solar energy instead of using fossil fuels where steam is produced by solar water heaters.
5. **Solar Furnaces**: In the solar furnace, the solar radiation is concentrated using sun-tracking mirrors on a given sample which raises its temperature up to the melting point.

1.3.1 Solar Heating of the Building

The heat obtained from the solar collectors is transferred to the space to be heated by using some suitable equipment to transfer the thermal energy from the solar collector to the building. There are two types of solar heating system, one uses air and the second uses water as a working fluid. (Kalogirou 2008)[7]. In the solar air heating system, the air is heated in the solar collectors and then pumping directly into the building by a fan to warm the building or space. The design of solar air heaters is not much different from solar water heaters except in the design of the absorber plate (Hobbi and Siddiqui 2009)[14]. In solar water heating systems, hot water is pumped from the solar collector to a radiator inside the space where heat exchange is carried out either naturally or forced. A thermal storage tank can be used in these systems to extend the working time of the system as much as possible. The size of the tank corresponds to the area of the solar heater (Yang, Wang, and Xiong 2017a)[15].

1.4 Solar Heaters Collectors

Solar heaters collectors work to convert solar irradiance into thermal energy and store it for later use. A solar water heater is a combination of a solar collector array, an energy transmission system, and a storage tank, as shown in Figure1.3. Mechanism of working solar heaters is convert the solar energy falling on the absorber plate into thermal energy, then the heat is transferred from the absorber to the working fluid that passes through the tubes fixed on the absorber plate. The working fluid is then transferred to the storage tank directly or indirectly via a heat exchanger. Thermal energy is used in heat water for domestic usage, heating building, generating steam, dry crops [16, 17, 18, 19 and 20].
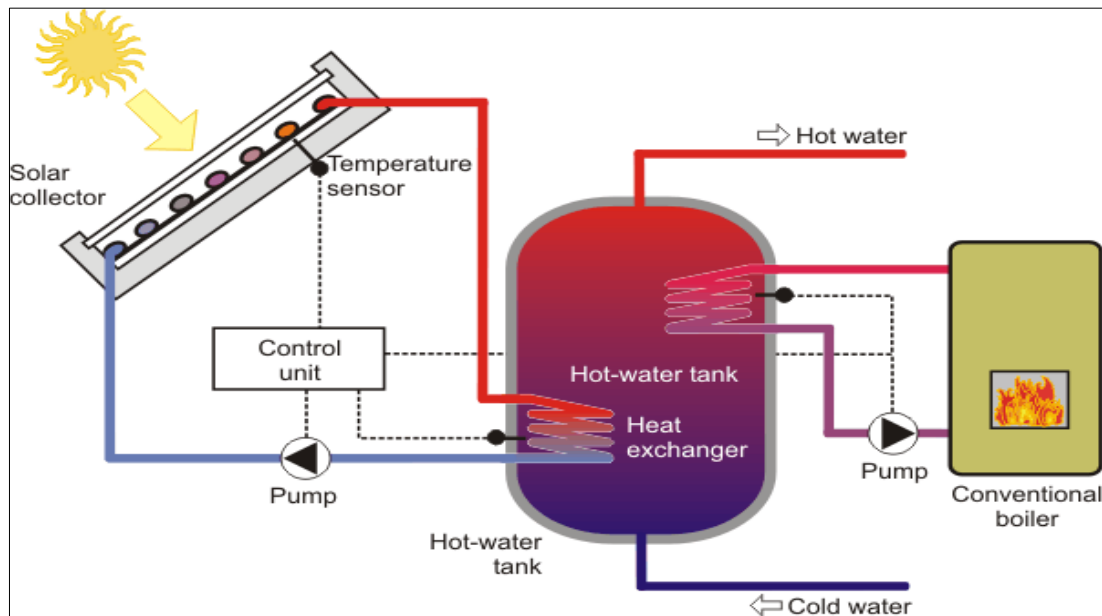
Fig. 1.3: schematic diagram of a solar water heater system (Haq 2012)[21]

Solar heaters are divided into two types according to the working fluid used:

1.4.1 Solar Air Heaters Collector

This type of heaters uses air as a working fluid and is characterized as cheaper and easier to operate and used to dry crops and heating building. These systems are classified as an active system type where a fan is used to pump air from the solar collector to the space. Although it produces thermal energy less than solar water heaters, but the solar air heater is less susceptible to damage and works for many years. The air temperature may rise between (20 -50) ℃ depending on the method of insulation in the system and the volume flow rate of air and the accumulation of dust on it (Kalogirou 2008)[7].

1.4.2 Solar Water Heaters Collector

Solar water heaters are used to supply hot water for domestic use, heating buildings and heating pool water. Solar heaters can be manufactured in several sizes to meet the needs of energy at temperatures required for water, whether warm (below 50 ℃) for swimming pools or heated (60-80 ℃) for domestic use or boil for steam to generate electricity, depending on the area and design of the solar heater (Kalogirou 2008)[7]. Solar water heaters work during the day and provide hot water directly and can be stored hot water by an insulated storage tank to cover the need during the blocking of the sun by clouds or at night. Solar water heater systems can be classified depending on the method of circulating the working fluids in the system:

- **Passive systems**: In these systems, the circulating the working fluid inside system does not require an external power source, but it depends on the free convection due to the difference in temperature between water in the solar heater and storage tank, which leads to a difference in densities, this causes movement of fluid from the high-density to the low density. The systems that operate in this way are called thermosiphon systems, as shown in Figure1.4.
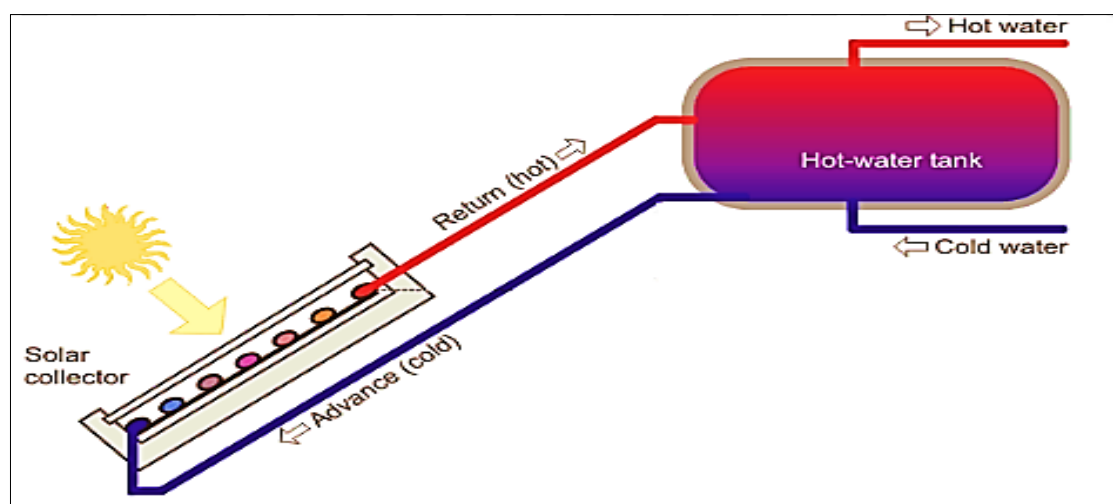
Fig. 1.4: showed Thermosyphon phenomenon in a solar water heater(Haq 2012)[21]

These systems are more economical because they do not need an external power source to circulate working fluid. The disadvantages of these systems, need high temperature difference between the solar heater and the tank in order to circulation working fluid, and the storage tank must be higher than the solar heater, which may be large.

- **Active systems**: In these systems, need to external power source where the working fluid is circulated inside the system by an electric pump. These systems are less economical but give more heat energy due to increased volume flow rate, thus improves the efficiency of the solar heater, as shown in Figure1.5.
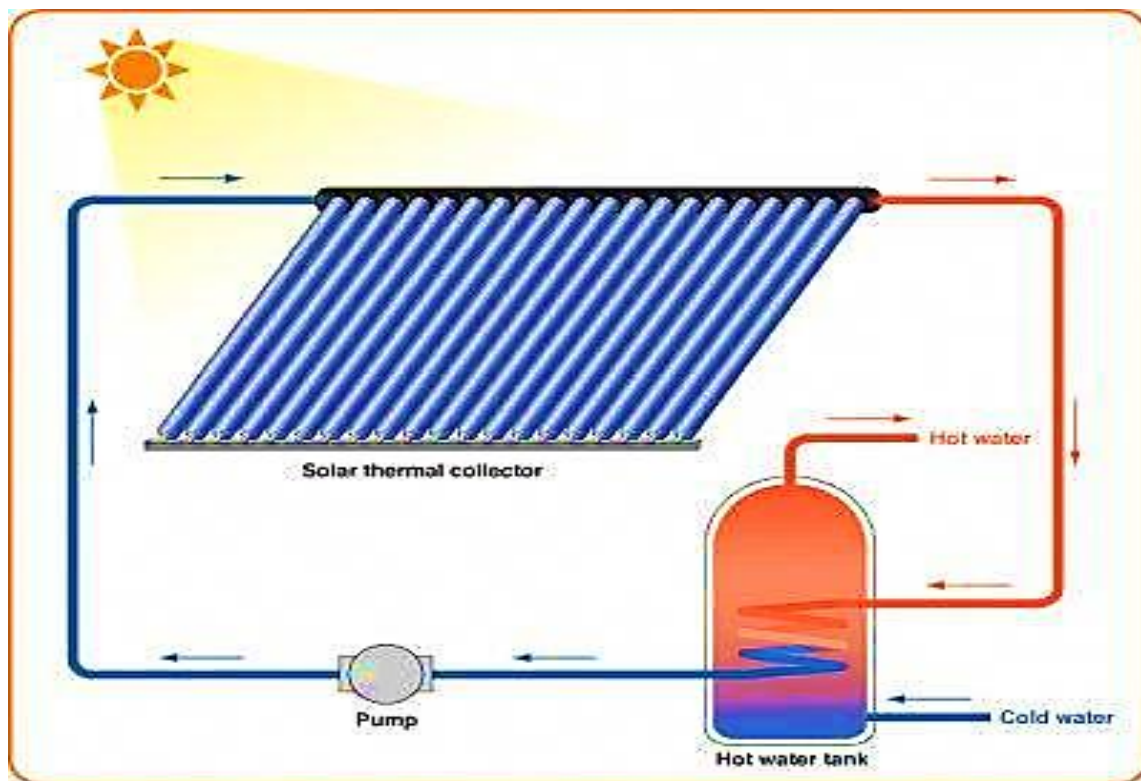
Fig. 1.5 Schematic diagram of the active solar water heater system.

There are another classification of the solar water heaters depends on the method of heating water:

- **Direct or open-loop systems**: In this system, the water is heated directly in the solar collector.

- **Indirect or closed-loop systems**: In these systems, water is heated indirectly by a heat transfer fluid that is heated in the collector and passes through a heat exchanger to transfer its heat to the domestic or service water, as shown in Figure1.3.

1.4.2.1 Type of Solar Water Heaters

Solar water heaters are usually used in domestic uses and in some industrial applications that require hot water at medium and low temperatures. The most prominent types are:

1. **Flat plate collector (FPC)**

    It is one of the most common solar heaters, especially in the residential sector for the supplying of hot water and heating buildings. It is easy to install, maintenance-free, longevity, and low price. This type of solar heaters will be the focus of this study for use in heating buildings. Figure1.6 showed main parts of flat plate collector (FPC).
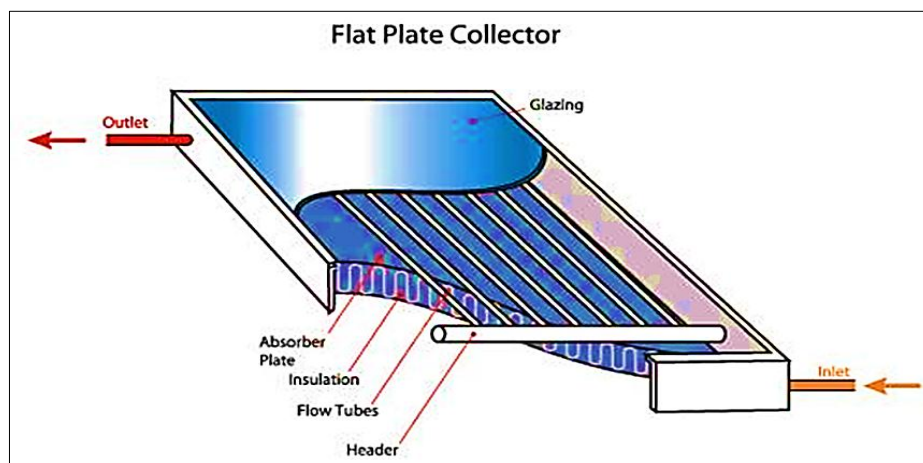
Fig. 1.6: shows the components of (FPC)

2. Evacuated Tube Collector (ETC)

This type of solar water heater is widely used in home use. These systems are characterized by the production of hot water with high temperatures of up to 90°C due to the small thermal losses (Guo et al. 2010)[22]. Figure1.7 showed main part of (ETC).
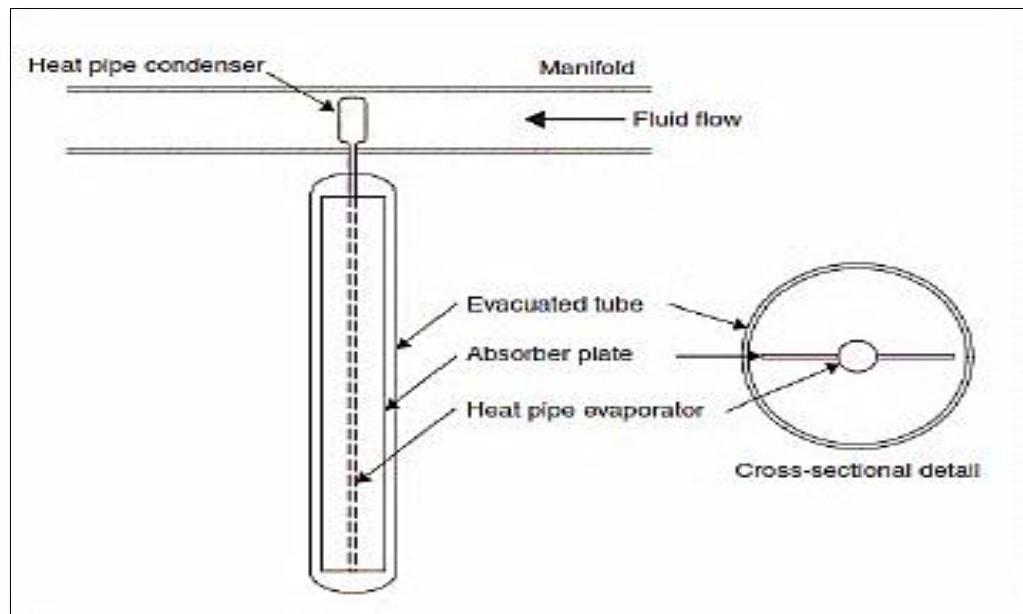
Fig. 1.7 schematic of evacuated tube collector (ETC) [7].

3. Integrated Collector Storage Systems (ICS)

In this system, the solar heater is mounted above the storage tank. The heat is transferred directly from the absorber to the storage tank. Hot water is pulled from the top and cold water enters from the bottom of the tank. One of the disadvantages of this solar heater is its large thermal losses due to the presence of the storage tank under the heater, and a large area of it is exposed to air.

1.5 Heating Load of Buildings

The heating load is the maximum thermal energy that may be provided into particular space to maintain suitable interior design condition. Heating load calculations are performed to determine the capacity of heating equipment for a particular space. There are several factors that affect heating calculations, the most important of which are the internal and external conditions of the space. In addition the building site and the properties of construction materials etc.(Kharagpur 2008)[23].The design of the interior conditions is based on the thermal comfort standard of the occupants. While in industrial and commercial applications, the interior conditions are designed to suit the production requirements or conditions suitable for storage. External design conditions are based on dry bulb temperature and wet bulb temperature in conjunction with the peak winter months. In other words, heat load calculations lead to guessing the amount of heat loss from the building during the winter and determining the required heating capacity [24, 25, 26, 27, 28 and 29].

1.6 Solar Heating Systems Economic Analysis

Solar energy is a free source of energy, but the equipment for collecting and transporting this energy is costly. Solar systems have high primary costs versus low operating costs. Therefore, when deciding to use solar heating systems it should be less than the cost of traditional systems to perform the same task. There must be an economic study that compares the initial cost with the operating and maintenance costs, and to have good knowledge of the various solar systems and components to determine the long-term thermal performance to obtain a realistic analysis and evaluation of the economic feasibility of these systems, so we get a convincing result for customers wishing to use these systems. Economic analysis also includes determining the correct size of the heating system for a particular application that

gives as much thermal energy as possible at the expense of using a conventional system. Life cycle analysis of the solar heating system reflects the cumulative benefits of solar energy use compared to conventional fossil fuel systems. In the long-term, the use of solar heating system saves cost after the end of the payback period compared to conventional heating devices. Life cycle analysis should include the initial and operating costs of a solar heating system and include the purchase of materials for the system and operation fuel and electricity costs for pumps, and maintenance(Kalogirou 2008)[7]. An important factor in the economic study is the payback period which means the length of time required (in years) to covering the initial investment cost by calculating the energy provided by the solar heating system compared to using conventional heating systems.

1.7 Objective of the Work

This work aims to achieve the following goals:

1- Construction a solar heating system for individual room and experimentally tested. Then calculating the amount of useful heat supplied by the system to heat the space and study the economic analysis.

2- Calculating the room's heating load in different climatic conditions for some days in January, February and March 2019 in the Najaf city.

3- Studying of the effect of the climatic conditions of the Najaf city on the thermal performance of the solar heating system.

4- Test different working fluids on the thermal performance of the solar heating system, as well as changing the amount of flow rate.

CHAPTER TWO

LITERATURE REVIEW

CHAPTER TWO

LITERATURE REVIEW

2.1 Introduction

Solar water heaters have undergone several developments by researchers during the past years to make them more efficient, via reducing production costs and increase the period of operation to achieve the highest possible economic feasibility within the highest specifications give high efficiency. These studies included the thermal performance of solar heaters for heating buildings and supplying hot water for domestic use under different operating conditions.

Researchers have varied their studies and methodologies in assessing the thermal performance of solar heaters. This chapter includes theoretical and numerical studies, experimental studies, and experimental and numerical studies.

2.2   Theoretical and Numerical Studies

(Morrison and Braun 1985)[30]   studied numerically thermosyphon approach to assess performance of solar water heaters which has two models: horizontal and vertical storage tank. There was a discrepancy between simulation results and data recorded from two locations. Results showed that the best performance of the solar water heater works by thermosiphon method when the daily production of hot water is approximately equal to the amount of daily consumption. The study showed that the horizontal tank system was the best performance during the day from the vertical tank system.

(Morrison et al. 2005)[31] investigated the flow rate of the circulation for the evacuated tube which is closed from one end using simulation model for a flow rate of water which related with heat transfer in an evacuated tube and flow measurement by Particle Image Velocimetry (PIV). Then worked non-dimensional correlation for circulation rate diffuse in collector tilted at an angle 45^0. This study showed that there is agreement between simulation and experimental results. The circulation flow rate inside tubes depends mainly on two factors, the rate of radiation intensity received by absorber surface and temperature of the storage tank. They found that the natural convection circulation rate can reach 35kg/h at a maximum rate of radiation intensity and temperature of the storage tank is 60 ℃.

(Chow et al. 2006)[32] evaluated produce of the Domestic Hot Water (DHW) in high- rise virtual building in Hong Kong by fixing central Solar Water Heaters (SWH) in the south and west vertical facades for building. The economic feasibility study was carried out in terms of technical and cost aspects. The results of the numerical model reported that the evaluated annual thermal energy produced was 904 GJ, and the thermal efficiency of solar water heater collector was 38.4%, average annual hot water temperature achieved was 41.4 ℃ and the payback period was 9.2 years. This period may be less if the electricity consumption of air-cooled appliances is taken into consideration due to the blocking of direct solar radiation on the facades of the building on which the solar collector is installed.

(Ucar and Inalli 2008)[33] searched in the comparative study of the thermal and economic performance of the central solar water heaters with seasonal storage in Turkey. Evaluation by using Simulation models for three types of seasonal storage: storage tank without insulation, another one with

insulation both mounted on ground and storage tank buried underground without insulation. Two types of collectors examined: a flat plate collector and evacuated tube collector. The results explained that the system with storage tank underground gives higher saving energy form other system and achieve higher solar fraction equivalent to three load sizes. Moreover, when the area of collector increased the solar fraction was also increased for three seasonal storage type.

(Mateus and Oliveira 2009)[34] presented the study to evaluate the possibility of utilization from solar energy to conditioning air applications. Combination of solar absorption cooling and heating system are adopted to reduce conventional fuel consumption that causes harmful environmental pollutants. The basic assessment was based on a simulation model by using TRNSYS software tools for different building such as hotel, residence, and office. Three different locations which have different climates are choosing which was Rome (Italy), Lisbon (Portugal) and Berlin (Germany).the results estimated that an annual solar fraction was between (20% - 60%). The use of solar integration for a single-family house and the hotel achieve maximum economic feasibility. Only Rome city has potential to attain tie case. It concluded the solar integration contribute to reduction exploitation costs between 35% and 45%.

(Hobbi and Siddiqui 2009)[14] studied the performance of solar water heaters with an indirect forced flow rate to provide domestic hot water for a single-family house in Montreal, Canada using flat plate collector and evaluated by simulation using TRNSYS software tool to analyze all main design parameters for system and collector and determining the optimum value for it. The solar fraction was considered as an optimization parameter. The simulation results explained that the rapid increases of solar fraction and collector efficiency when circulation rate increases. And the system can

produce 83–97% in summer and 30–62% in winter from hot water needs. They found the collector non-selective coated locally made can provide 54% from annual water heating demands which obtained by solar energy.

(Allen et al. 2010)[35] searched the impact of environmental and economical for integrated assessment of solar water heaters for the housing sector in the UK. Energy evaluation performed by reducing dependence on the conventional energy source: electrical heater, oil boiler, and gas boiler. then integrated with solar water heaters which can be stopped or reduce using traditional energy sources, especially fossil fuels. as a result, it reduces carbon emissions. The economic assessment explained in current time have high costs and give a negative indication of the various scenarios assessed. Future anticipation refers to reduce capital costs, which contribute to enhancing the economics of performance. The results refer to the annual energy produced of (SWH) was 1940–3520 MJ while the range of solar fraction was 28–52%.

(Ayompe et al. 2011)[36] a developed comparative study to validate the performance of solar water heaters with forced flow rate using flat plate collector and evacuated tube collector installed in Dublin, Ireland. The comparison was performed by simulation models with TRNSYS software tool for (FPC), (ETC) collectors. Also, they verified the validity of the model with measured data that is more acceptable in simulations with long-term performance under different operating and weather conditions. Results of modeling and trail field data in term percentage mean absolute errors for output temperature of collectors and heat collected by collector and heat delivered to load of 16.9%,14.1%, and 6.9% respectively for the flat plate collector, and 18.4%, 16.8% and 7.6% respectively for evacuated tube collector.

(Serale et al. 2014)[37] presented the enhance of thermal performance of a flat plate collector which produces limited temperature. Thermal enhancement can be achieved by using latent heat. which can be obtained by fitted slurry phase change material (PCS) with water and surfactants. So heat carried the fluid are evaluated. This study suggested that conceptual proposals to an integrated solar thermal system with slurry (PCMs) were presented. Also, a prototypal system based on n-eicosane (PCS) was developed. This leads to give the system thermo-physical and rheological properties and material behavior that interest flat-plate solar thermal collectors. To interface possible problems is to use of PCSs as Heat Transfer Fluid (HTF) such as clogging in pipes, high-pressure drop, some sedimentation in the storage tank and capsule rupture as a result of pumping work.

(Ekramian et al. 2014) [38] investigated numerically analysis was used to study the effect of different parameters on thermal efficiency of flat plate solar collectors. Various geometries and operating conditions were examined in order to assess the influence of riser position, shape of tube area section, mass flow rate, absorber thickness, absorber material, absorber absorptivity, and glass transmissivity on thermal efficiency of solar collectors. Results show that the efficiency of collector with risers on top of the absorber plate is 4.2% more than that of the collector with risers on bottom. Also the tube cross-sectional geometry shows strong effect on the efficiency. the efficiency of collectors with circular tubes is 38.4% more than that of collectors with triangular cross sections. Thermal efficiency of solar collectors increases with increasing the fluid flow rate, plate absorptivity, absorber thickness, and glass transmissivity.

(Yao et al. 2015)[39] evaluated performance of solar water heaters of single tube collector inserts inside it a twisted tape. A simulation model

studied flow rate and heat transfer inside the tube. Numerical data explained that the twisted tube decreases velocity value and makes temperature field uniform. For series of investigations, mean result number of (SWH) with a relative twisted ratio of the twisted tape (m) 2.5m and 4m respectively was 1.07% less and 9.29% higher than the ordinary solar water heater.

(Guo et al. 2017)[22] analyzed the thermal performance and economics of solar water heaters, through optimal correspond between collector area and storage tank size for heating space applications. The simulation results showed that the (SWH) using for heating space, the perfect ratio between storage tank size and collector area relies on total area of collector, and analysis the examined model gives reasonable accuracy (±10%) for transient storage temperature distribution and (±3%) for accumulated heat flow accumulated over the entire heating season.

(Sami et al. 2018)[40] investigated the energetic and economic possibility of the integration of flat plate collector solar water heaters system with high energy performance housing. They choose four houses in different locations to have a distinct climatic zone in Algeria to study this case. The evaluation based on calculations depending on using F-Chart method (which is empirical to characterize the long-term performance of solar heating systems) with monthly meteorological data characterizing each region. The study focused on finding the optimum solar collector area, which minimized the cost of installation in versus economic and energetic aspects. The results showed that the(SWH) contributed to saving the traditional energy reach to 46% and 57% in northern and southern regions respectively and in the same time-saving in the annual operating cost of the solar system reached 51% and 69% respectively.

2.3   Experimental Studies:

(Naphon et al. 2008)[41] studied improvement thermal efficiency of the heat pipe by enhancement thermal properties for working fluids over alteration fluid transport and flow characteristic of working fluid. The heat pipe experience using nanofluids (alcohol and titanium nanoparticles) and compared the output when heat pipe working with fluid transport was de-ionic water once and alcohol again. The results showed when volume concentration of nanoparticle was 0.10%, the thermal efficiency has improved 10.60% higher than that with the based working fluid.

(Reindl et al. 2008)[42] modified the thermal storage system of the solar water heaters which work with indirect circulation: external heat exchanger and storage tank. The modified system uses a spiral-jacketed storage tank which achieves the function of heat exchanger and storage tank. The experimental results showed a decrease in the thermal performance of the modified system in ranges between (6%-11%) compared with the conventional system. So this leads to an increase in the temperature of fluid supply to collector thus heat losses in collector increased.

(Al-Madani 2006)[43] evaluated experimentally of cylindrical solar water heaters which consist of cylindrical glass tube has length 0.8m, outer diameter 0.14m and thickness of 6 mm. coil tube made from coppers has shaped as spiral rings. The tube has inner and outer diameter 2mm and 3.175mm respectively. The system was tested during March and April 2002. The result showed that the maximum temperature difference between inside and outside of (SWH) was 27.81℃ at a circulation rate of 9 kg/h. Maximum thermal efficiency achieved during the above period was 41.8%.

(Ayompe, Duffy, Keever, et al. 2011)[44] compared the annual thermal performance for flat plate collector and evacuated tube collector having area 4m^2 and 3m^2 respectively. The test was done under the same conditions for both collectors in Dublin, Ireland. The results explained that for an annual total in-plane solar insolation of 1087 kWh.m^{-2}. The total thermal energy obtained by (FPC), (ETC) system was 1984 kWh and 2056 kWh respectively, Annual thermal efficiency rates were 46.1% for (FPC) and 60.7% for (ETC). The economic analysis indicates the lack of commercial application for both (SWH) system because net present value ranging between 4264€ and 652€ while simple payback period (years) varied between 13 years and 48.5 years. The results of energy analysis showed that the 4m^2 (FPC) system has an advantage compared with (ETC) when fitted with a 300L storage tank.

(Parida 2011)[45] studied experimentally design and fabrication hybrid solar water heaters flat plate collector for heating pool water. (FPC) fabricated from the material locally available, system operating to make a pool water temperature at a comfort level. The experiment was tested for many values of flow rate. Results revealed that the optimal flow rate was 15L/min for favorable heating, unglazed solar collectors gives efficiency of 27.8 %.

(Yousefi et al. 2012)]46] evaluated the effect of nanofluid (Al$_2$O$_3$-water) as an absorbing medium to the enhancement of the thermal efficiency of flat plate collector. Nanofluid tested with a weight fraction (wt) of 0.2% and 0.4 %, With or without used surfactant Triton X-100. The nanoparticle has diameter 15 nm and circulation rate varied (1-3) L/min. Experiments showed that the thermal efficiency of (FPC) system enhancement reached 28.3% by using nanofluid 0.2 wt% Al$_2$O$_3$ in comparison with water base fluid. Maximum improvement efficiency by using surfactant was 15.63%.

(Gang et al. 2012)[47] studied the performance of Compound Parabolic Collector (CPC)-type solar water heaters based on experiment and exergetic analysis. The experiment rig installed with U-pipe and the study was conducted in December at Hefei in the eastern region of China. The system was in the steady condition during winter and the Heating water of the tank from the temperature 26.9 ℃to 55, 65, 75, 85, and 95 ℃. The empirical study and exergetic analysis of the five experiments showed that the overall thermal efficiency of the (CPC) solar water heaters was always above 49% when the temperature is reached 95℃ and exergetic efficiency of above 4.62% When the temperature is reached 55 ℃. It is mentioned above (CPC) type solar water heaters with U-pipe gives an excellent thermal performance achieving a high temperature which has Possibilities to use in different applications.

(Nouvelles et al. 2012)[48] investigated the performance of Integrated Collector Storage (ICS) solar water heaters with fixed compound parabolic concentrator reflector is conducted in Ghardaia, Algeria. The experiment rig consists of one horizontal cylindrical tank set up in fixed symmetrical compound parabolic concentrating reflector. This study focused on obtaining low-cost (SWH) by using: absorber surface with high emittance, curved reflectors has low cost and single glass cover. The results explained that the solar water heaters system provided (120L/day) were attaining to enough energy-saving.

(Ahmad 2012)[49] searched the potential to reduce energy consumption in building by using Concentrating Water Solar Collector (CWSC) to achieve two functions: blocking the incident solar radiation by mounted (CWSC) as adjacent to southern side of the room to reduce obtain energy for cooling space and in the same time (CWSC) provided a hot water

for some special usage. This work experience on the room has $1m^2$ area for each side conducted in Baghdad in days, July 28, 29 and September 21, 22 and 23, 2010. The experiment data explained that the concentrator water solar collector contributes for decreasing heat gain to the wall by 30% through summer season, and (CWSC) has instantaneous thermal efficiency 45%. This system is suitable for small hotel and hospital which need cooling in the long term as well as hot water required in some special cases.

(Pei et al. 2012)[50] evaluated experimentally the performance of evacuated tube collector(ETC) with and without a mini-compound parabolic concentrator (CPC) reflector. A series of experiments were conducted under the same time and conditions for two types SWH; water tank was heated from 26.9 to 55, 65, 75, 85, and 95℃. The results indicated that when water is required at low temperature, ETC without mini CPC has higher thermal and exergy efficiencies than ETC with mini CPC . And when water is required at high temperature, ETC with mini CPC has higher thermal and exergy than ETC without mini CPC. These results are taken for average and instantaneously values.

(Wayne 2012)[51] developed the performance of the experimental apparatus of solar water heaters for domestic usage. The system operating by thermosyphon methods, (SWH) fitted with a tracking mechanism to increase heat absorbed by the collector. The results explained that the water tank was heated by solar energy absorbed by the collector also thermosyphon affected by water temperature measurements in the tank for different height inside it. moreover, the natural flow rate increases when water demands increase.

(Cruz-Peragon et al. 2012)[52] investigated experimentally the characterization of solar collectors is based on experimental techniques next to validation of associated models. It serves to characterize the device by

means of critical coefficients. The first step consists of identifying those significant parameters that match the selected model with the experimental data, via nonlinear optimization techniques, applied to steady state conditions. Second, new correlations must be adopted. Finally, the overall model must be checked in transient regime. To illustrate the technique, a tailor-made prototype flat plate solar collector has been analyzed. An intermediate complex collector model has been proposed (2D finite-difference method). Both steady and transient states were analyzed under different operating conditions. Parameter identification is based on Newton's method optimization. For parameter approximation, exponential regression functions through multivariate analysis of variance is proposed among many other alternatives. Results depicted a robustness of the overall proposed method as starting point to optimize models applied to solar collectors.

(Fazilati and Alemrajabi 2013)[53] investigated improving the performance of solar water heaters by using phase change material (PCM) as a storage medium. The solar tank is of jacketed shell type, Three levels of radiation intensity were studied (weak, middle and strong). Experimental data revealed improving in thermal performance of (SWH) system using (PCM) which leads to increase the time of 25% for supplied hot water from system, highest improvement in thermal energy was 39% when the temperature was 80℃. exergy efficiency reached 16% when the temperature was 40℃.

(Ayompe and Duffy 2013)[54] evaluated annual thermal performance for (SWH) evacuated tube collector in a temperate climate which was performed with recalling a field trial installation in Dublin city, Ireland (Lat. 53.3, Long. -6.26) . The system takes into consideration the effects between (ETC), thermal storage tank and immersion heater which provide

auxiliary energy when collector is incapable of reaching the obtaining temperature. Results revealed that the higher temperature of the outlet fluid collector was 70.3℃. The mean annual energy produced was 20.4 MJ/day, and the thermal efficiency of collector was 63.2 %.

(Mongre 2013)[55] studied experimentally the performance of flat plate solar water heaters fitted with circulating pump linked by aluminum pipes. Testing of an apparatus conducted in September 2012 and November 2012. The results showed that there is a marked increase in immediate efficiency of 55.24 % when glazing area increased. This system can be used in remote areas to supply hot water usage.

(Ogie, et al. 2013)[56] developed designing and fabricating flat plate collector solar water heaters for domestic usage at low cost utilizing from material available locally as much as possible. The study arrived the possibility to construction (SWH) system which has low cost, cover domestic requirements of hot water, leading to saving cost and electrical energy, and reducing harmful emissions in the long term. Experimental results showed the higher temperature of output fluid was 55℃.

(Sharma and Joshi 2013)[57] promoted the thermal performance of V-through flat plate collector (corrugated absorber plate) by novel design improving heat transfer technique and reducing cost by fabricated from available material. Each zone consists of two aluminum plates that are installed diagonally and pass through two tubes. This design increases absorbed solar energy and enhanced thermal performance for the system. Results showed the system produced 30L at average water temperature of 50℃ at 5:00 pm.

(Madan and Sirse 2015)[58] investigated evaluating thermal efficiency of flat plate collector solar water heaters. Thermosyphon system was tested

in Nagpur (21.15ºN, 79.09ºE), , Maharashtra, India during winter. The results reached was higher outlet temperature of 73℃ and higher obtained efficiency was 65%.

(Pandey et al. 2015)[59] searched experimentally the thermal performance of open system solar water heaters evacuated tube collector has U-shape copper tubes based on energy and exergy analysis. The system was examined with different flow rate:10, 15, 20, 25 and 30 liters per hour (L/hr) to reach optimum value giving the best heat and mass transfer mechanism. Results revealed the optimum performance of the system for 15 (L/hr), temperature reached 79℃, energy efficiency was 66.57%, and exergy efficiency was 13.38 %.

(Luo et al. 2017)[60] evaluated saving energy for residential heating buildings using solar water heaters as an assistant with a heat pump. Many experimental tested in Xi'an(34°20'N and 108° 56E) located in the northwest of China, satisfied comfortable conditions for occupants. Results showed that integrated solar water heaters with a heating pump contributed to saving energy in the rate was greater than 60% from total energy consumption.

(Lokhande and Dubey 2017)[61] investigated analysis performance of solar water heaters fitted with heat exchanger. system fabricated, distilled water used to flow in collector to enhance efficiency and tested in various condition to reach the best performance. System tested on 30th March 2016 from 9:00 A.M. to 5:00 PM. The weather was sunny for a few hours, cloudy sky and sun completely faded away. Results of the experiment showed the system gave temperature reach for more 50℃ when the weather was sunny, so when the sun completely vanishes, or weather was cloudy, the system gives satisfactory results.

(Bellos and Tzivanidis 2018)[62] improved analytical model of solar water heaters for daily performance and validated with experimental work. The developed model examined with experimental data from an integrated laboratory system with a flat plate collector. Model extended with real weather data for the climate conditions of Athens city, Greece (37° 59' N and 23° 43' E). Evaluation of the system from energetic and economic aspects is by testing a day of each month in the year. Results indicated the energy produced during the year by the system was 2171 kWh, average thermal efficiency reached 54.24% and payback period reached 5.03 years.

2.4 Experimental and Numerical Studies:

(Koffi et al. 2008)[63] Searched experimentally and theoretically enhancement efficiency of SWH system work according to thermosyphon approach, fitted with internal heat exchanger. An exchanger manufactured from the copper tube which is rolled and mounted inside storage tank diagonally. This study found a good consensus between experimental and theoretical results; results indicated that the outlet water temperature of collector was more than 85.5℃, and thermal efficiency of the collector was 58% when heat flux reaches major value.

(Budihardjo and Morrison 2009)[64] Evaluated numerically model of a water-in-glass evacuated tube, the experimental measurement for the system can be presented. Model of thermosyphon system water-in-glass evacuated tube and experimental measurement study to describe the characteristics of the system. Results showed that the water-in-glass evacuated tube system consists of 30 tubes array. It has slightly less energy saving than the two systems (3.7 m^2) of flat plate collector. Moreover, the

performance of ETC system shows little response to the size of the tank than the FPC system.

(Li, Dai, and Wang 2015)[65] Used a new design of solar water heaters evacuated tube collector which was fixed vertically on the wall of balcony in high rise buildings in Shanghai, Chine. The system was studied by two methods, the numerical simulation model for water consumption are presented, and experimental data of the system were compared with the numerical model and found a good agreement between them. Results explained that the average daily efficiency of the collector was 40%, total annual energy derived from the tank was 2805.3 MJ/m^2.

(Yang, Wang, and Xiong 2017b)[15] Searched potential heating space using thermal solar system in Lhasa, chine. The study focused on calculation distribution of temperature in the storage tank to reach the optimized solar thermal system using numerical simulation taking into account the effects of instantly charging and discharging operation mode and then validated with experimental measurements. The coefficient of performance (COP) of the system computed dependent on experimental data. Results indicated that the system has a high (COP) with instantly charging and discharging operation mode and good heating effect.

(Koholé and Tchuen 2018)[66] Investigated optimization of solar water heaters flat plate collector worked with thermosyphon approach. Experimental and numerical studies to obtain an optimization system combined between the perfect design of parameter and higher performance of FPC collector, and there is good agreement between experimental and numerical results. Results revealed that the higher thermal efficiency and outlet fluid temperatures were 64.93 % and 63.66 %, 65.19 ℃ and 64.10 $°C$ obtained by experimental and simulation, respectively.

(Liu et al. 2018)**[67]** Studied heating space using a new hybrid solar heating system which consists of solar Kang system (An ancient Chinese heating system based on burning animal waste), direct gain window, and Trombe wall. This study examined the impacts of five solar system operation method on the hourly temperature inside building in the Qinghai-Tibetan plateau. Results revealed that there was a good consensus between numerical and experimental results. Moreover, solar Kang system operating along the day on the contrary from another system, combined application: solar Kang system, direct gain window and Trombe wall can provide the optimum indoor thermal environment, especially in rural domestic buildings.

2.5 Summary Of Results For The Literature Review

A review of previous studies shows that there is an interest in the development of solar water heaters for various domestic, commercial and industrial applications These studies focused on four essential aspects that contribute to increasing the efficiency of solar heating systems:

1-   Solar water heater design, geometric shape, dimensions of solar collector components and type of materials used in its composition.

2-   Testing several types of working fluids or improve the thermal performance of them by improving some physical properties.

3-   Studying the impact of changing climate conditions on the performance of solar heaters.

4-   Using techniques to increase the heat exchange in the storage tank in closed systems such as use phase change meterial PCM to increase the amount of heat energy stored for cloudy times or at night.

In addition to the above, the researchers included feasibility studies for using solar water heaters, calculating the amount of electrical energy that can be saved and reducing environmental pollution rate, so that their use will be more widespread and achieve sustainable economic development in the future. Table 2.1 provides information summarizing previous research discussed in this chapter and presenting the most important findings of the researchers.

Table 2.1 showing the summary of results for the literature review

No.	reference	Study type	Collector type	Working fluid circulating method	Efficiency	Useful heat	Output temperature	other
1	(Morrison and Braun 1985)	numerically	FPC	thermosyphon	---------	-------------	------------	Horizontal tank is better than vertical in thermosyphon
2	(Morrison, Budihardjo, and Behnia 2005)	numerically	ETC	Thermosyphon	---------	-----------	60 C^O	----------
3	(Chow et al. 2006)	numerically	FPC	forced	38.4% (annual average)	904GJ (annual)	41.4C^o	----------
4	(Ucar and Inalli 2008)	numerically	FPC & ETC	Thermosyphon	-------	----------	(40-100)C^o	--------
5	(Mateus and Oliveira 2009)	numerically	FPC & ETC	forced	35%-44%	-----------	(70-90)C^o	--------
6	(Hobbi and Siddiqui 2009)	numerically	FPC	forced	41%	-----------	-----------	-------
7	(Allen et al. 2010)	Theoretically	FPC	forced	-----	(1940–3520) MJ (annual)	---------	Expensive in the current time

No.	reference	Study type	Collector type	Working fluid circulating method	Efficiency	Useful heat		Output temperature		other
8	(Ayompe, Duffy, McCormack, et al. 2011)	numerically	FPC & ETC	forced	Results of modelling and trail field data in term percentage mean absolute errors					-------
					------	FPC	ETC	FPC	ETC	
						14.1%	16.8%	16.9%	18.4%	
9	(Serale et al. 2014)	Theoretically & numerically	FPC	forced	PCMs Enhanced from 5% to 9%	--------		---------		
10	(Yao et al. 2015)	numerically	Tube collector	Thermosyphon	mean nessult number of SWH with a relative twisted ratio of the twisted tape (m) y=2.5m and y=4m respectively was 1.07% less and 9.29% higher than normal solar water heater.					---------
11	(Guo et al. 2017)	numerically	ETC	forced	-------	(±3%) for accumulated heat flow accumulated over the entire heating season		(±10%) for transient storage temperature distribution		-----------
12	(Sami et al. 2018)	Theoretical	FPC	Thermosyphon		SWH contributed to saving the traditional energy 46% and 57% in northern and southern regions		------------		Saving in annual operating cost of the solar system reached 51% and 69% respectively

No.	reference	Study type	Collector type	Working fluid circulating method	Efficiency		Useful heat		Output temperature	other
13	(Naphon, Assadamongkol, and Borirak 2008)	Experimental	ETC	forced	Nanofluid enhanced by10.60%		------------		----------	--------
14	(Reindl et al. 2008)	Experimental	-------	forced	Modified system reduced (6%-11%)		---------		----------	---------
15	(Al-Madani 2006)	Experimental	Cylindrical SWH	Thermosyphon	--------		41.8%		The maximum temperature difference between inside and outside of SWH was 27.81C	---------
16	(Ayompe, Duffy, Keever, et al. 2011)	Experimental	FPC & ETC	forced	Annual average		Annual average		---------	4264€ -652€
					FPC	ETC	FPC	ETC		
					46.1%	60.7 %	1984 kWh	2056 kWh		
17	(Yousefi et al. 2012)	Experimental	FPC	forced	Nanofluid enhanced of 28.3%		surfactant enhanced of 15.63%.		----------	---------

No.	reference	Study type	Collector type	Working fluid circulating method	Efficiency		Useful heat	Output temperature	other
18	(Gang et al. 2012)	Experimental	CPC	forced	49%		---------	95C^o	-------
19	(Nouvelles, Seminar, and Energies 2012)	Experimental	CPC	-----------	SWH system provided hot water of (120 L /day)				--------
20	(Ahmad 2012)	Experimental	FPC	forced	45%			----------	
21	(Pei et al. 2012)	Experimental	ETC & ETC with CPC	forced	ETC / Higher for low temp.	ETC with CPC / Higher for high temp.	---------	(55-95)C^o	--------
22	(Wayne 2012)	Experimental	FPC	Thermos-yphon	----------		---------	--------------	--------
23	(Fazilati and Alemrajabi 2013)	Experimental	Solar tank	forced	thermal energy 39%		---------	80C^o	--------
					exergy efficiency 16%		--------	40C^o	
24	(Ayompe and Duffy 2013)	Experimental	ETC	Thermosyphon	63.2%		annual mean energy produced was 20.4 MJd^{-1}	70.3oC	--------
24	(Mongre 2013)	Experimental	FPC	forced	55.24 %		--------	---------	--------

No.	reference	Study type	Collector type	Working fluid circulating method	Efficiency		Useful heat	Output temperature	other
25	(Ogie, Oghogho, and Jesumirewhe 2013)	Experimental	FPC	Thermosyphon	----------		---------	55 C^{o}	Low cost (use the material available locally)
26	(Sharma and Joshi 2013)	Experimental	FPC	Thermosyphon	--------		--------	50C^{o}	Low cost (use material available locally
27	(Madan and Sirse 2015)	Experimental	FPC	Thermos-yphon	65%		---------	73C^{o}	---------
28	(Pandey et al. 2015)	Experimental	ETC	forced	energy 66.57%	Exergy 13.38 %	---------	79C^{o}	---------
29	(Luo et al. 2017)	Experimental	ETC	------	Solar energy contributed by 60% from total energy to heating space		---------	----------	-------
30	(Parida 2011)	Experimental	FPC	forced	27.8% (for unglazed solar collectors)		1.7 M Watts (for 6 hours)	--------	--------

No.	reference	Study type	Collector type	Working fluid circulating method	Efficiency	Useful heat	Output temperature	other
31	(Lokhande and Dubey 2017)	Experimental	FPC	Thermos-yphon	_____	--------	50C^O	--------
32	(Bellos and Tzivanidis 2018)	Experimental	FPC	forced	54.24%	2171 kWh (in year)	-------	2432 € payback period reached 5.03 years
33	(Koffi et al. 2008)	Experimental & theoretical	FPC	Thermos-yphon	%58	---------	85.5^{o}C	------
34	(Budihardjo and Morrison 2009)	Experimental & numerical	ETC	Thermosyphon	water-in-glass evacuated tube system consist of 30 tubes array It has slightly less energy saving than two systems (3.7 m2) of flat plate collector. Moreover, the performance of ETC system Shows little response to the size of the tank than the FPC system.			
35		Experimental & numerical						
36	(Li, Dai, and Wang 2015)	Experimental & numerical	ETC	Forced	40%	annual energy derived from the tank was 2805.3 MJ/m2	---------	---------
37	(Yang, Wang, and Xiong 2017)	Experimental & numerical	FPC	forced	an average value of COP system (3)			---------

No.	reference	Study type	Collector type	Working fluid circulating method	Efficiency	Useful heat	Output temperature	other
38	(Koholé and Tchuen 2018)	Experimental & numerical	FPC	Thermos-yphon	64.93 % and 63.66 % obtained by experimentation and simulation respectively	---------	63.66 %, 65.19 °C obtained by experimentation and simulation respectively	-------
39	(Liu et al. 2018)	Experimental & numerical	ETC	forced	-------	---------	-------------	-------

CHAPTER THREE

THOERETICAL ANALYSIS

CHAPTER THREE

THOERETICAL ANALYSIS

3.1 Introduction

This chapter presents the theoretical analysis of heating load calculations as well theoretical study of the solar heating system. The derivation of the mathematical model that describes the operation of a flat plate collector are presented. The representation of different heat exchangers under transient conditions, three-dimensional, incompressible flow and heat transfer has been solved of the collector. The proposed method for solving this model will be presented in this chapter.

3.2 Heating Load Calculations

The heating load is the amount of heat added to the space to obtain internal design conditions which is suit the comfort of the occupants. Heating load is calculated to estimate capacity of the equipment required to heat the space. In general, the heating load is almost equal to the heat loss from the building by walls, ceilings, floors, windows, and doors, as well as air leakage through the openings of the windows and doors. The heating load consists of sensible heat which transmitted directly by conduction, radiation, and convection, and the latent heat transmitted to space with the air accompanying the moisture. Calculation of the heating load to the room has a dimension (2 * 5) m and height of 3 m, as shown in Figure 3.1.
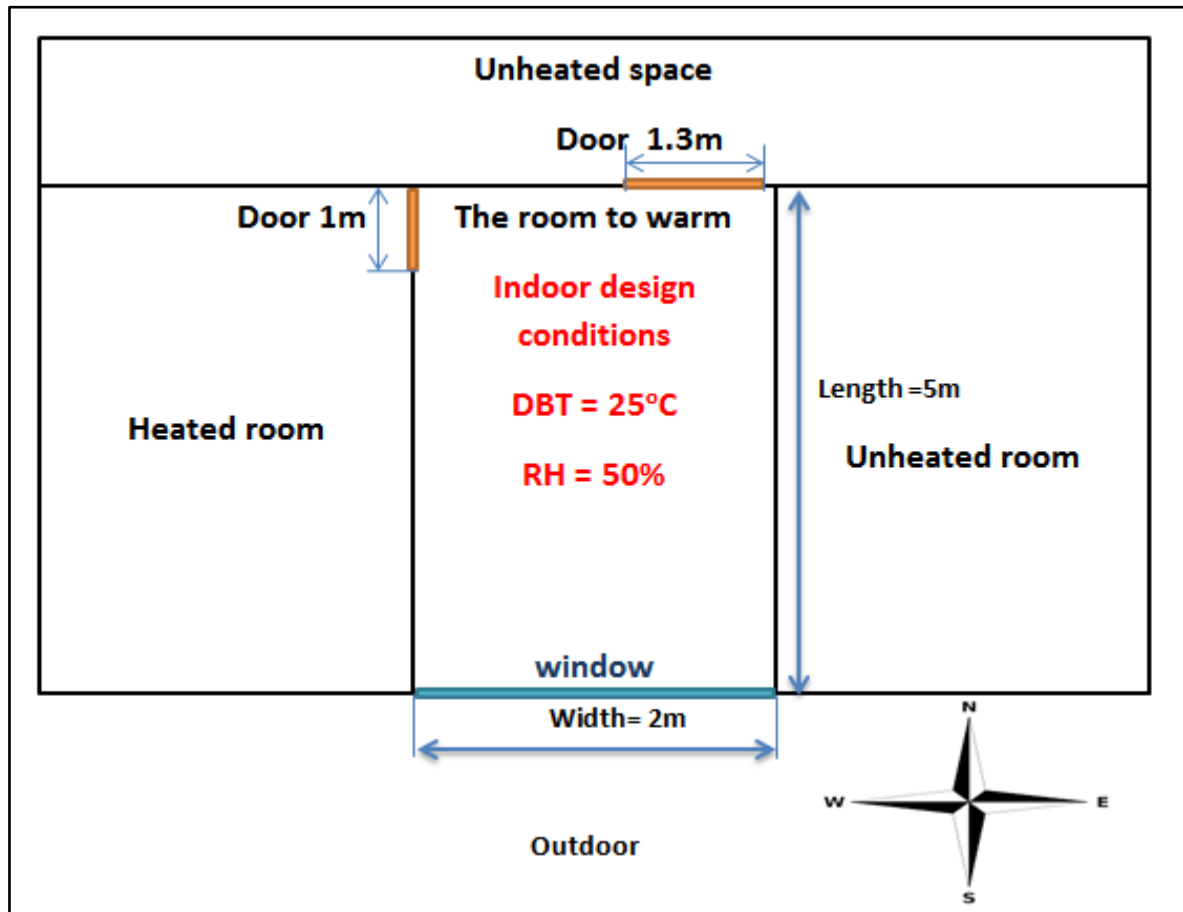
Fig.3.1: shows room location to be heated

There are some basic rules that are taken into consideration in heating load calculations:

1- All heat losses are instantaneous heating loads while neglecting the effect of heat stored in the structure of the building.

2- Internal heat sources and solar heat gain are neglected in heating load calculations.

The following are calculations of the heating load due to thermal losses from the various parts of the room structure, which are either sensible or latent heat (Kharagpur 2008)[23].

a) Sensible heat transfer rate through the walls:

Heat is transmitted through the walls from the space to the outside by conduction. It is assumed that the walls are composed of homogeneous materials, and heat transfer is one-dimension. Two walls of the room are shared with adjacent rooms and one common wall with an internal corridor, while the southern wall is exposed to the outdoor. The heat transfer in the wall is neglected if it is located between two rooms under heating.

1- Sensible heat transfer through the walls given by:

$$(Q_S)_{walls} = A_w * U_w(T_r - T_o) \qquad \qquad ....(3.1)$$

Where:

$A_w = Wall\ area\ (m^2)$.

$U_w = Overal\ heat\ transfer\ coefficient\ of\ the\ wall\ \left(\frac{W}{m^2.K}\right)$.

$T_r = Room\ air\ temperature\ \ °C.$

$T_o = Outdoor\ air\ temperature\ \ °C.$

b) Sensible heat transfer through the roof

The ceiling is assumed to be monolithic, and the heat is moving in one direction. The room to be heated is located on the ground floor, and above it is the first floor only.

$$(Q_S)_{roof} = A_r * U_r(T_r - T_o) \qquad \qquad ....(3.2)$$

Where:

$A_r = Roof\ area\ (m^2).$

$U_r = Overal\ heat\ transfer\ coefficient\ of\ the\ roof\ \left(\frac{W}{m^2.K}\right).$

c) **Sensible heat transfer through the floor**

It was assumed that the floor was composed of a homogeneous material and that the heat was moving in one direction.

$$(Q_S)_{floor} = A_f * U_f(T_r - T_o)$$ ....(3.3)

Where:

$A_f = Floor\ area\ (m^2)$.

$U_f = Overal\ heat\ transfer\ coefficient\ of\ the\ floor\ \left(\frac{W}{m^2.K}\right)$.

d) **Sensible heat transfer rate through the glass:**

$$(Q_S)_g = A_g\ [U_g(T_r - T_o) + SHGF_{max}.SC]$$ ....(3.4)

Where:

$A_g = Glass\ area\ exposed\ to\ solar\ radiation\ (m^2)$.

$U_g = Overal\ heat\ transfer\ coefficient\ of\ the\ glass\ \left(\frac{W}{m^2.K}\right)$.

$SHGF_{max} = Maximum\ Solar\ Heat\ Gain\ Factor.$

$SC = Shading\ Coefficient.$

e) **Heat transfer due to infiltration**

The heat transmitted by air infiltration is sensible and latent heat.

1- Sensible heat transfer due to infiltration

$$(Q_S)_{inf} = m_{inf}\ cp_m(T_r - T_o) = V_m\ \rho_m cp_m(T_r - T_o)$$ ....(3.5)

Where:

$$V_{\dot{m}} = \text{Infiltration volume flow rate } \left(\frac{m^3}{s}\right).$$

$$\dot{m}_{inf} = \text{Infiltration mass flow rate } \left(\frac{kg}{s}\right).$$

$$\rho_m = \text{Density of the moist air } \left(\frac{kg}{m^3}\right).$$

$$cp_m = \text{Specific heat of the moist air } \left(\frac{J}{kg.K}\right).$$

2- Latent heat transfer due to infiltration

$$Q_{l,inf} = \dot{m}_{inf}h_{fg}(W_{out} - W_{in}) = V_{\dot{m}}\,\rho_m h_{fg}(W_{out} - W_{in}) \quad \ldots\ldots\ldots..(3.6)$$

Where:

$$h_{fg} = \text{Latent heat of vaporization of water } \left(\frac{KJ}{kg}\right).$$

$$W_{in}\&W_{out} = \text{Indoor and outdoor humidity ratio.}$$

The infiltration rate relies upon many factors such as the tightness of the building that includes the windows, walls, and doors, as well as the prevailing wind speed and direction. The infiltration rate is obtained by using the air change method given by:

$$\dot{m}_{inf} = ACH.V/3600 \quad (m^3/s) \qquad\qquad \ldots\ldots\ldots\ldots.(3.7)$$

Where:

$$ACH = \text{Number of air changes per hour.}$$

$$V = \text{Gross volume of the conditioned space in } (m^{3)}.$$

The total sensible heat calculated from following equation:

$$Q_{s,total} = (Q_S)_{walls} + (Q_S)_{roof} + (Q_S)_{floor} + (Q_S)_{glass} + (Q_S)_{inf} \quad \ldots(3.8)$$

The total latent heat calculated from following equation:

$$Q_{l,total} = Q_{l,inf} \qquad\qquad\qquad \text{...................(3.9)}$$

The total heating load of the room equals the sum of sensible and latent heat transferred from the room.

$$Q_h = Q_{s,total} + Q_{l,total} \qquad\qquad \text{...................(3.10)}$$

3.3 Energy Balance Equations Of Flat Plate Collector

In this section, we will explain the energy balance equations that describe the thermal energy transfer between parts of a flat plate collector that operates under transient conditions for its various components. In this model, a control volume containing one tube and five areas (glass cover, air gap, absorber plate, the working fluid, insulation) was taken vertically to the flow direction, as shown in Figure 3.2.
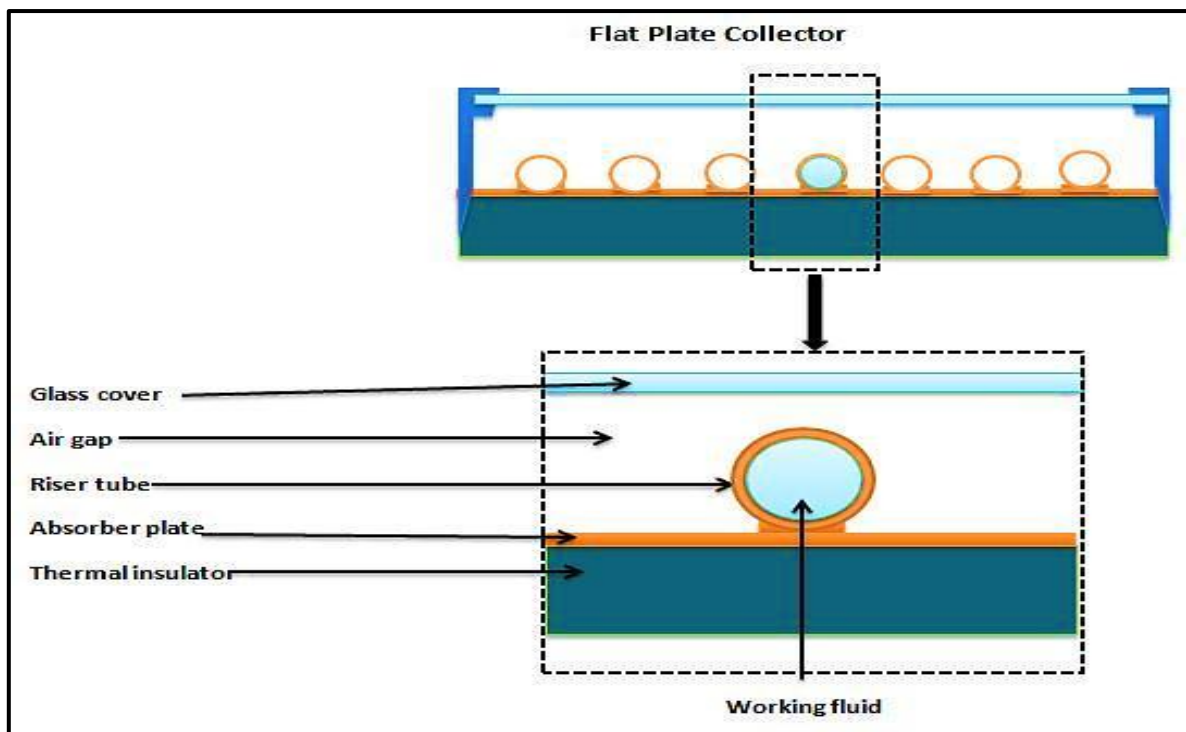
Fig. 3.2: Schematic diagram of the five areas analyzed in the flat-plate collector.

There are several heat transfers process occur between different parts of collector as shown in Figure 3.3. The temperature of the collector depends on the direction of the fluid flow, Taking into account the section of areas in the flow direction . The mathematical model will be applied through the general energy balance it will be applied to each zone of the collector in the control volume analysis; the general energy balance is given by:

$$\frac{dU_s}{dx} = Q_{in} - Q_{out} + Q_v \qquad\qquad\qquad\qquad\qquad (3.11)$$

where:

$\dfrac{dU_s}{dx}$ = Change the internal energy of the system in control volume *(W)*.

Q_{out} = Heat transfer outlet the system in control volume *(W)*.

Q_{in} = Heat transfer inlet the system in control volume *(W)*.

Q_v = Heat generation inside the system in control volume *(W)*.
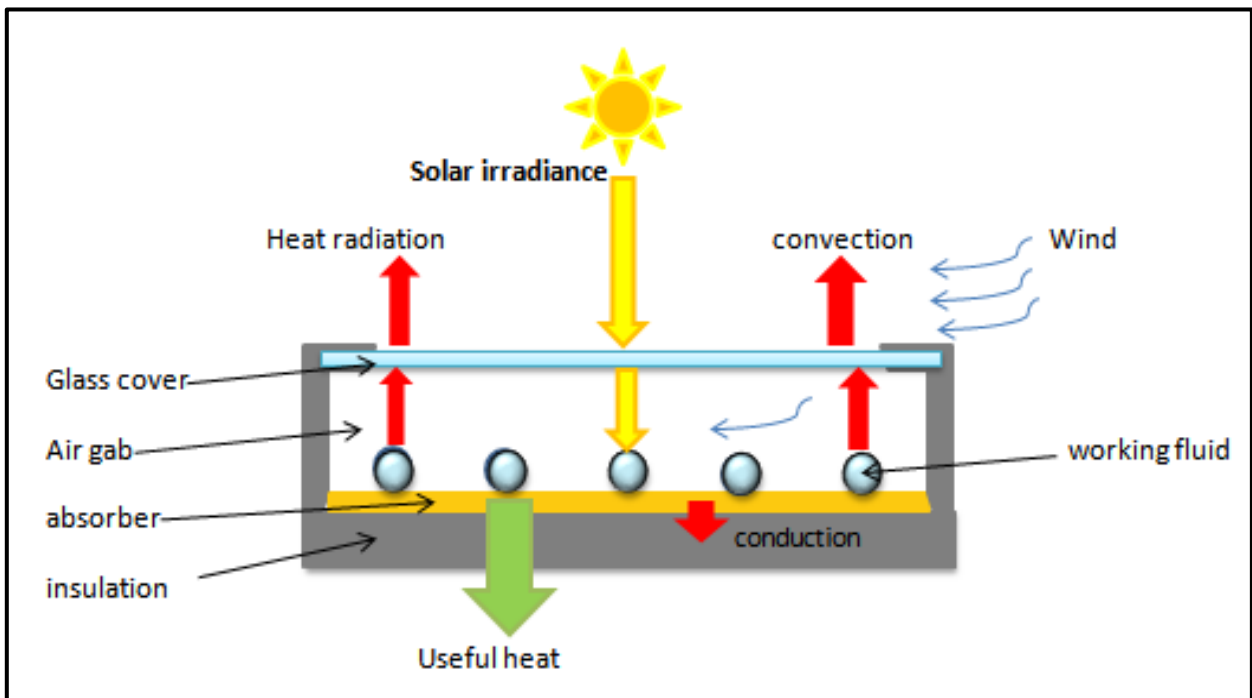

Fig.3.3 Heat transfers process occur between different parts of collector

The following assumptions will be considered to simplify the analysis of flat plate solar collector:

1. Uniform mass flow rate in each tube of the collector.

$$m_t = \frac{m_f}{n} \qquad\qquad \text{............... (3.12)}$$

   where:

   m_f= *The total mass flow rate inlet the solar collector (kg/s).*

   m_t= *the mass flow rate in each tube (kg/s).*

   n = *number of tubes of the solar collector.*

2. The heat does not move by conduction in the flow direction and the thermal energy transferred in the flow direction by mass transfer.
3. Neglecting heat transferred from the edges of the collector.
4. Insulation and glass properties remain constant when temperature changes (independent of temperature).
5. The thermal properties of the air gap change as the temperature changes (dependent temperature).
6. The ambient conditions, wind speed, and sky radiation are changing with time.
7. The side and back of the collector exposed to the same ambient temperature.
8. Consider the sky as a black body for long-wavelength radiation at an equivalent sky temperature (Kalogirou, 2008)[7].
9. Neglecting the effect of dust and dirt on the collector.
10. The header and riser of the collector were fixed on a sheet with parallel tubes.
11. Consider the heat passing through the cover in one direction.

The energy balance equations of the flat plate solar collector parts as follows:

3.3.1 The Glass Cover

The glass cover is at the top of the collector and has relatively thin thickness, which makes the temperatur uniformly distributed. Thus its thermal properties can be considered constant. The governing equation can be derived from an energy balance in a differential volume of thickness δ and an area of (pΔz). Convection heat transfer occurs between the glass and the ambient air and air gap, and by radiation between the glass and both the sky and absorber, as shown in Figure 3.4.

Therefore, equation (3.11) is written as follows:

$$Cp_g\rho_g V_g \frac{dT_g}{dt} = \left[hc_{g-am}(T_{am} - T_g) + h_{r1}(T_{am} - T_g) + h_{r2}(T_{ab} - T_g) + hc_{g-a}(T_a - T_{g)} + \alpha G \right] P \Delta z \qquad \text{... ... ...} (3.13)$$
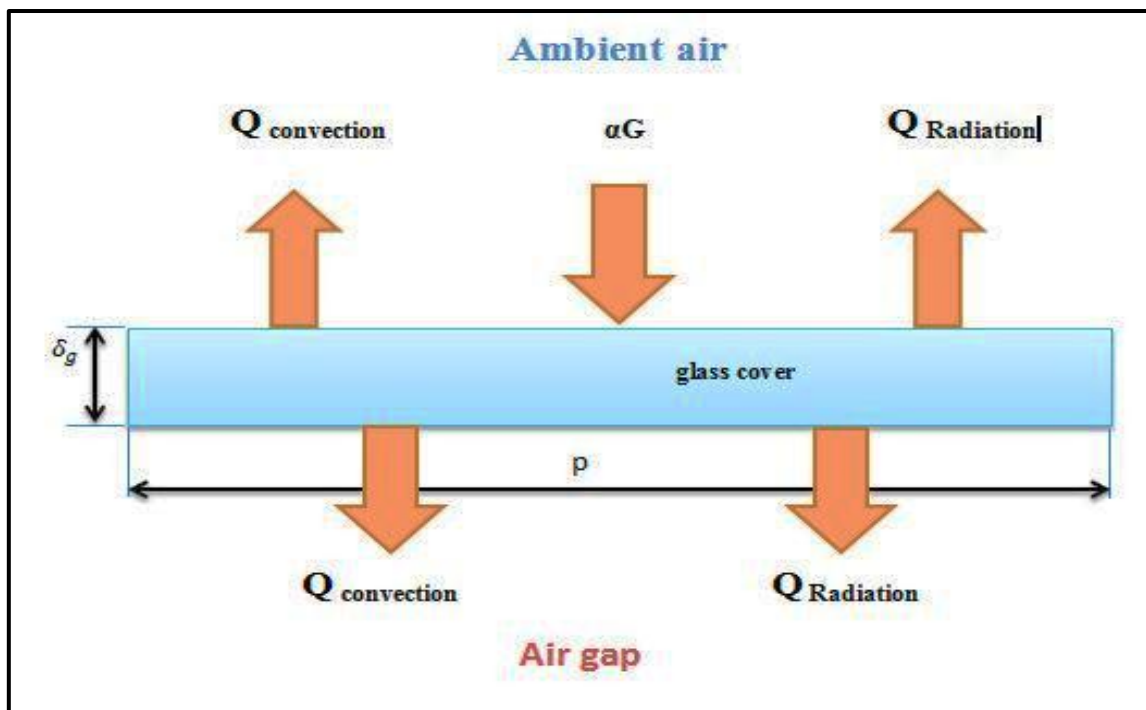
Fig. 3.4: 1-D heat transfer in the glass cover

3.3.2 The Air Gap Between the Glass Cover and the Absorber

The air gap lies between the glass cover and the absorber plate, considering an analysis of the air gap area in the control volume. The air gap has transient thermal properties. Heat transfers by convection between air gap and both the glass cover and the absorber, as shown in Figure 3.5.
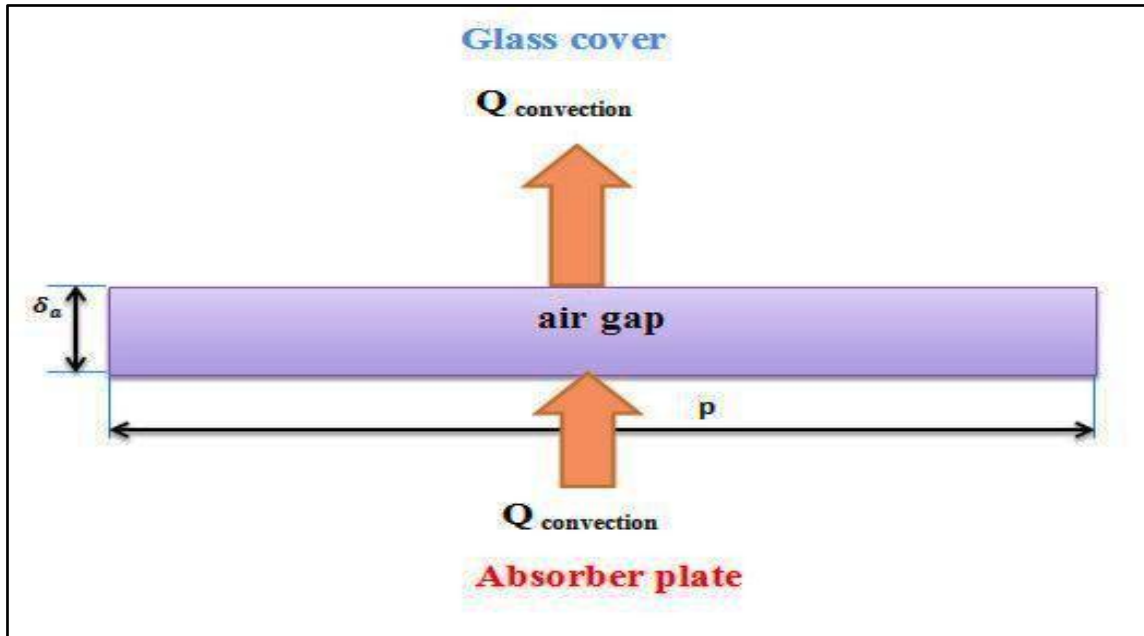

Fig. 3.5: 1-D heat transfer in the air gap between cover and absorber

By applying the energy balance equation (3.11) is written as follows:

$$Cp_a(T_a)\rho_a(T_a)V_a \frac{dT_a}{dt} = \left[hc_{g-a}(T_g - T_a) + hc_{ab-a}(T_{ab} - T_a) \right]P\Delta z \quad \ldots \ldots \ldots (3.14)$$

3.3.3 The Absorber

The absorber plate is the central part of the solar collector. Its temperature is high relative to other parts and assume the thermal properties are constant. Energy balance of the control volume of the absorber region and the consideration of the fall of solar radiation on it. Heat transfer via radiation between the absorber and the glass cover, convection heat transfer between the absorber and the air gap,

and by conduction between the absorber and the insulation zone, as well as the heat transfer to the working fluid via convection as shown in Figure 3.6.
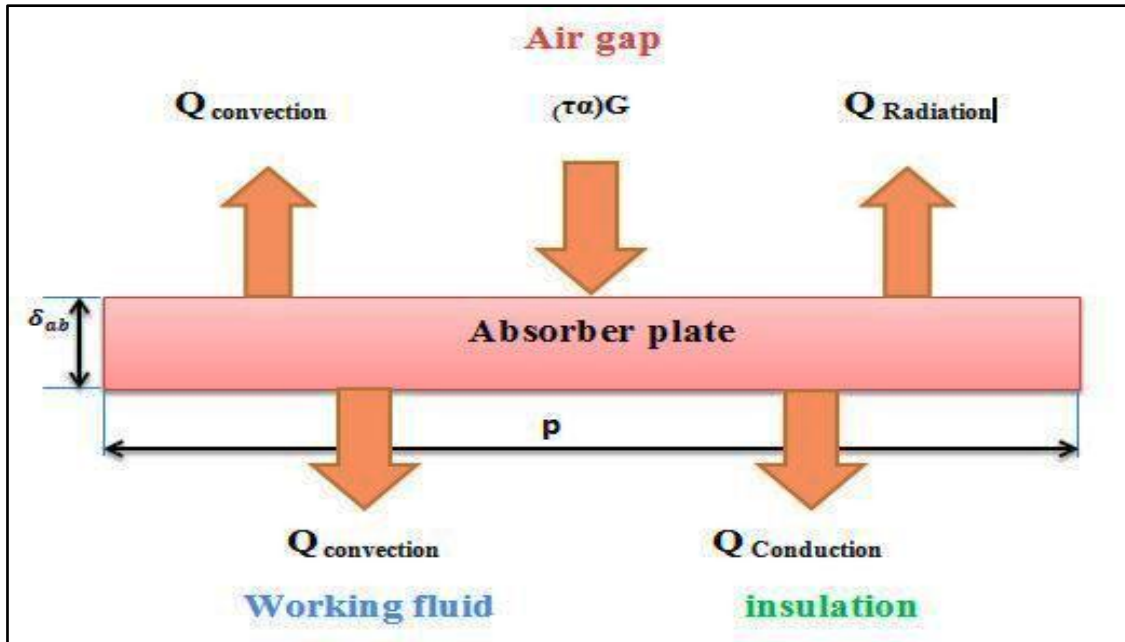

Fig. 3.6: 1-D heat transfer in the absorber

By applying energy balance, equation (3.11) is as follows:

$$Cp_{ab} \, \rho_{ab} V_{ab} \frac{dT_{ab}}{dt} = \left[G(\tau\alpha) + h_{r3}(T_g - T_{ab}) + hc_{ab-a}(T_a - T_{ab}) + \frac{k_{ins}}{\delta_{ins}}(T_{ins} - T_{ab}) \right] P\Delta z + \pi d_i \Delta z \, h_f(T_f - T_{ab)} \qquad \dots\dots\dots\dots\dots\dots(3.15)$$

3.3.4 The Working Fluid

Figure 3.7 shows the energy balance in a control volume of the working fluid in a flat-plate solar collector. Taking in consideration the change in total energy with time and the total heat transferred into the fluid control volume, the energy balance under transient properties of the working fluid can be written as:
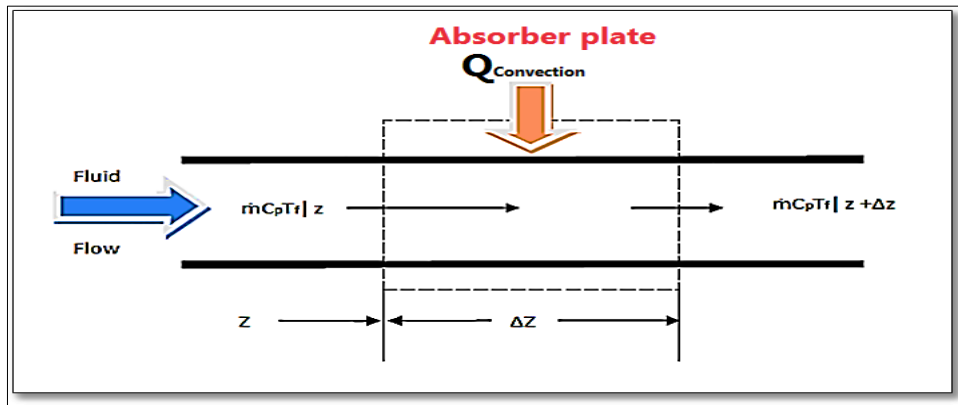
Fig. 3.7: Energy balance in a control volume of the working fluid in the flat-plate solar collector

By applying energy balance, equation (3.11) is as follows:

$$Cp_f\rho_f \, A \, \frac{\partial T_f}{\partial t} = \pi d_i \, h_f \, (T_{ab} - T_f) + m_f cp_f \frac{\partial T_f}{\partial z} \qquad \dots\dots\dots\dots\dots\dots\dots(3.16)$$

3.3.5 The insulation

The insulation part is the back of the solar collector and is directly adjacent to the absorbent. By analyzing the insulation zone in the control volume, thermal properties of it is constant. Conduction heat transfers occur between the absorber and insulation, also via radiation between the insulation and the surrounding air, as shown in Figure 3.8.
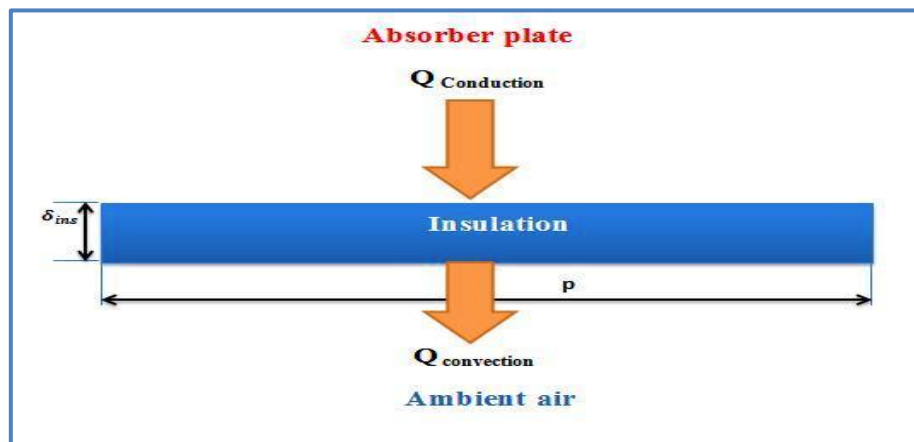

Fig. 3.8: 1-D heat transfer in the insulation

By applying energy balance, equation (3.11) is as follows:

$$Cp_{ins}\,\rho_{ins}V_{ins}\frac{dT_{ins}}{dt} = [\frac{k_{ins}}{\delta_{ins}}(T_{ab} - T_{ins}) + hc_{ins-am}(T_{am} - T_{ins})]P\Delta z \quad .... (3.17)$$

3.4 The Useful Heat And energy Equations Balance Of Indoor Radiator

The radiator is an essential part of the heating system, and it is a heat exchanger that works to transfer heat from working fluid to air inside the room. The radiator is generally composed of upper and lower manifolds connected with each other by a set of tubes. The sides of each tube are connected to the fins as shown in Figure3.9.
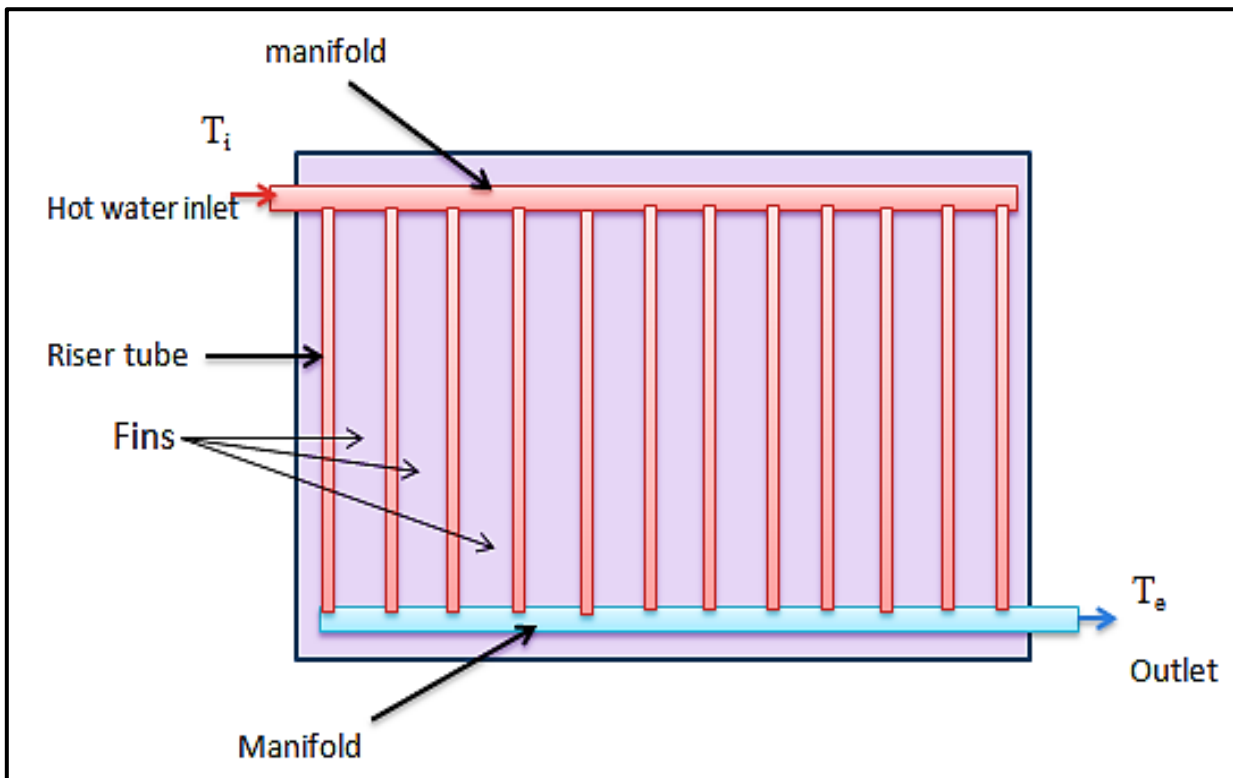

Fig. 3.9 shows the schematic diagram of radiator

The useful heat of the radiator is the amount of heat transferred from the radiator surfaces to the room air. The useful heat increases as the difference between the temperature of the radiator and room air are high. The useful heat of the radiator can be calculated according to the following equation:

$$q_u = m^{\cdot} \; cp(T_i - T_e) \qquad\qquad\qquad \text{...........................} \; (3.18)$$

3.5 System Modeling and Simulation:

Flat plate collector is studied by 3-D numerical investigations which performed by CFD technique and governing equations were solved by COMSOL Multiphasic 5.3 software. In this study, the model exposed to radiation heat transfer and convection between glass cover and side walls with the surrounding. Moreover, conduction heat transfer in insulation base, and conduction between the absorber plate and risers tubes are considered. The absorbed solar energy was simulated by taking data of weather for Najaf city (31.59^o N Lat., 44.19^o E Long.) on January 9, 2019 which was recorded by a weather station in the laboratory. Data recorded are ambient temperature, wind speed, and global solar irradiance that uniformly distributed over the absorber plate.

3.5.1 Computational Domain

Numerical simulations are carried out on a model of with a 2 m^2 solar water heater flat plate collector. Due to the significant difference in the dimension of hydraulic tube diameter (0.008 m) and absorber tube length (1.8 m), an excellent grid distribution is needed in the cross-section of the tube. Therefore, some assumptions on the computational domain are considered as follow:

- The heat loss by radiation from margins of the collector is ignored.

- The heat loss from the bottom base of the collector is neglected

- The flow rate in all riser tubes remains constant and is divided equally in all risers in the collector.

- The flow field is symmetric concerning y–z plane, take one half of the riser tube, and absorber plate on one side is considered for the simulation study.
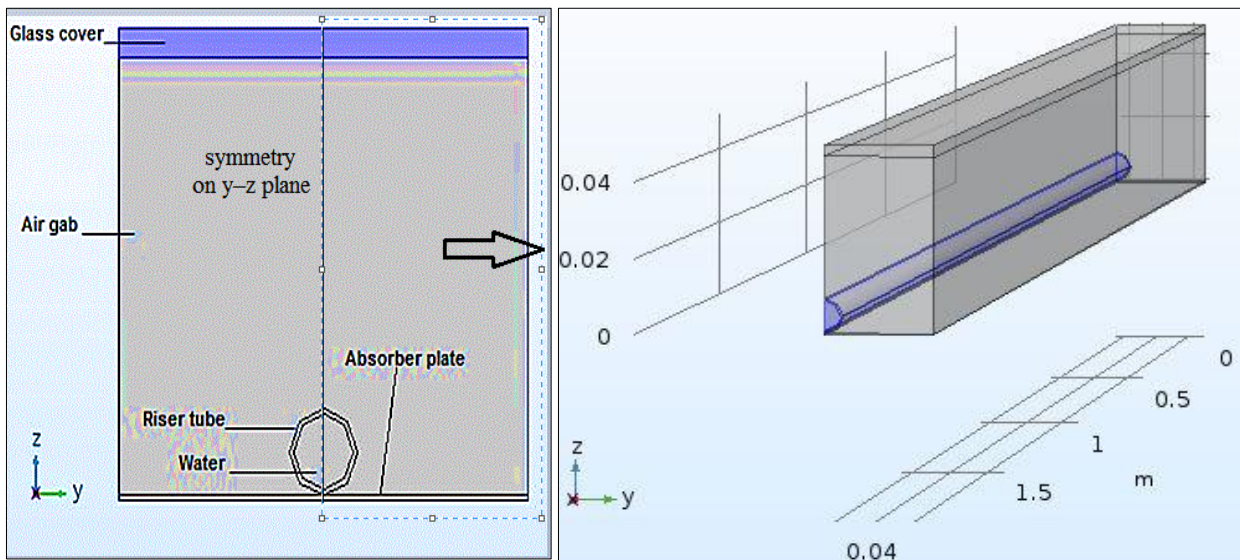
The computational domain of the model is shown in Figure 3.10.

Fig .3.10: Schematic diagram of the CFD model

The boundary conditions are defined as:

1- At the inlet:

   i. $\int \rho.u_{in}dA$ ……….…….…..…….(3.19)

   When $\dot{m}=(0.016667/7)$kg/s

   ii. Inlet water temperature changes continuously with time

   $T_{in} = T_{in}(t)$ ……….…….…..…….(3.20)

2- At outlet:

    i. $P_o = 0$ (Gage pressure)   …………………..….(3.21)

    ii. $\dfrac{\partial T}{\partial x} = 0$ ………..……….…..…….(3.22)

3- At the wall, the no-slip boundary condition was imposed on the walls

         U=0   ...….…….……….…….(3.23)

4- The condition "Symmetry" was assumed on the wall in the middle of the riser tube.

   Normal component of velocity equal zero $u_n = 0$ ...….…..……..…….(3.24)

     $q_{\cdot n} = 0$ ....….…….…..…….(3.25)

5- Initial temperature $T_i = T_{am}(9)$ $at\ 9{:}00\ Am$ …………….…..…….(3.26)

6- Convective heat flux on outer glass cover

     $Q_c = h_c\, A_c (T_g - T_{am}\,(t)\,)$ …....……………….....(3.27)

     $h_c = 5.7 + 3.8 V_{out}\,(t)$ (Kalogirou, 2008)[7]   ………………….…...(3.28)

     Where $V_{out}(t)\ is$ wind speed, which is changing with time taking values from a weather station.

7- Heat absorber by glass cover

     $Q_g = A_c \cdot G(t) \cdot \alpha$ for glass $\alpha = 0.05$.……………..(3.29)

     $where\ G(t) = solar\ irradiance\ (\dfrac{W}{m^2})$

     $A_{c=Aparture}$ area of collector

8- Heat absorbed by the absorber plate

$$Q_{ab} = A_c . G(t) . \alpha_{ab} \quad \text{for glass } \alpha_{ab} = 0.95 \qquad \text{................(3.30)}$$

9- Insulation wall $q._n = 0$ ....(3.31)

3.5.2 The Governing Differential Equations

Many heat transfers process occur in the solar collector, where these processes tend to balance the heat within collector due to exposed the collector to climatic conditions (transient conditions). The solar radiation converting into heat in the absorber and transferring heat from the absorbent to the riser tubes by conduction. Heat is transferred to the water inside the tubes by forced convection. On the other hand, there are losses between the collector and the surrounding. To evaluate the thermal performance of a flat plate collector, the equations of heat transfer, and fluid flow should be considered. These assumptions are taken into account incompressible, laminar, unsteady flow, and the three-dimensional constant-properties viscous Newtonian flow inside a flat plate collector is governed by the continuity, momentum and energy equations.. through the above assumptions, the continuity equation may be written as (Potter and Wiggert 2008)[68]:

$$\frac{\partial u}{\partial x} + \frac{\partial v}{\partial y} + \frac{\partial w}{\partial z} = 0 \qquad \text{.............................(3.32)}$$

The momentum equations in x, y, and z directions can be written as:

$$\frac{\partial u}{\partial t} + \frac{\rho u \partial u}{\partial x} + \frac{\rho v \partial u}{\partial y} + \frac{\rho w \partial u}{\partial z} = -\frac{\partial P}{\partial x} + \mu \left[\frac{\partial^2 u}{\partial x^2} + \frac{\partial^2 u}{\partial y^2} + \frac{\partial^2 u}{\partial z^2} \right] \qquad \text{............(3.33)}$$

$$\frac{\partial v}{\partial t} + \frac{\rho u \partial v}{\partial x} + \frac{\rho v \partial v}{\partial y} + \frac{\rho w \partial v}{\partial z} = -\frac{\partial P}{\partial y} + \mu \left[\frac{\partial^2 v}{\partial x^2} + \frac{\partial^2 v}{\partial y^2} + \frac{\partial^2 v}{\partial z^2} \right] \qquad \text{............(3.34)}$$

$$\frac{\partial w}{\partial t} + \frac{\rho u \partial w}{\partial x} + \frac{\rho v \partial w}{\partial y} + \frac{\rho w \partial w}{\partial z} = -\frac{\partial P}{\partial z} + \mu \left[\frac{\partial^2 w}{\partial x^2} + \frac{\partial^2 w}{\partial y^2} + \frac{\partial^2 w}{\partial z^2} \right] - \rho g z \qquad \text{..........(3.35)}$$

The energy equations for fluid and the structure of collector are as following:

$$\rho \, Cp \left(\frac{\partial T}{\partial t} + u\frac{\partial T}{\partial x} + v\frac{\partial T}{\partial y} + w\frac{\partial T}{\partial z} \right) = k \left[\frac{\partial^2 T}{\partial x^2} + \frac{\partial^2 T}{\partial y^2} + \frac{\partial^2 T}{\partial z^2} \right] \qquad \ldots\ldots\ldots(3.36)$$

3.6 Thermal Efficiency of Flat Plate Collectors:

The thermal efficiency of the collector is the main parameter that describes thermal performance of it; collector performance can be envisioned by an energy balance that shows the distribution of solar energy which turn into useful heat and thermal losses. The solar radiation absorbed by the absorber plate (S) and converted into heat. The heat losses from the collector to the surrounding air by convection heat transfer and radiation can be expressed by the heat transfer coefficient (U_L), efficiency defined as the ratio of the useful heat delivered to the solar radiation incident on the aperture area of collector. The incident solar flux consists of direct and diffuse radiation. While flat-plate collectors can collect both (Deceased and Beckman n.d.)[8].

$$\eta = \frac{Q_u}{G.A_c} \qquad \ldots\ldots\ldots\ldots\ldots\ldots\ldots..(3.37)$$

$$Q_u = A_c[S - U_L(T_{ab} - T_a)] \qquad \ldots\ldots\ldots\ldots\ldots\ldots..(3.38)$$

Where:

$Q_u = $ Useful heat of collector (W).

$G = $ Solar irradiance $\left(\frac{W}{m^2}\right)$.

$Ac = $ Collector area $(m^{2)}$.

$S = $ Absorbed solar radiation (W).

$U_L = $ Overall heat loss coefficient of collector$(\frac{W}{m^2.K})$.

The useful heat can also be calculated from the following equation:

$$q_u = m_f \; cp(T_{in} - T_{out}) \qquad\qquad \dots\dots\dots\dots\dots\dots\dots\dots\dots..(3.39)$$

$m_f = $ Mass flow rate of working fluid in collector $\left(\frac{kg}{s}\right)$.

$T_{in} = $ Temperature of inlet working fluid of collector °C.

$T_{out} = $ Temperature of outlet working fluid of collector °C.

3.6.1 Absorbed Solar Radiation:

To predict the thermal performance of the solar collector, it is necessary to know the amount of solar radiation absorbed by the absorber plate. The solar radiation that falls on the solar collector has three components: beam, diffuse, and ground-reflected radiation. This calculation depends on the radiation model will that used. Using the isotropic model on an hourly basis, calculating absorbed radiation (S) (Kalogirou 2008)[7], by multiplying each term with the appropriate transmittance– absorptance product as follows:

$$S = I_B R_B (\tau\alpha)_B + I_D (\tau\alpha)_D \left[\frac{(1+\cos\beta)}{2}\right] + \rho_G(I_B + I_D)(\tau\alpha)_G \left[\frac{(1-\cos\beta)}{2}\right] \quad \dots\dots..(3.40)$$

$$(\tau\alpha) = \tau\alpha \sum_{n=1}^{\infty}[(1-\alpha)\rho_D]^n = \frac{\tau\alpha}{[1-(1-\alpha)\rho_G]} \qquad \dots\dots\dots\dots.....(3.41)$$

Where

$R_b = $ Beam radiation tilt factor.

$\beta = $ tilt angle of collector (degree).

$I_{B=}$ Beam solar radiation.

$I_{d=}$ *Diffuse solar radiation.*

$(\tau\alpha) \cong 1.01\tau\alpha$

$S = (\tau\alpha)_{av}I_T$

$(\tau\alpha)_{av} \cong 0.96(\tau\alpha)_B$

Absorbed solar radiation $S = I_T\,(\alpha\tau)\,A_c$ ….......…......(3.42)

3.6.2 Tilt Angle Of Flat Plate Collector

The flat plate solar collector is installed on a fixed structure in a southward direction. It is very important to determine the angle of inclination that achieves the highest abundance of solar radiation; the geographic latitude (L) represents the approximate tilt angle of the collector from the horizontal plane. It has been empirically determined that the optimal tilt angle for annual yield can be approximated as shown in equations (3.43) and (3.44) (Kalogirou 2008)[7]:

$\beta = 0.764L + 2.14^{\circ}$ \qquad for L $\leq$ 65° \qquad ………………. (3.43)

$\beta = 0.224L + 33.65^{\circ}$ \qquad for otherwise \qquad ………………. (3.44)

The city of Najaf is located in the geographical latitude (32° 1' N), Therefore, equation (3.43) will be used to find the optimal tilt angle of the solar collector.

3.6.3 Losses Of Solar Collector:

To study the thermal performance of any thermal system it is necessary to determine its thermal losses. In the solar collector, solar radiation falls on the absorbent plate, which converted into thermal energy, part of it moves to the working fluid as useful heat, and the thermal loss is transmitted by various methods of heat transfer from the collector to the surroundings as shown in Figure 3.3. Determination of the thermal losses of a flat solar heater collector has a single glass

cover by creating a network of thermal losses in terms of conduction, convection, and radiation. The different thermal losses from the solar collector can be combined into a simple thermal resistance R_L as shown in Figure 3.11, which represents thermal resistance to heat transfer from the absorber to surroundings (Kalogirou 2008)[7], So the energy losses of the solar collector can be as follows:

$$Q_L = (T_{ab} - T_{am})/R_L = U_L A_c (T_{ab} - T_{am}) \qquad\qquad ....\text{.......}(3.45)$$

Where: $Q_L = Heat\ losses\ from\ collector\ (w)$

$$R_L = Total\ thermal\ resistance\ (\tfrac{W}{°C}).$$

$U_L = U_t + U_b + U_e$ ....(3.46)

Where: U_t = *heat transfer loss coefficient from top of the collector (W/m² K).*

U_b = *heat transfer loss coefficient from bottom of the collector (W/m² K).*

U_e = *heat transfer loss coefficient from edge of the collector (W/m² K).*
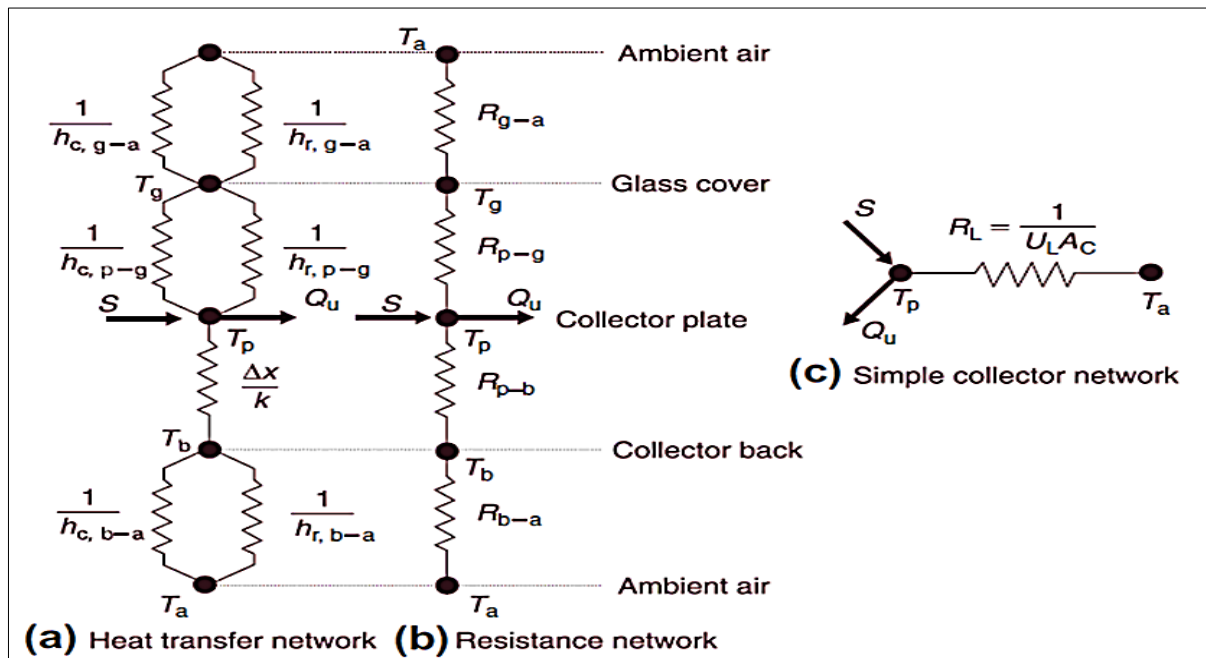
Fig. 3.11: Shows Thermal network for flat plate collector has single-cover in terms of (a) heat transfer by conduction, convection, and radiation ; (b) resistance between parts of the collector; and (c) a single collector network. (Kalogirou 2008)[7]

3.6.3.1 Calculations the Top Heat Loss Coefficient of Collector (U_t)

Heat losses from absorber plate to glass cover occur by convection and radiation. It can use resistances network expression to represent losses. Assuming heat losses from absorber plate to glass cover equal heat losses from glass cover to ambient.

$Q_{t, \text{absorber plate to glass cover}} = Q_{t, \text{glass cover to ambient}}$

$$Q_{t,\text{absorber plate to glass cover}} = A_c hc_{ab-g}(T_{ab} - T_a) + \frac{A_c \sigma (T_{ab}^4 - T_g^4)}{\left[\left(\frac{1}{\varepsilon_{ab}}\right) + \left(\frac{1}{\varepsilon_g}\right) - 1\right]} \quad \text{..........(3.47)}$$

Heat transfer coefficient (hc_{ab-a}) can be determined from nusselt number equation After knowing the rest of the variables.

$$Nu = hc_{ab-a} \cdot \frac{L}{K} \quad \text{..............(3.48)}$$

The value of a Nusselt number can be found according to the following empirical equation(Kalogirou 2008)[7]:

$$Nu = 1 + 1.446\left[1 - \frac{1708}{R_a \cos\beta}\right]^+ \left\{1 - \frac{1708[\sin(1.8\beta)]^{1.6}}{R_a \cos\beta}\right\} + \left\{\left[\frac{(R_a \cos\beta)}{5830}\right]^{0.333} - 1\right\}^+ \quad \text{..........(3.49)}$$

hince

$$(R_a) \text{ Rayleigh numbers} = \frac{g\acute{\beta}P_r(T_{ab} - T_g)l^3}{\nu^2} \quad \text{.................(3.50)}$$

where

g = gravitational constant, = 9.81 m²/s.

$\acute{\beta}$ = volumetric coefficient of expansion; for ideal gas, $\acute{\beta}$ = 1/T.

P_r = Prandtl number.

l = absorber to glass cover distance (m).

v = *kinetic viscosity of air gap (m²/s).*

Then $hc_{ab-a} = Nu.K/L$

But regarding to radiation heat transfer coefficient between absorber plate and the glass cover can be found from following equation:

$$hr_{ab-g} = \frac{\sigma(T_{ab}+T_g)(T_{ab}^2+T_g^2)}{\left[\left(\frac{1}{\varepsilon_{ab}}\right)+\left(\frac{1}{\varepsilon_g}\right)-1\right]} \qquad \qquad ....(3.51)$$

$$Q_{t,absorber\ plate\ to\ glass\ cover} = A_c\left(hc_{ab-a} + hr_{ab-g}\right)\left(T_{ab} - T_g\right) = \frac{(T_{ab}-T_g)}{R_{ab-g}} \qquad ....(3.52)$$

$$R_{ab-g} = \frac{1}{A_{c\left(hc_{ab-a}+hr_{ab-g}\right)}} \qquad \qquad ....(3.53)$$

1- Heat losses from glass cover to ambient by convection and radiation.

$$Q_{t,glass\ to\ ambient} = A_c\left(hc_{g-am} + hr_{g-am}\right)\left(T_g - T_{am}\right) = \frac{(T_g-T_{am})}{R_{g-am}} \qquad ....(3.54)$$

Where:

hc_{g-am} = Convection heat transfer coefficient between the glass cover and ambient due to the wind *(W/m² K).*

hr_{g-am} = Radiation heat transfer coefficient between the glass cover and ambient *(W/m² K).*

$$hr_{g-am} = \varepsilon_g\sigma\left(T_g + T_{am}\right)\left(T_g^2 + T_{am}^2\right) \qquad \qquad ....(3.55)$$

$$hc_{g-am} = 8.6V_{out}^{0.6}/L^{0.4} \qquad \qquad ....(3.56)$$

$$R_{g-am} = \frac{1}{A_c(hc_{g-am}+hr_{g-am})}$$ …..……......(3.57)

Since resistances R_{p-g} and R_{g-am} are in series, their resultant is given by:

$$R_t = R_{ab-g} + R_{g-am} = \frac{1}{U_t A_c}$$ …….......(3.58)

Where heat transfer from the top of the collector can be written as follows:

$$Q_t = \frac{(T_{ab}-T_{am})}{R_t} = U_t A_c(T_{ab} - T_{am})$$ …..…......(3.59)

CHAPTER FOUR

EXPERIMENTAL WORK

CHAPTER FOUR

EXPERIMENTAL WORK

4.1 Introduction

This chapter illustrates the experimental section which will be divided into three parts. The first part explains the construction, the equipment, and the components of the heating system and parts of the flat plate solar heater collector. The second part shows the measurement tools. The third part clarifies the specifications of the practical part and the experimental procedure.

4.2 Experimental Rig

The solar heating system consists of several devices to perform certain functions. The essential part of the system is a flat plate solar water heater it is placed on the roof of the building. The radiator that is placed inside the room to be heated. An electric pump that is circulating the working fluid inside the system. The flowmeter is installed before the collector to control the flow rate and is controlled by the valves. Hot water passes from the solar collector to the radiator via isolated polyethylene pipelines, as shown in Figure 4.1.
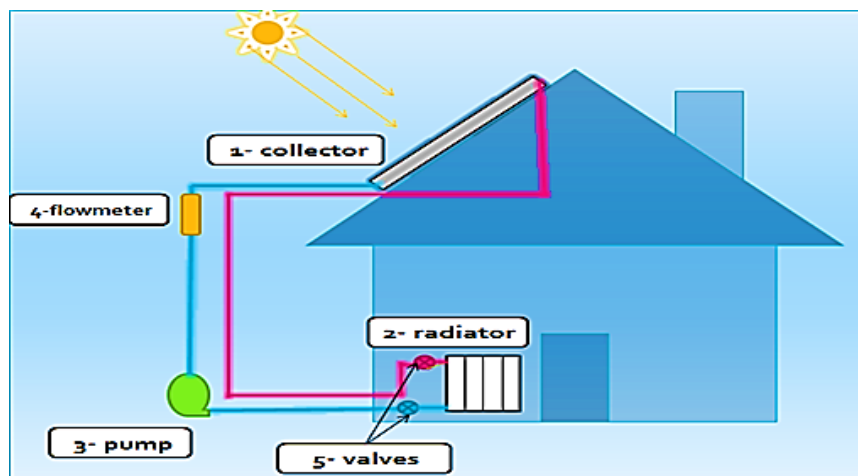
Fig.4.1: Scheme of the experimental rig

4.2.1 Flat Plate Collector (FPC)

Figure 4.2. shows the flat plate collector which was one of the most widely used solar water heaters. It is easy to manufacture from locally available materials, cheap and easy to maintain and is suitable for thermal applications that require medium or low temperatures. The solar heater is the power unit that supplies heat energy for the selected application, where it converts solar energy into heat energy and transfers it to the working fluid.

Fig.4.2: Flat plate collector

Figure 4.3 showed main parts of the flat plate collector (FPC).
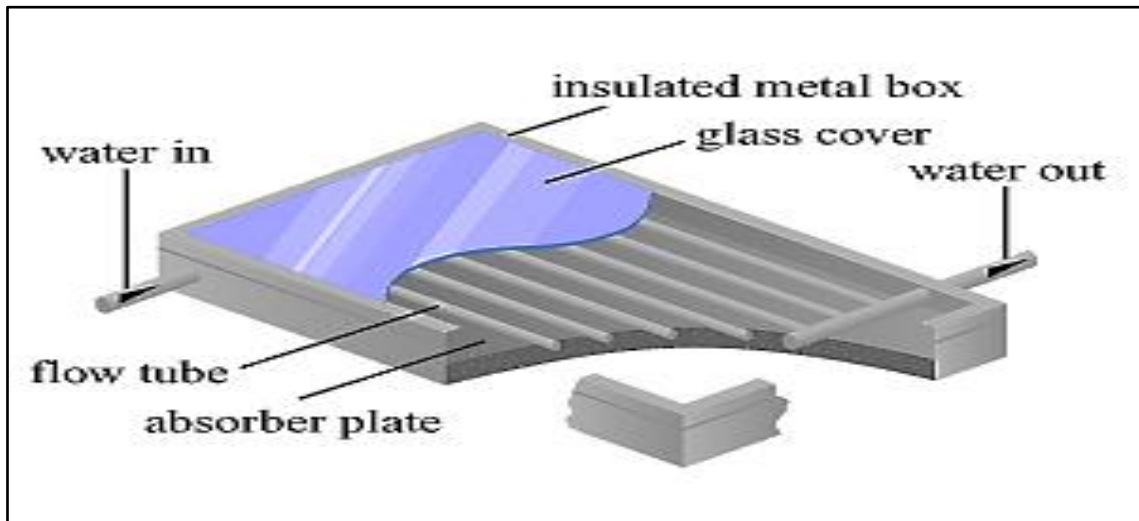
Figure 4.3 Main parts of the flat plate collector

a) **Glass Cover**

Glass is widely used to cover solar heaters because it allows to transmit short-wave solar radiation to exceed 90% and prevents long-wavelength radiation emitted from it. Glass thickness (3.2mm) with low iron content has an advantage in use because it is highly transparent. The other function of the glass cover prevents direct contact between the surrounding air and the absorbent plate, which reduces the losses by convection heat transfer.

b) **Absorber Plate**

The absorber is the essential part of the collector surrounded by insulation from the bottom and edges covered with glass from the top. It converts the solar radiation transmitted across the glass cover into thermal energy. The absorber metal usually has high absorbance with excellent thermal properties such as copper. Moreover, it is coated with a special black paint to increase absorption for short wavelength radiation and low emittance for long-wavelength (selective surface). Riser pipes fixed on the absorber plate by laser welding in parallel, as shown in Figure 4.4. The welding material should be of

high conductivity in order to increase heat transfer from the fins to the pipes. The absorber edges are surrounded by a rubber section (Seal section) that closes tightly the area between the absorber plate and the glass cover and between the insulating and absorber on the other side. It works to prevent air leakage to and from the collector and thus will reduce thermal losses by convection.
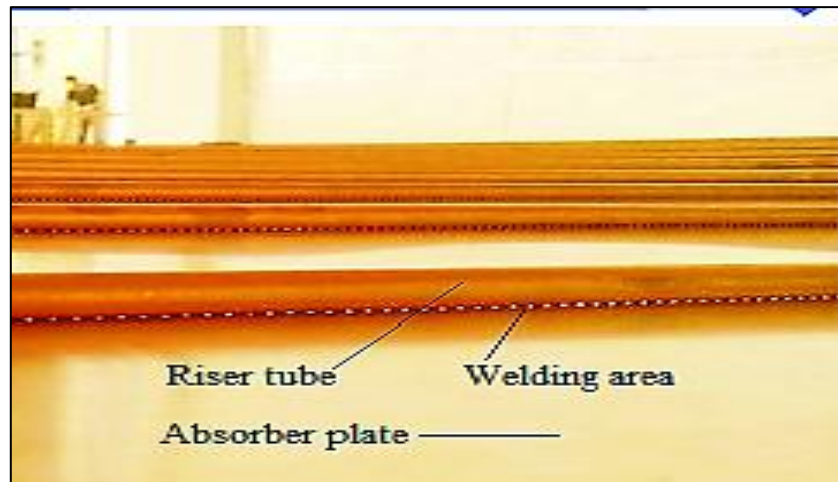

Fig.4.4: shows riser tubes fixed on the absorber plate by laser welding

c) Headers and Risers

Water pipes are usually made of high conductivity material such as copper. The collector contains two header tubes, the inlet header distributes the water on the riser tubes, and the outlet header collects water from them. The riser tubes distributed longitudinally in parallel, as shown in Figure 4.5.
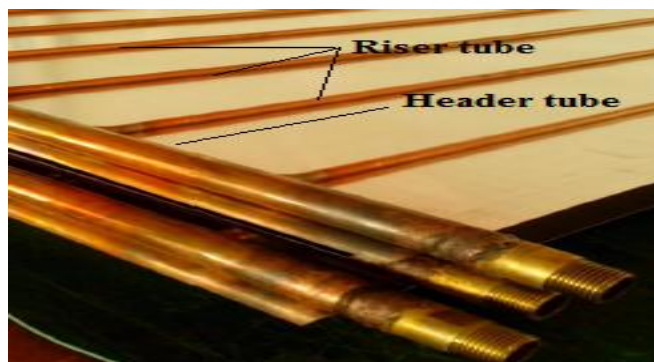
Fig.4.5: Header and riser tube of collector

d) Insulation

The insulating material placed on the back and sides of the collector. It reduces the thermal losses from collector to surroundings. Fiber glass is used for thermal insulation.

e) Container or Casing

Container functions to surround all components of the solar collector and protect them from dust and moisture. It is made from aluminum frame 2mm thickness, and from the back, it is covered with a panel of wood.

Table 4.1 shows the specifications of the flat-plate solar collector.

Table 4.1: The specifications of the flat-plate solar collector

Specification	Details
Dimension of collector	(2000x1000x80) mm
Glass cover thickness	3.2 mm
Transmittance of glass	95%
Aluminum Absorber plate thickness	0.4 mm
Absorber plate absorptivity	95%
Absorber emissivity	5%
Copper header tube diameter	22 mm / 2 headers
Copper riser tube diameter	8 mm / 7 risers
Space between riser tube	110 mm
Fiber glass insulation thickness	30 mm
Fiber glass density	60 kg/m^3
Air gap spacing between glass and absorber	25 mm

4.2.2 Radiator

The radiator is a heat exchanger that transmits heat from the working fluid flowing through it to the room air to be heated. It consists of two front and rear plates, each one contains two manifold and connect between them 30

sub-passages. So it contains two valves to control the flow rate of hot water, as shown in Figure 4.6.

Fig.4.6: The indoor heating radiator

4.2.3 Electric Pump

The electric pump is located between the radiator and the solar collector at the top of the building. The pump circulates hot water directly in a closed system from the solar collector to the radiator.

4.2.4 Pipelines

The parts of the system are connected by polyethylene plastic pipe. Where supplying pipe connected from the collector at the building to the radiator in the room. There is another tube that returns working fluid from the radiator to the collector through the electric pump. The length of the pipes supply and back is long because of the height of the building about (8m). The long distances for the pipes and the zigzag paths led to the appearance of two problems. The first, which caused

increased thermal losses, and by covering the pipes with insulating material to minimize losses. The other problem is the difficulty of water passing through the pipelines due to the blockage of air bubbles inside the zigzag pipes. This problem was eliminated by using air bleeding tubes. Two valves were installed on the supply and return pipes to control the flow rate of working fluid. Outer pipes diameter are 0.5 inches it is covered with insulation then coiled from the outside by thermal tapes, as shown in Figure 4.7.

Fig.4.7: shows the supply and return insulation pipes

4.3 Measurements Devices

Measuring devices are an important role in conducting experiments and synthesizing results during the test period. This research experiments used several measuring devices to connect with the components of the heating system to measure the necessary parameters such as temperature, relative humidity, solar radiation, fluid flow rate, and wind speed. The weather station at the college lab was used to obtain weather conditions during the test days.

4.3.1 Temperatures

The temperatures of inlet and outlet working fluid of the solar collector and the indoor radiator, ambient air and room air are measured to study the performance of the heating system by changing climatic conditions during daylight hours. The temperatures measurements of the collector is done through the use an Applent digital thermometer type (AT-4532x) 64 channel used thermocouples type (T) with accuracy ($\pm 1C^o$) as shown in Figure 4.8, connected to the seven thermocouples. Three thermocouples are installed in three different places on the glass cover; Two thermocouple measures the temperature of the inlet and outlet working fluid of collector. A thermocouple is installed on the side edge, and one is installed behind the collector. As shown in Figure 4.9.

Fig.4.8: Data logger multi-channel thermometer device
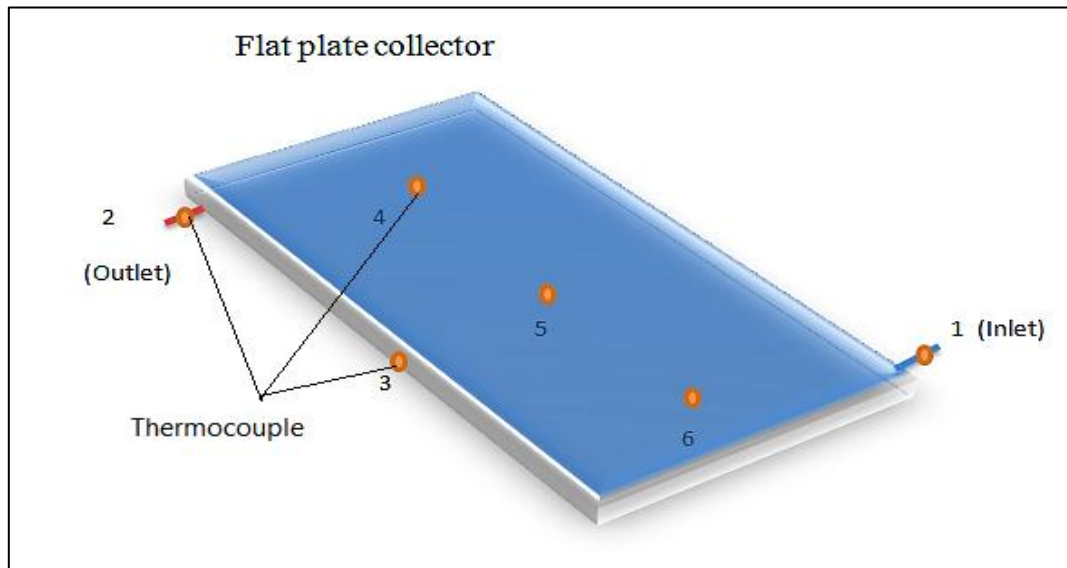
Fig. 4.9: Shows the thermocouple locations on the collector

Another 8 Channel Temperature Data Logger type V2 has range (-55+125 °C) with Accuracy (±0.5°C) as shown in Figure 4.10 was used to measure the indoor room temperature, two thermocouples to measure the inlet and outlet water temperatures of radiator, Five thermocouples were installed in different places on the radiator surface,

Fig.4.10: shows the data logger type V2 Channel Temperature

As for the measurement of ambient air temperature, it was recorded from the weather station located in the laboratory of the Technical College in Najaf.

4.3.2 Solar Radiation

The solar radiation Pyranometer is used to measure the variation of solar radiation during day hours. It is measured by a Tenmars device of the type (TM-207). It is a Taiwanese industry, accuracy (± 10 W/m^2) as shown in Figure 4.11, and the readings were taken every 15 minutes from sunrise to sunset in Iraq, Najaf (31.59^o N Lat., 44.19^o E Long.)

Fig.4.11: The pyranometer device

4.3.4 Wind Speed

Measuring wind speed is important in knowing its impact on the thermal performance of the solar collector. Wind speed readings were taken from the weather station system in the laboratory inside the college, as shown in Figure 4.12.

Fig.4.12: The weather station system

4.3.5 Relative Humidity

Figure 4.13 shows the humidity meter (hygrometer), which measured relative humidity inside the room to determine the change in the value during the heating process and its effect on the comfort of the occupants.
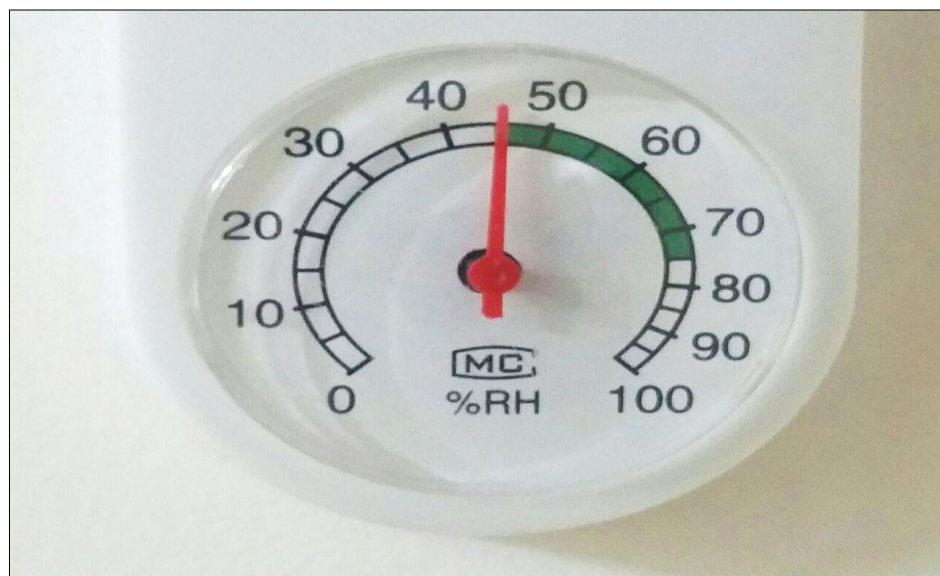
Figure 4.13: The humidity meter (hygrometer)

4.3.6. Flowmeter

Flowmeter device was installed in the inlet pipe of the collector to the measured flow rate of working fluid inlet to the solar collector, as shown in Figure 4.14. The flowmeter has a range of flow rate (0.5-4)L/min.
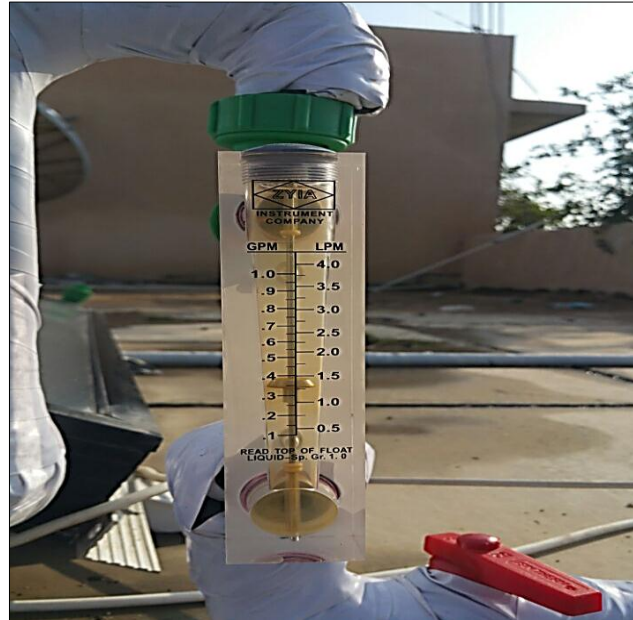
Fig 4.14: shows flowmeter and valve

4.4 Mechanism of The Solar Heating System of the Room

The heating space mechanism by the solar heating system takes place after sunrise. The solar radiation falls on the solar collector and is carried out through the glass cover. After that, the solar radiation falls on the absorber plate where the solar radiation turns into heat energy due to the high absorbance of the absorbed metal, where it leads to a temperature rise of it. The heat then transfer by convection from the absorber to the working fluid, causing a temperature rise of it. The working fluid is circulated from the collector to the radiator via electric pump inside insulated pipes at the recommended flow rate of the solar collector. Then the hot water enters the radiator where the hot water passing through the upper manifold tube of the radiator; then it divided into vertical smaller passages. The hot water

then collects in the bottom manifold pipe to return to the collector. Heat transfer by convection occurs between hot water and radiator surface, and thus a thermal exchange occurs between the radiator surface and the room air via free convective heat transfer and by radiation between radiator surface and the walls of the room. In this process, the room air temperature gradually increases from the initial temperature until it reaches the interior design temperature reaches or below them. Room to be heated has a length of 5 m, a width of 2 m, and a height of 3 m, with one window on the south side with a distance of (1.2*2) m. It contains two doors to have dimensions of (1.3*2) m and the other (1*2) m. Table 4.2 showing the heat transfer coefficient of for room parts.

Table 4.2: showing the coefficient of heat transfer (U) for room parts(Nicklas et al. 2016)[69].

Item	coefficient of heat transfer (U) [W/(m^2 .°C)]
Roof	0.61
Walls	0.68
Windows glass	3.8
Floor	0.03

4.6 The aspects that examined the experimental work

Many factors that affect the performance of the solar heating system, in this work will be suggest to study the impact of weather conditions and the effect of working fluid type.

4.6.1 Study impact of the weather condition on the performance solar heating system

The effect of weather conditions on the thermal performance of a solar heating system was examined. Tested on certain days in three different months to know the performance of the system during varying periods in climatic conditions. This procedure gives a right conception of testing the system during winter and to assess the economic viability of the system over the long term.

4.6.2 Study impact of working fluid type on the performance solar heating system

The type of working fluid has an important effect on improving the thermal performance of a solar heating system. This test aims to reach the best working fluid that enhances the capacity and efficiency of the system and get the best desired result. In this study, water and ethylene glycol-water mixture and engine oil grade (10W-30) were tested because they are considered to be an available fluid with high heat transfer capacity.

These working fluids have different physical properties that make them show different behavior in the test, Tables 4.3, 4.4, and 4.5 it illustrated the physical properties of water and ethylene glycol-water mixture (50-50)% and engine oil.

Table 4.3 Physical properties of liquid Water (Kalogirou 2008) [7]

T (°C)	$\rho \left(\dfrac{kg}{m^3}\right)$	$cp \; (KJ/(kg*C)$	$v \left(\dfrac{m^2}{s}\right)$	$K \; (W/(kg*C)$
0	1002.28	4.2178	$1.788*10^{-6}$	0.552
20	1000.52	4.1818	$1.006*10^{-6}$	0.597
40	994.59	4.1784	$0.658*10^{-6}$	0.628
60	985.46	4.1843	$0.478*10^{-6}$	0.651
80	974.08	4.1964	$0.364*10^{-6}$	0.668
100	960.63	4.2161	$0.294*10^{-6}$	0.680

Table 4.4 Physical properties of ethylene glycol-water mixture(50-50)%
(Propylene and Transfer n.d.)[70]

T (°C)	$\rho \left(\dfrac{kg}{m^3}\right)$	$cp\ (KJ/(kg * C)$	$\mu\ (Pa.sec)$	$K\ (W/(kg * C)$
0	1053.9	3.455	$18.28 * 10^{-3}$	0.327
20	1044.0	3.532	$6.62 * 10^{-3}$	0.341
40	1032.1	3.609	$3.10 * 10^{-3}$	0.353
60	1018.2	3.686	$1.75 * 10^{-3}$	0.362
80	1002.2	3.763	$1.12 * 10^{-3}$	0.367
100	984.1	3.841	$0.79 * 10^{-3}$	0.370

Table 4.5 Physical properties of engine oil grade (10W-30)(Alghamdi 2018)[71]

T (°k)	$\rho \left(\dfrac{kg}{m^3}\right)$	$cp\ (KJ/(kg * C)$	$\mu\ (Pa.sec)$	$K\ (W/(kg * C)$
0	908	1.76	12.23	0.149
20	896	1.83	2.170	0.146
40	884	1.91	0.486	0.144
60	872	1.99	0.141	0.141
80	860	2.08	0.053	0.139
100	848	2.16	0.025	0.137

4.7 Experimental Procedure

The Steps for conducting the experimental work:

1. After connecting the parts of the experimental model with measuring devices, which are:

   a) Two data loggers were used, one is connected with the solar collector and the other is associated with the radiator. The calibration between the thermocouples and the mercury standard thermometer was performed and create the calibration curve, and the calibration equation was found as in Appendix A.

   b) Relative humidity probe: The relative humidity meter was placed inside the room to be heated, and readings were taken every 15 minutes.

c) Solar radiation sensor: The solar radiation sensor is placed in the same tilt angle of the solar collector and readings are taken every 15 minutes.

d) Wind speed measuring: Wind speed measurements were taken from the weather station at the college, and the readings were taken every 10 minutes.

e) Flow rate measuring: Flow rate measurement was taken one time and remain constant through the period test.

2. Most measuring devices would be run to record data from (9:00 am) until (17:00pm) periodically.

3. The thermometer will record the data automatically, while the other devices, the data would be recorded every 15 minutes manually, like solar radiation and relative humidity except wind speed taken for ten minutes.

4. All experiments were conducted at the Technical Engineering College in Najaf, Iraq on months January, February and March, 2019 to study the effect of different climatic conditions on the performance of the solar collector.

CHAPTER FIVE

RESULTS ANS

DISCUSSIONS

CHAPTER FIVE

RESULTS ANS DISCUSSIONS

5.1 Introduction

This chapter presents the results of the theoretical and experimental studies that performed during three months (January, February, and March) 2019 of the outlet fluid temperature of the collector, useful heat, and efficiency of the solar collector, and inlet fluid temperature and useful heat of the indoor radiator. The study included the effect of several parameters on the thermal performance of the solar collector, such as type of working fluid, volume flow rate, and weather conditions. and heating load calculation for the room and finally energy-saving analysis and costs.

5.2 Numerical results

Numerical results were done by using COMSOL multiphysics ver. 5.3 software tool. Simulation studies are necessary to verify the results with previous studies and present experimental results which study the effect of changing flow rate, working fluid type, and weather conditions on performance of a flat plate collector (FPC).

5.2.1 Validation Model

The theoretical study of this work was validated by compared with previous studies. (Ekramian et al. 2014) [23] presented his work numerically and compared with experimental results presented by (Cruz-Peragon et al. 2012) [37] for same parameters and conditions which performed on a flat plate solar collector contains

15 riser tubes. Solar incident irradiation was constant at a value of 936.8 W/m^2. Inlet water temperature, ambient temperature, and water mass flow rate remains constant has values 31˚C, 23.2˚C and 6.42 kg/h respectively. The thickness of glass cover and absorber plate are 4mm and 2mm, respectively. The inner diameter of risers was 10mm, and distance between risers was 30 mm with riser's length of 450mm. Numerical results of E. Ekramian showed that the percentage mean absolute errors between the experimental and numerical results is about 5.5%. In our work, a numerical study conducted on the same solar collector and operation condition presented by Cruz-Peragon. Numerical results were obtained more accurate and approximate to experimental results, and the percentage mean absolute errors of experimental data to numerical results is about 0.062%. As shown in Figure 5.1.
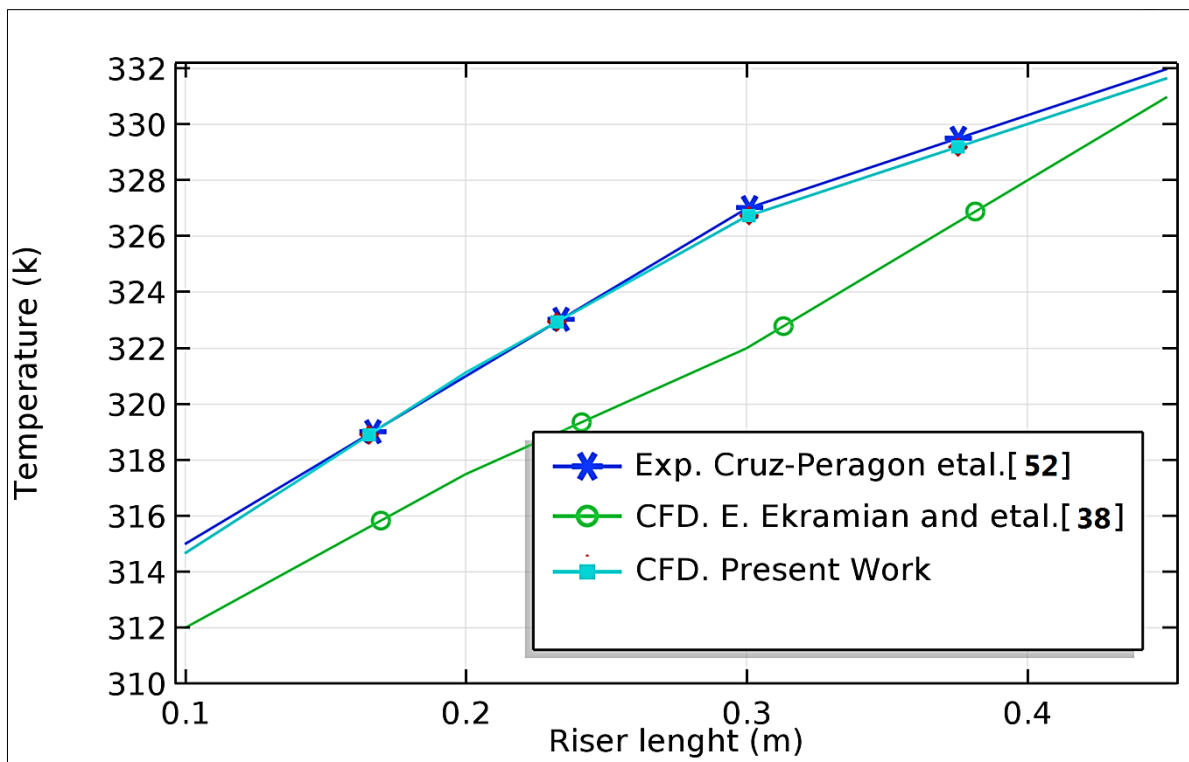
Fig. 5.1: Comparison between experimental and numerical temperature

5.2.2 Effect of the volume flow rate on the performance of a flat plate solar collector

The studies of the effect of variation volume flow rate of working fluid on the thermal performance of solar collector were conducted by using water as working fluid on volume flow rate values (30, 40, 60) L/hr. The weather conditions were chosen on January 9,2019 in each simulation studies which remain same at each variation of volume flow rate in the simulation studies. weather parameters data taken from experimental data recorded from the weather station. Figure 5.2.(a),(b) shows time variation of solar irradiance, ambient temperature, and wind speed on January 9, 2019. The inlet water temperature of the collector was taken from experimental data on the same day, as shown in Figure 5.2 (b). The weather conditions on January 9, 2019 were a clear sky day. The solar radiation was within the average limits and reached the highest of 987W/m². The ambient air temperature has low in the early morning time and gradually increased until it stabilized at about 17˚C. Wind speed was active most of the test time ranged from (1.8-4)m/s.

The numerical results for different volume flow rates indicated there is a clear difference in the outlet water temperature values T_{out} and the temperature difference between outlet and inlet water of collector ΔT, as shown in Figure 5.3 (a),(b). The numerical results under flow rate (30,40,60) L/h gave the highest T_{out} during the test time were 66.3˚C, 60˚C, 53.7˚C, respectively. While the highest ΔT during the Test time was 22.17˚C, 17.16˚C, 9.8˚C, respectively. The results showed that the T_{out} and ΔT values increase when the flow rate of the working fluid decreases and vice versa. About the useful heat, there was a convergence in the results in tests when volume flow rate (30,40) L/hr while there was a significant difference when volume flow rate was 60 L/hr liters as shown in Figure 5.3 (c). The useful heat

values during tests in volume flow values (30, 40, 60) L/hr were 773W, 798W, and 684W respectively.
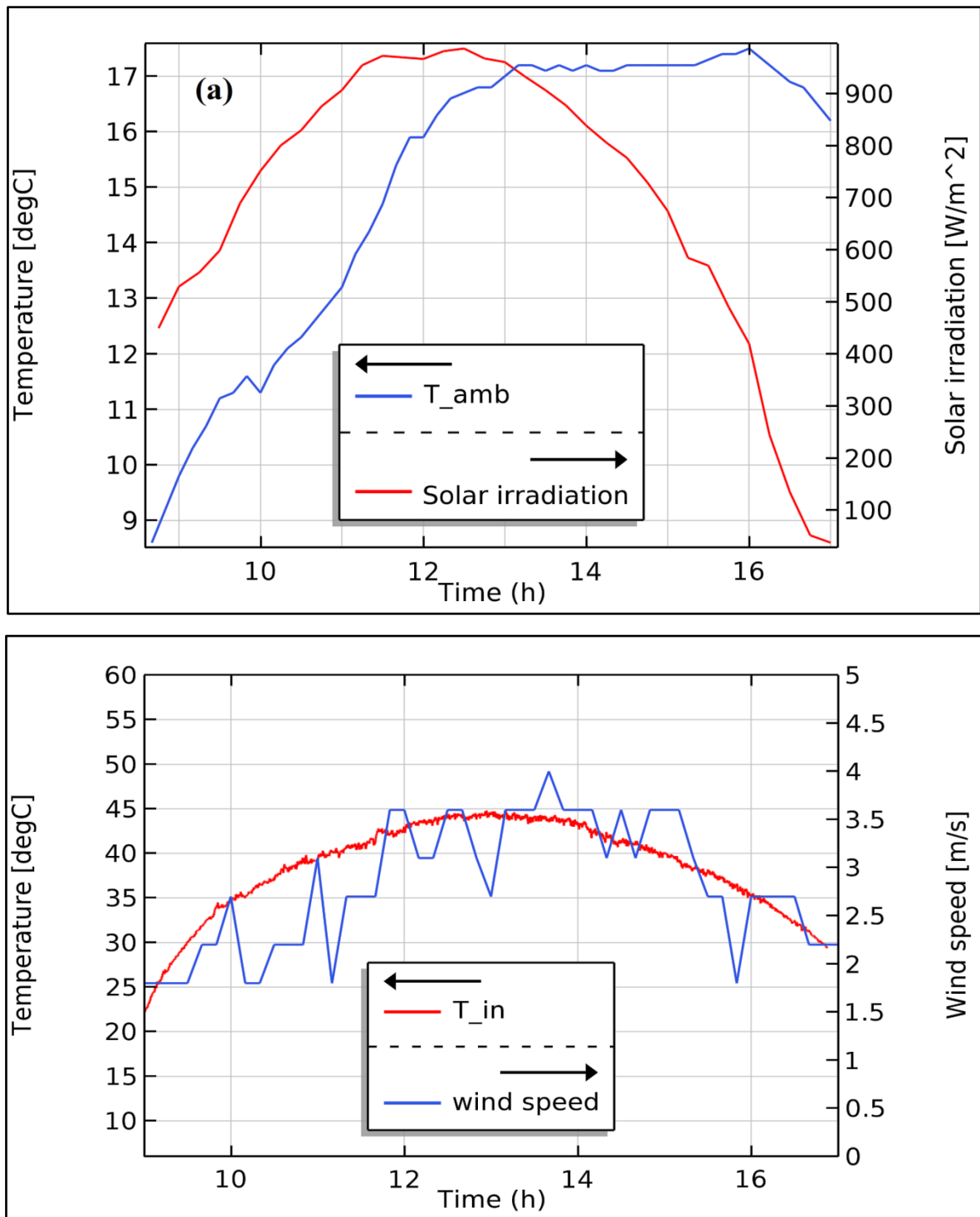

Fig.5.2: Hourly variation for several quantities on 9/1/2019 of (a) Solar irradiance and ambient temperature, (b) Inlet water temperatures and wind speed.
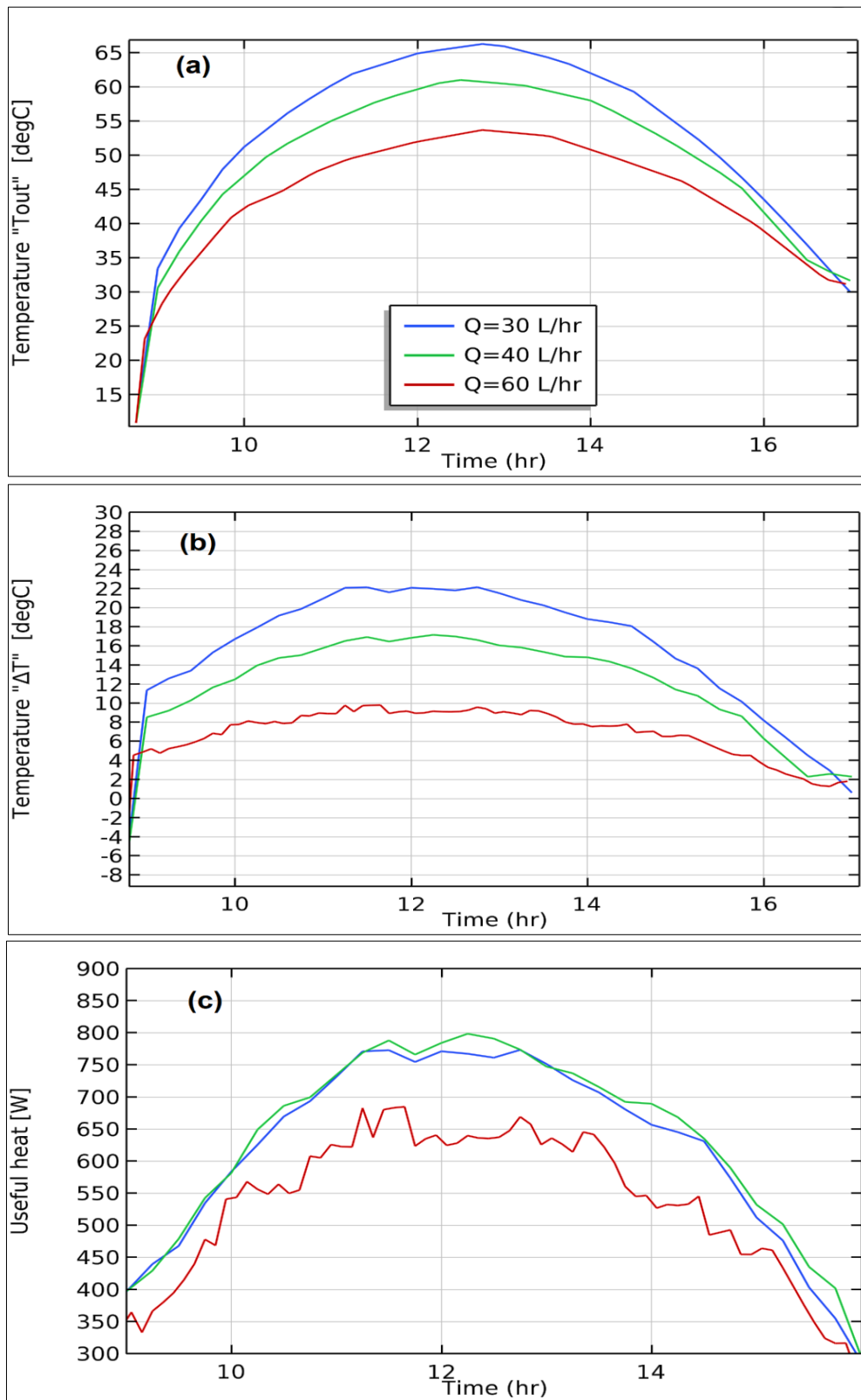
Fig. 5.3 hourly variation of (a) Outlet water temperatures of a collector
(b) temperatures difference between outlet and inlet of water to the collector
(c) Useful heat of collector. (**on January 9, 2019**)

81

5.2.3 Effect of the working fluid type on the performance of a flat plate solar collector

Numerical simulation was conducted to study the effect of the use of various working fluids which are water, ethylene glycol-Water mixture and engine oil grade (10W-30) on the thermal performance of the flat plate collector. study aims to predict the best working fluid to transfer heat from the collector . The same input data of weather conditions on January 9, 2019 are adopted in all studies. The time variation of the weather conditions parameters indicated in Figure 5.2 (a),(b). The inlet working fluid temperature to the solar collector was constant during the test time and was 20 C^o. The working fluid flow rate was 60L/hr in all numerical studies. Figure 5.4 (a),(b) shows time variation of T_{out} and ΔT for different working fluids. Where the highest T_{out} was 41.94˚C recorded in engine oil test. The ethylene glycol-Water mixture test gave the highest temperature of 38.71˚C while the highest temperature recorded in the water test 31.7˚C. The highest ΔT when the engine oil test was 21.94˚C. In the ethylene glycol-Water mixture test, the highest ΔT was 18.71˚C. The water test achieved the lowest ΔT from the rest of the fluids and was 11.7˚C.

For useful heat, the results gave a different behavior than in the T_{out} and ΔT. The results showed that the highest values of useful heat for engine oil, ethylene glycol-Water mixture, and water tests were 727W, 1149W and 819W, respectively as shown in Figure 5.4(c). It was observed that the engine oil, although achieved higher T_{out} and ΔT, but it gave less useful heat compared to other fluids because the specific heat of engine oil is more lower than the specific heat of water and ethylene glycol-water mixture. It noted that the ethylene glycol-water mixture is the effective fluid that is transferring the highest amount of heat compared to other fluids at specific test conditions.
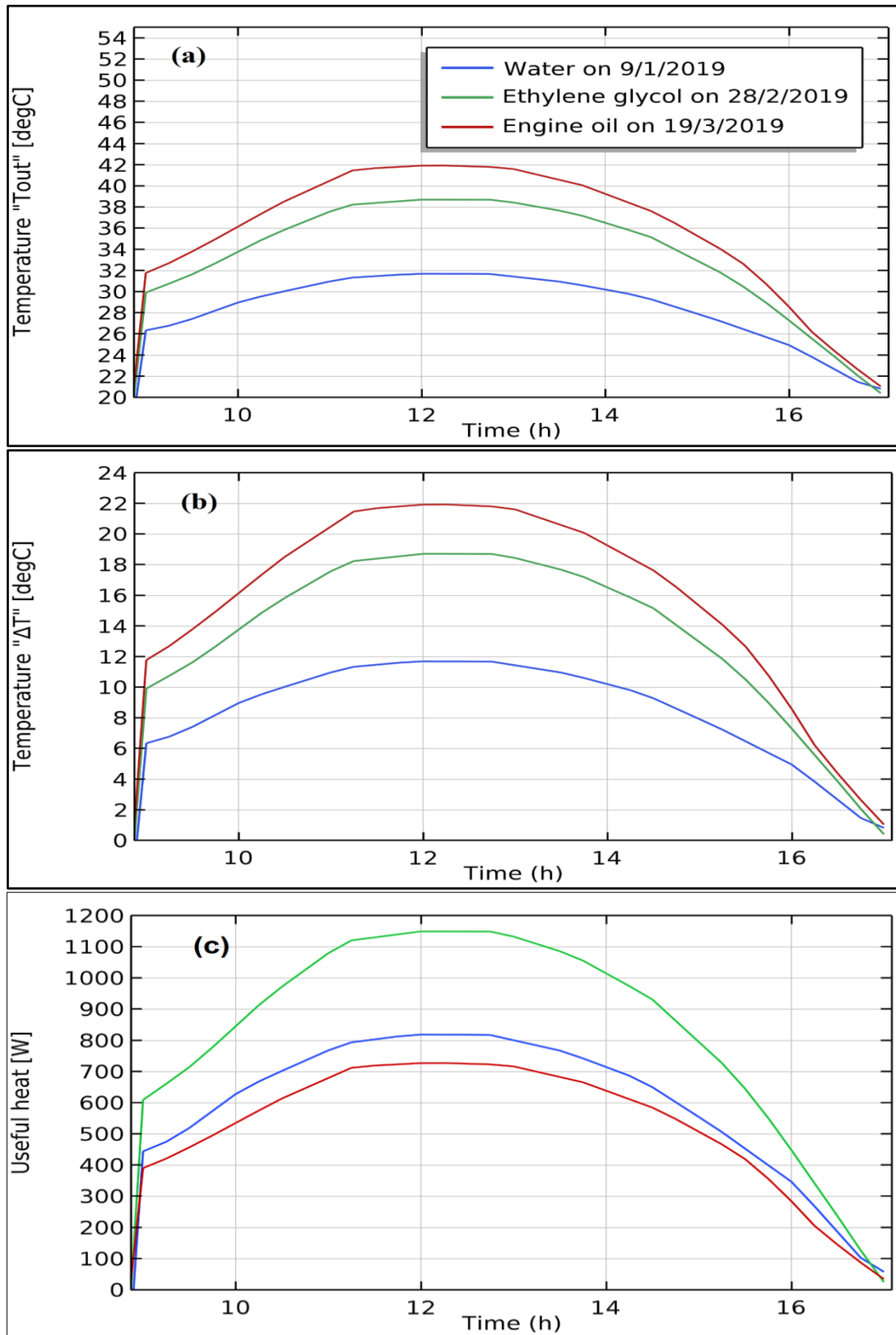
Fig.5.4: time variation of (a) Outlet working fluids temperatures (b) Temperature difference for the fluid inside and outside of collector (c) useful heat of collector

5.2.4 Effect of the weather condition on the performance of a flat plate solar collector

Studying the effect of weather condition on flat plat solar collector by numerical simulation are presented. Climate conditions were chosen for three different days in Najaf city, Iraq. Test days were January 9, February 28 and March19, 2019. Figure 5.5 (a),(b),(c),(d),(e),(f) show the time variation of parameter of weather condition in these days. It was observed that on January 9, 2019 the weather was clear sky day and stable irradiative regime. The wind speed was relatively high, with a significant decrease in ambient air temperature. On February 28, 2019, the weather was clear sky day and stable irradiative regime, and in the afternoon the weather was partly cloudy for intermittent periods, and the wind speed was relatively moderate with a decrease in ambient air temperature. On March19, 2019, the weather was nearly clear sky day and stable irradiative regime, and the wind speed was relatively low, while the ambient temperature was moderate most of the time.

Water was selected as a working fluid in all numerical studies and inlet temperature of it taken constant value which was 20˚C. The water volume flow rate was constant has value 60L/hr in all studies. It is noted that outlet water temperatures are directly affected by changes in the rate of solar radiation, There is an obvious similarity between the variation of outlet water temperature T_{out} and the difference between the inlet and outlet water temperatures of collector ΔT, on the one hand, and solar irradiance falling on the collector, on the other hand.

Figure 5.6 (b) showed there was matching in variation between T_{out} and ΔT during test days; also it noted gap in T_{out} and ΔT on February 28, 2019 near the back mimics the short period with the cloud shadow. The results of the simulation indicate that the lowest T_{out} was on January 9, 2019 because the solar radiation in

this day less than other days and also the relatively high wind speed contributed to increasing the thermal losses of the collector. While T_{out} on February 28 and March19, 2019 was higher than the T_{out} on January 9, 2019 because these days were characterized by relatively high radiation rates and low wind speed and T_{out} were close at most times because of the relative convergence in the climatic conditions in them. The highest T_{out} for January 9, February 28, and March 19, 2019 were 31.7Co, 34.3˚C and 34.95˚C respectively. While the highest ΔT were 11.7˚C, 14.37˚C and 14.95˚C respectively as shown in Figure5.6 (a),(b),(c). As for the useful heat, the maximum values of them are 819W, 1003W and 1043W respectively, as shown in Figure5.6 (d),(e),(f).
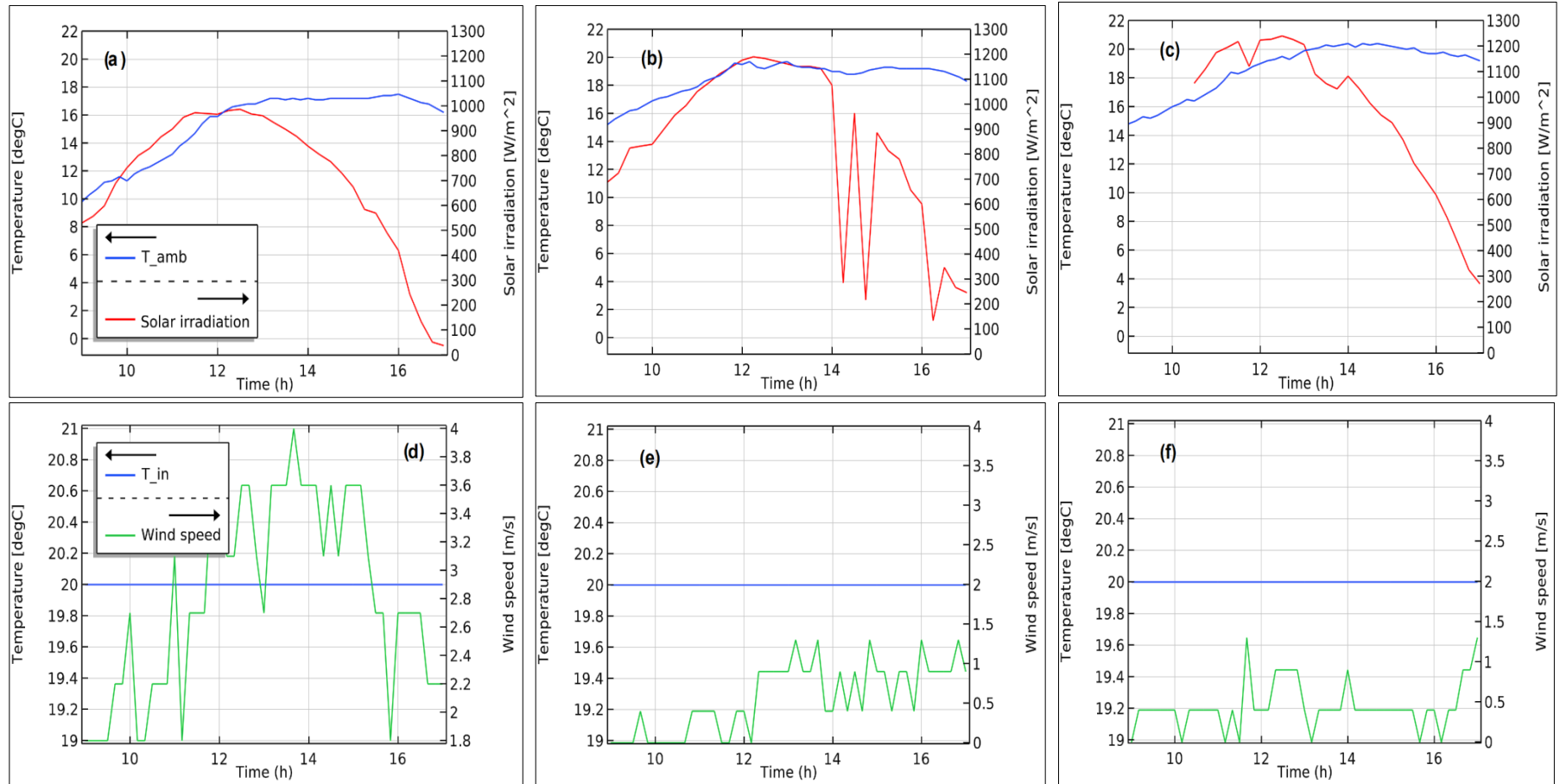
Fig. 5.5: Time variation of solar irradiance and ambient temperature of (a) on 9/1/2019 ; (b) on 28/2/2019 ;(c) on 19/3/2019. and Inlet water temperatures to collector and wind speed (d) on 9/1/2019 ; (e) on 28/2/2019 ;(f) on 19/3/2019.
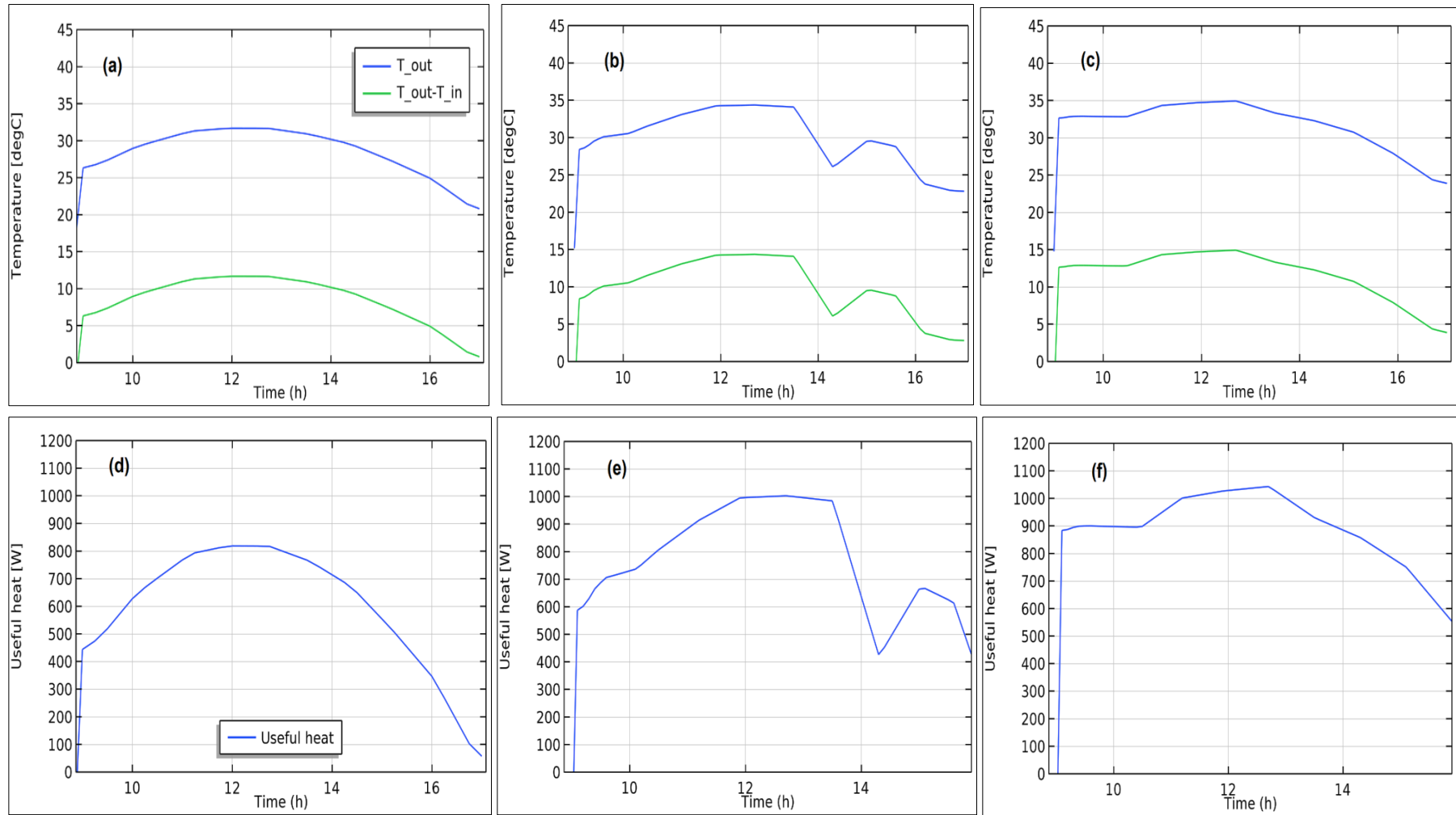
Fig.5.6: Hourly variation of outlet water temperatures and temperatures difference between outlet and inlet water of the collector (a) on 9/1/2019 (b) on 28/2/2019 (c) on 19/3/2019. And useful heat of solar collector (d) on 9/1/2019 (e) on 28/2/2019 (f) on 19/3/2019.

5.3 Experimental results

The solar heating system was tested on several days in winter months in Najaf city. The effect of climatic conditions and testing various operating fluids on the thermal performance of a solar heating system was studied.

5.3.1 Comparison between numerical and experimental results of a flat plate solar collector

A comparative study was carried out between the numerical and the experimental results of the thermal performance of a flat plate solar collector. Numerical studies were conducted during the same days of the experimental tests, which conducted in three days in three different months in winter season of the city of Najaf, Iraq. Various working fluids have been tested in those days to find which is more effective fluid in the thermal performance of the collector. The numerical study conducted in same data used in experimental work such as; weather conditions parameters data for these days, The working fluid type and fluid volume flow rate, which is described in Table 5. Figure 5.5 (a),(b),(c),(d),(e),(f) shows several quantities of solar radiation, ambient air temperature and wind speed, Figure 5.7 showed time variation of inlet water temperature of collector for the three test days.

Table 5.1 shows the details on the tests data

Test no.	test date	working fluid type	volume flow rate (L/hr)
(1)	9/1/2019	water	60
(2)	28/2/2019	Ethylene glycol-Water	60
(3)	19/3/2019	Engine oil	120
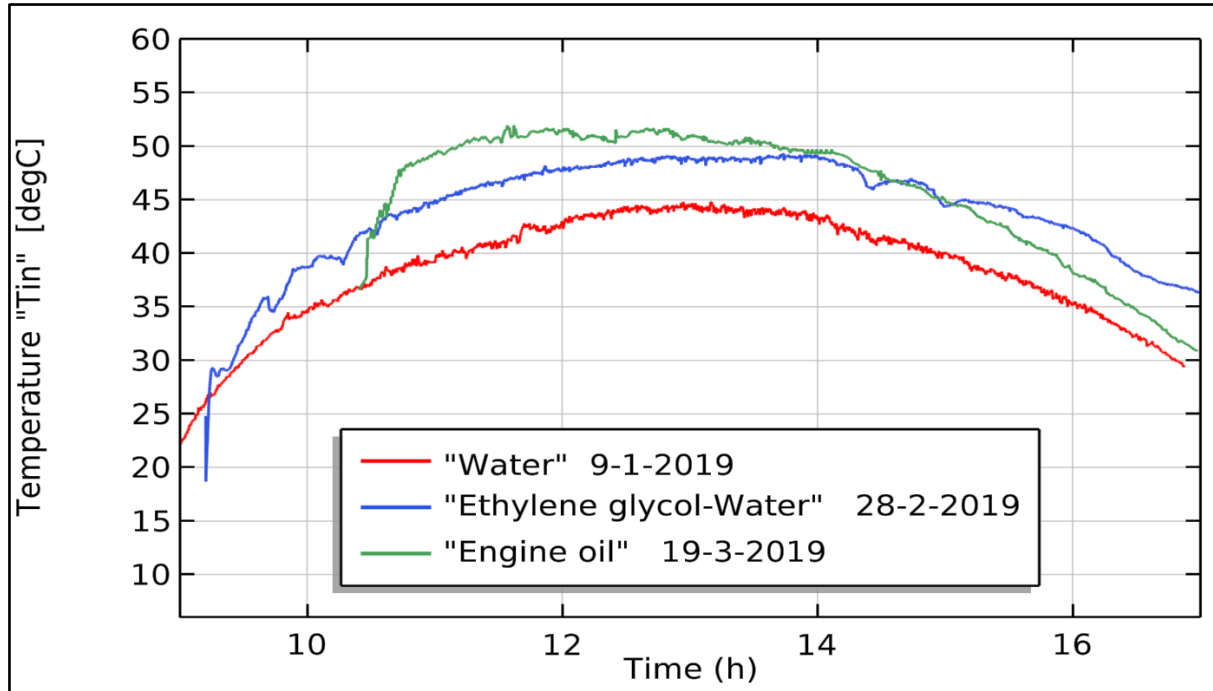
Fig.5.7: Time variation of Inlet fluids temperatures to a collector during days test

Three-day simulation studies using three different working fluids were computed. In this comparison, the focus will be on computing outlet fluid temperatures of the collector T_{out} and the difference between experimental and numerical temperatures, which is an indicator of the amount of error. By studying the simulation results to evaluate the thermal performance of the solar collector for the three days and comparing them with the experimental results during the similar days, it was found that there is acceptable agreement between numerical and experimental results and acceptable accuracy in most tests.

On January 9, 2019 test, The working fluid used was water with a volume flow rate of 60 L/hr. It is noted that the time variation of experimental and numerical temperatures T_{out} was almost identical, and this indicates the high accuracy in solving the numerical study. Time variation of the difference between

experimental and numerical temperatures was ranged between (1.2 to -2.8)°C as shown in Figure 5.8(a)

In the February 28, 2019 test, Ethylene glycol-Water was used as a working fluid with a volume flow rate of 60L/hr .The computed and measured temperatures were usually convergence and spread slightly in a few times, as shown in Figure 5.8(b) The difference between experimental and numerical temperatures ranged from (4.8 to   -6.85) °C.
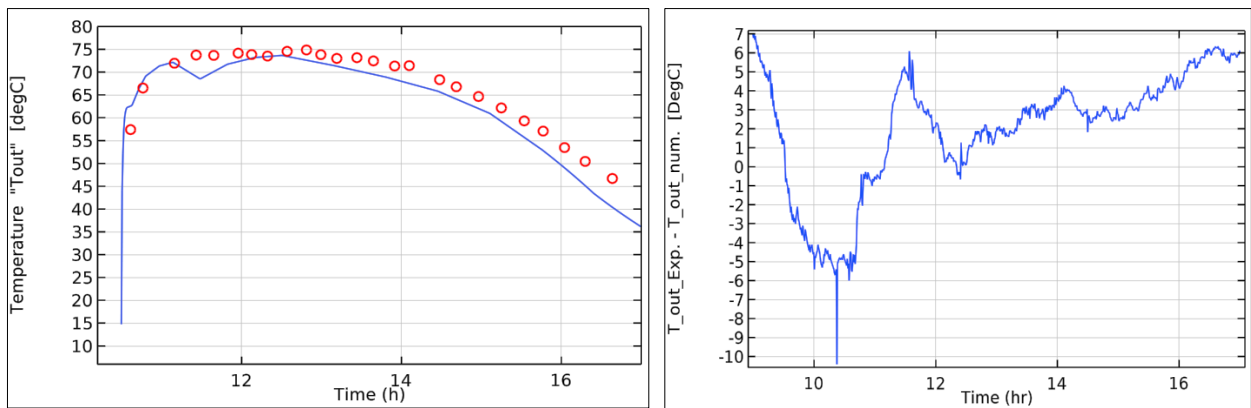
Finally, on March 19, 2019, the engine oil used as a working fluid, and the volume flow rate was 120 L/hr. The hourly variation of numerical and experimental temperatures was identical before noontime and then slightly diverged in the afternoon, as shown in Figure 5.8(c), the difference between experimental and numerical temperatures ranged from (7 to -6)°C.
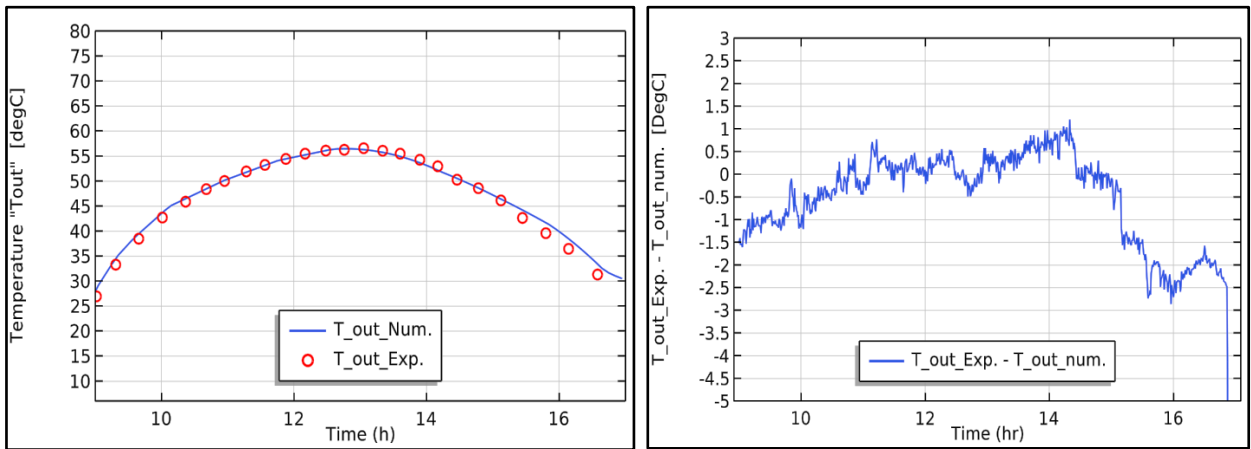
(a)
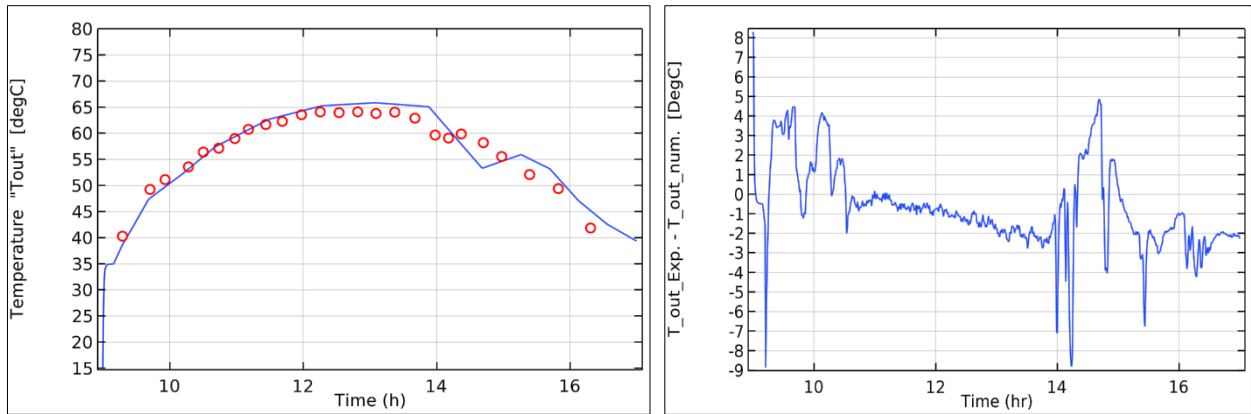
(b)

(c)

Fig. 5.8 shows time variation of experimental and numerical T_{out} of collector and difference between experimental and numerical temperatures of (a) on January 9, 2019(b) on February 28, 2019 (c) on March 19, 2019.

5.3.2 Effect of the weather condition on the performance of a flat plate solar collector

Experimental tests were conducted to study the effect of the weather conditions on the performance of the flat plate collector solar water heater. Four different days were selected to done these tests, which on (January 9,20) and (February 20,24), 2019. The weather data were recorded during test days from the weather station system and portable measuring instruments, where it recorded the solar radiation, wind speed, and ambient air temperatures. Figure 5.9 shows solar radiation during test days. Figure 5.10 and Figure 5.11 show the hourly variation of wind speed and ambient air temperatures during the test days.
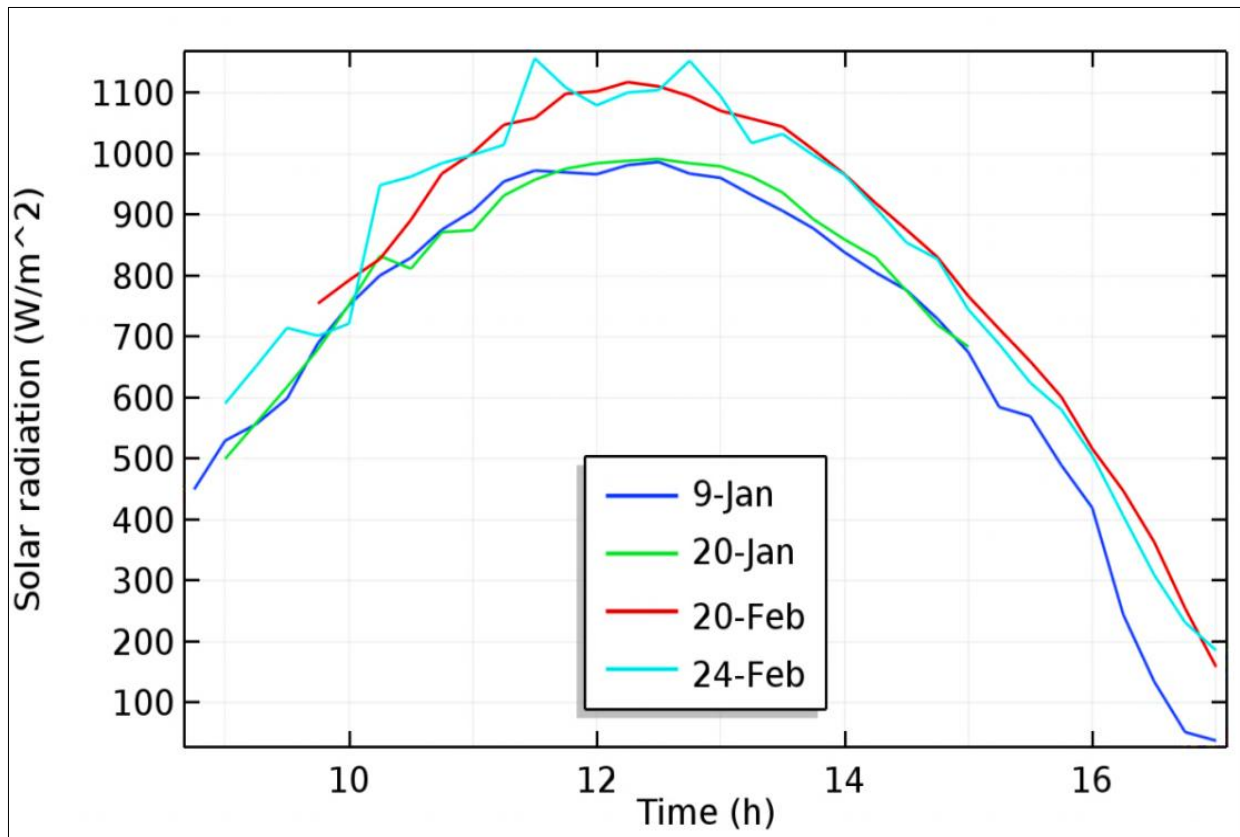
Fig.5.9: Hourly variation in solar irradiance during testing days
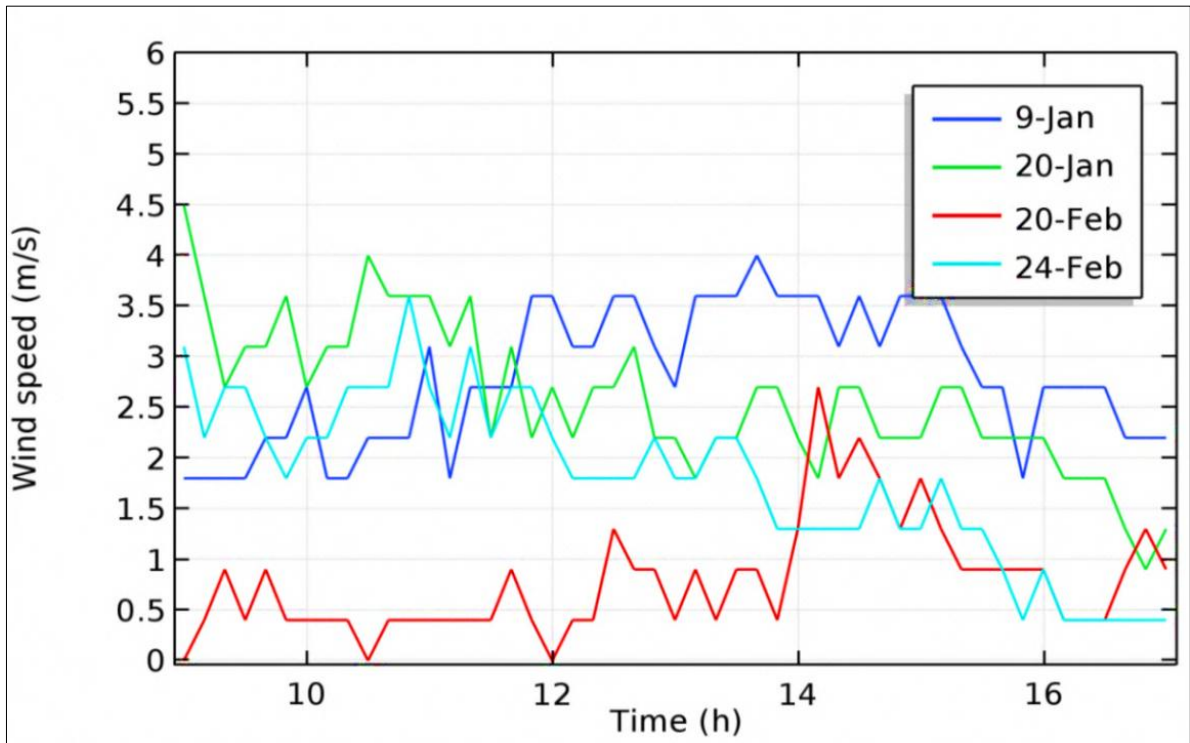
Fig. 5.10: Hourly variation of wind speed during testing days
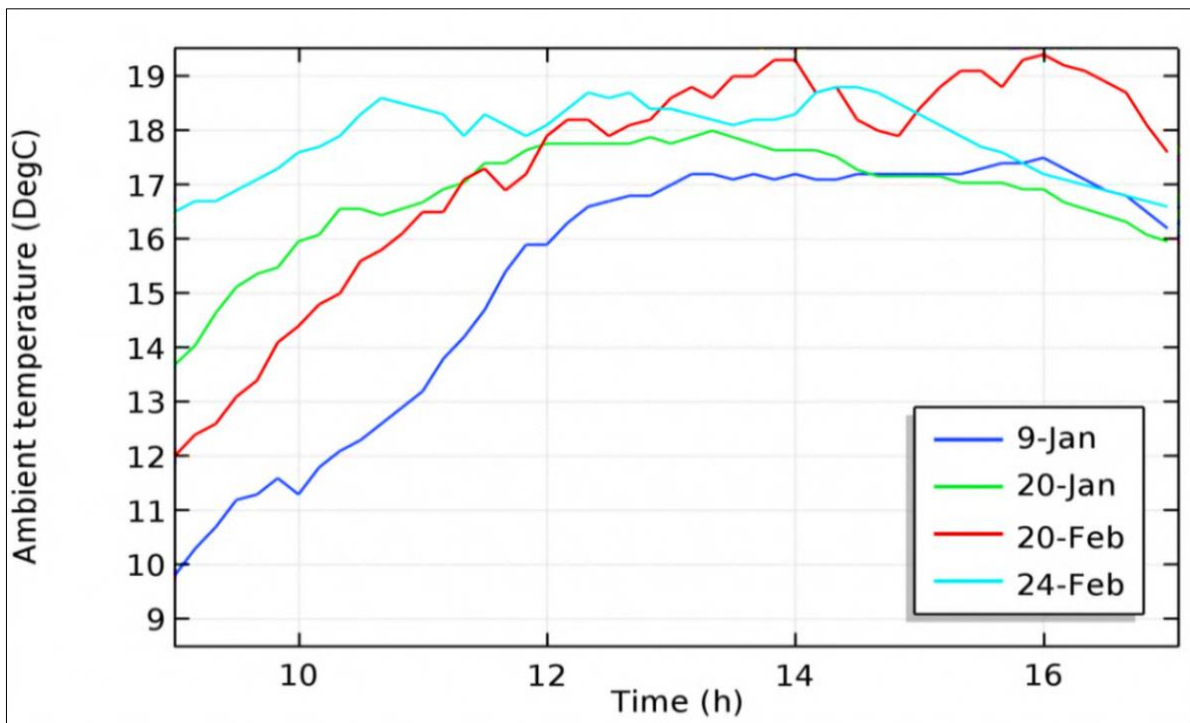
Fig.5.11: Hourly variation of ambient air temperatures during testing days

The heating system was tested in most days from 9:00 am to 5:00 pm. the working fluid used was water. The volume flow rate was 60L/hr in all days, except on 20 January, the volume flow rate was 30 L/hr. Figure5.12 shows time variation of outlet water temperatures T_{out} and the temperature difference between outlet and inlet water ΔT of solar collector. There is a remarkable similarity between the variation of T_{out} and ΔT on the one hand and variation of solar radiation on the other hand. The results showed the T_{out} was convergent on January 20 and February 20,24, 2019 between the hour 12:30 and 13:30 pm, where the highest T_{out} for these days was 64.6°C,64.7°C, and 64.5°C Respectively. On February 20,24,2019 variation in T_{out} were close because variation in solar radiation was convergent. While on February 20, 2019 variation in T_{out} was close to the previous two days, although the solar radiation was significantly less, because of the volume flow rate was lower than the previous two days. While on January 9, 2019 the highest T_{out} was 57.1°C. It was noted that time variation of ΔT for days on January 9 and February 20,24, 2019, were almost identical in values during most hours of the day and reached the highest value of 12.7°C, 13.9°C, and 13.8 °C respectively. While on 20 December 2019, ΔT was twice as high as the other days and its greatest value was 24.5°C, This is a big difference in temperature because the volume flow rate of working fluid in this day was lower than other days, which was 30L/hr while the volume flow rate in other days was 60L/hr. This difference is beneficial to compare solar heaters and represents an indicator of the thermal performance of the solar heater.

From above, it was noted that the most important climatic factors that affect the change of water temperature are solar radiation, which is the source of thermal energy in the solar collector. The ambient air temperature and wind speed contribute to increase and decrease the thermal losses of a collector.
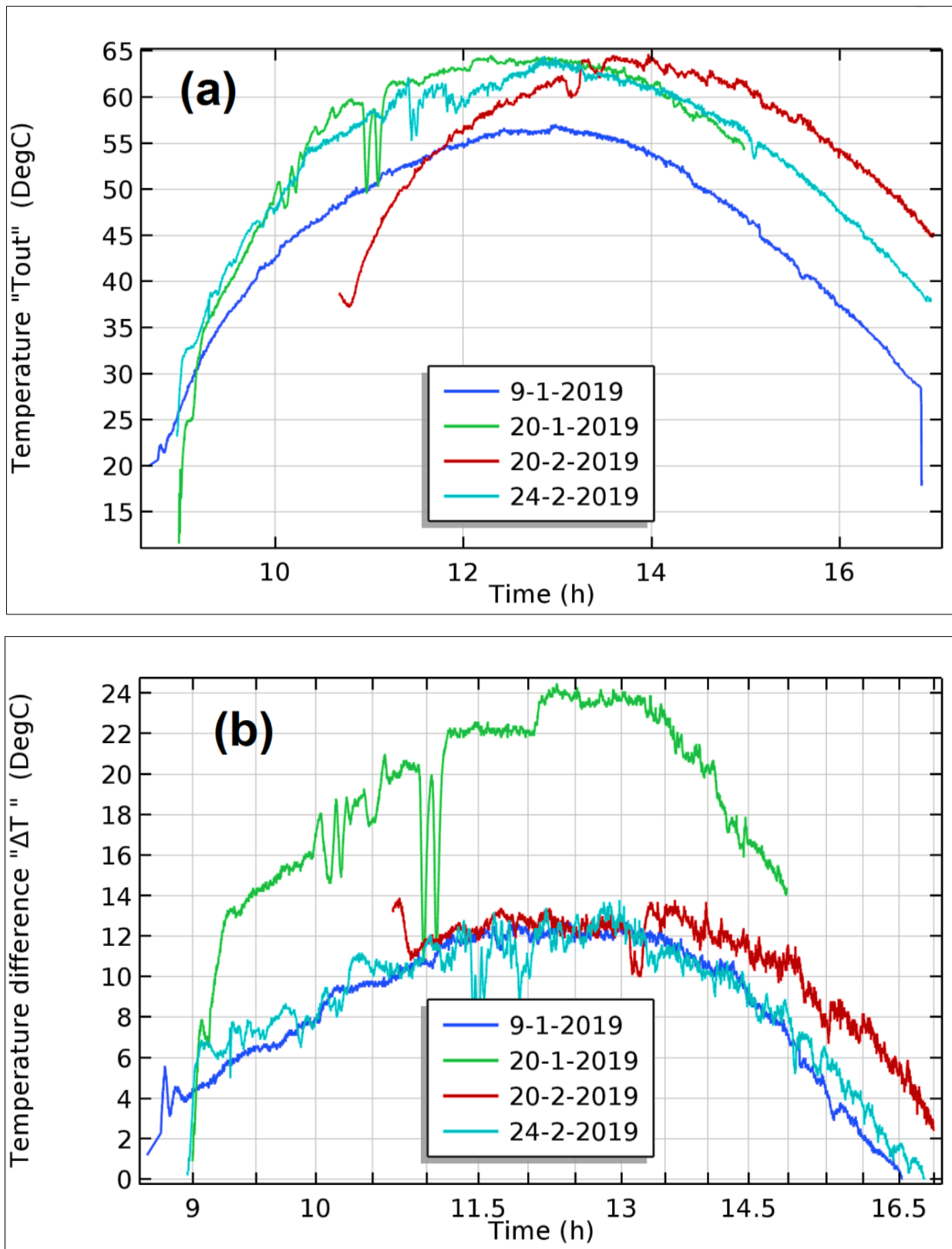
Fig.5.12: Hourly variation of (a) outlet water temperatures (b) temperature difference between outlet and inlet water of the solar collector during testing days

Figure 5.13 shows hourly variation of useful heat of the flat plate solar heater collector calculated from the experimental data of the temperature recorded for the water inlet and outlet of the solar collector. The hourly variation of useful heat of a flat plate collector during the test days on January 9,20 and February 20,24, 2019 reached the highest values during the test period are 886.3W, 854.85W, 956.1W and 963.1W respectively. The useful heat is directly affected by changes in solar radiation during the test time because they are produced by the heat generated in the absorbent part inside the solar collector due to solar radiation falling on it minus the thermal losses from the collector.
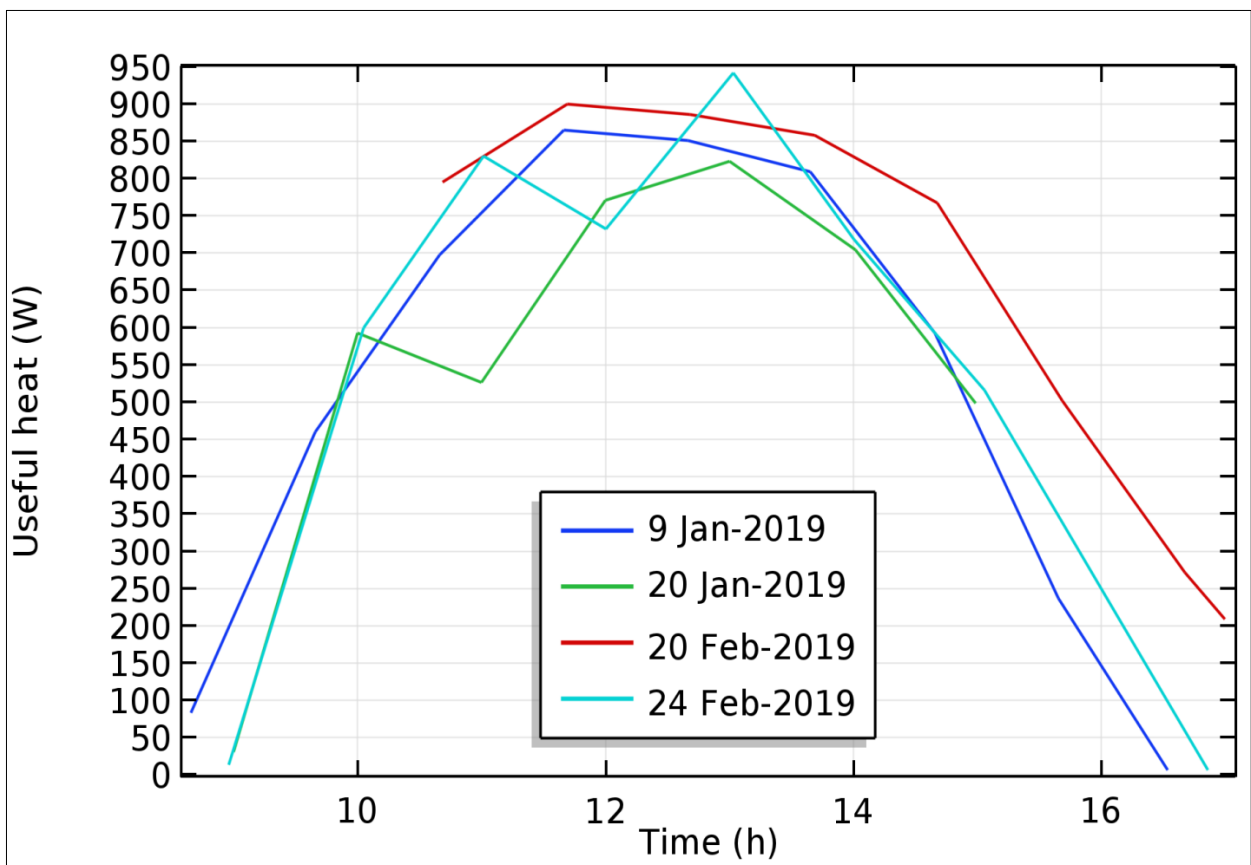
Fig.5.13: Shows hourly variation of the useful heat of the collector during testing days

Figure 5.14 shows the time variation of the thermal efficiency of the flat plate solar collector during the four test days. The thermal efficiency values of the solar collector were calculated for the test days on January 9,20 and February 20,24, 2019, and highest values reached 50.52%, 47.37%, 47.39%, 46.78% respectively.

The highest thermal efficiency value recorded on January 9, 2019 reached 50.52 %. Although the solar radiation rate was lower than other days, The wind speed rate was higher, and the ambient air temperature was lower than the rest of the test days. Because the thermal losses on January 9, 2019 were less than the other days and this can be deduced from knowing the difference between the average temperature of the glass cover of the collector and the temperature of the surrounding air where it reached its value of 5.8˚C at 1:00 pm. While the value of this difference reached 17.4 ˚C at 1:00 pm on February 24, 2019. This difference in temperature contributes to increased thermal losses by convective heat transfer and radiation between collector and surroundings., This shows that the thermal losses on February 24, 2019 were high and contributed to reducing the efficiency of the collector even though the weather conditions were better. In any case, the thermal efficiency of the solar heater was convergent in values , and all were below 50%. This gives an essential indication that thermal losses in the collector are large and exceed half of the input energy, and this is a disadvantage of flat plate solar collector.
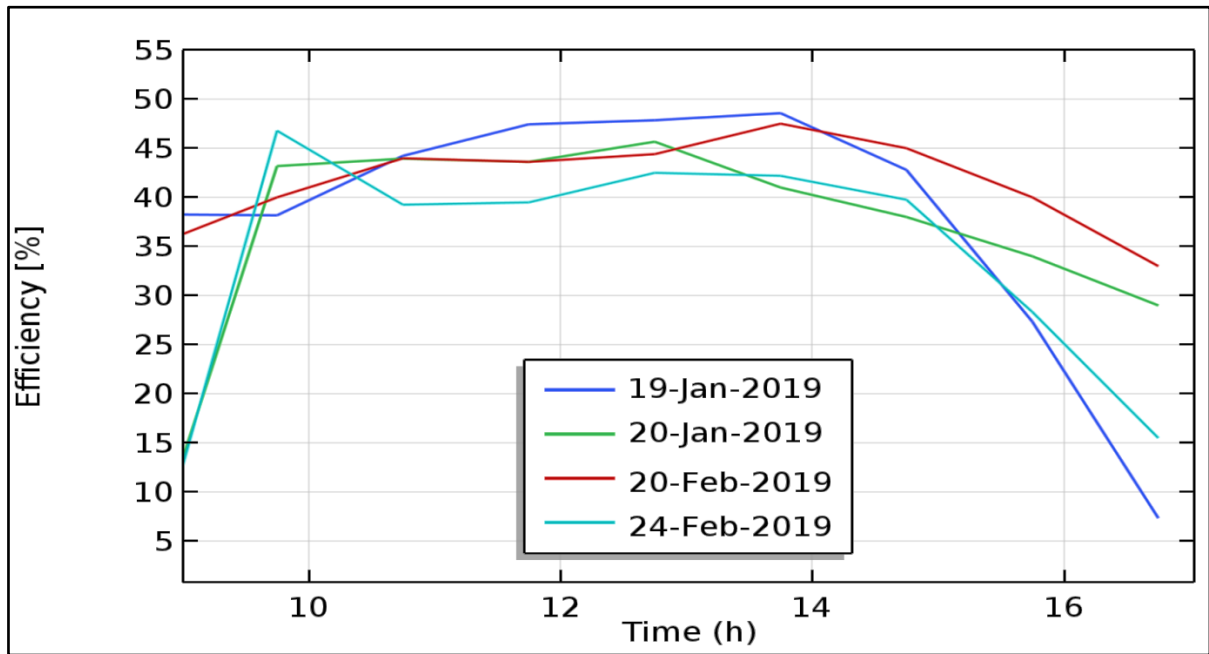
Fig.5.14: shows the thermal efficiency of the flat plate solar collector during the
test days.

5.3.3 Effect of the weather condition on the performance of the indoor radiator

The performance of the radiator inside the room is directly affected by changes in weather conditions parameters because its work is directly related to the solar collector. Figure 5.15 shows the time variation of inlet water temperature T_i of the radiator during the four test days.

It was noted that the highest Ti during the test days was 57.4°C at 12:55 pm on February 20, 2019, and the lowest temperature of 51.6°C at 1:02 pm on January 9, 2019. Figure 5.16 shows time variation of the temperature difference of inlet and outlet water of radiator ΔT, The results showed convergence in ΔT for the days of January 9, 2019, and February 20,24, 2019, the highest values are were 8.5°C, 9.7°C, and 9.3°C, respectively.
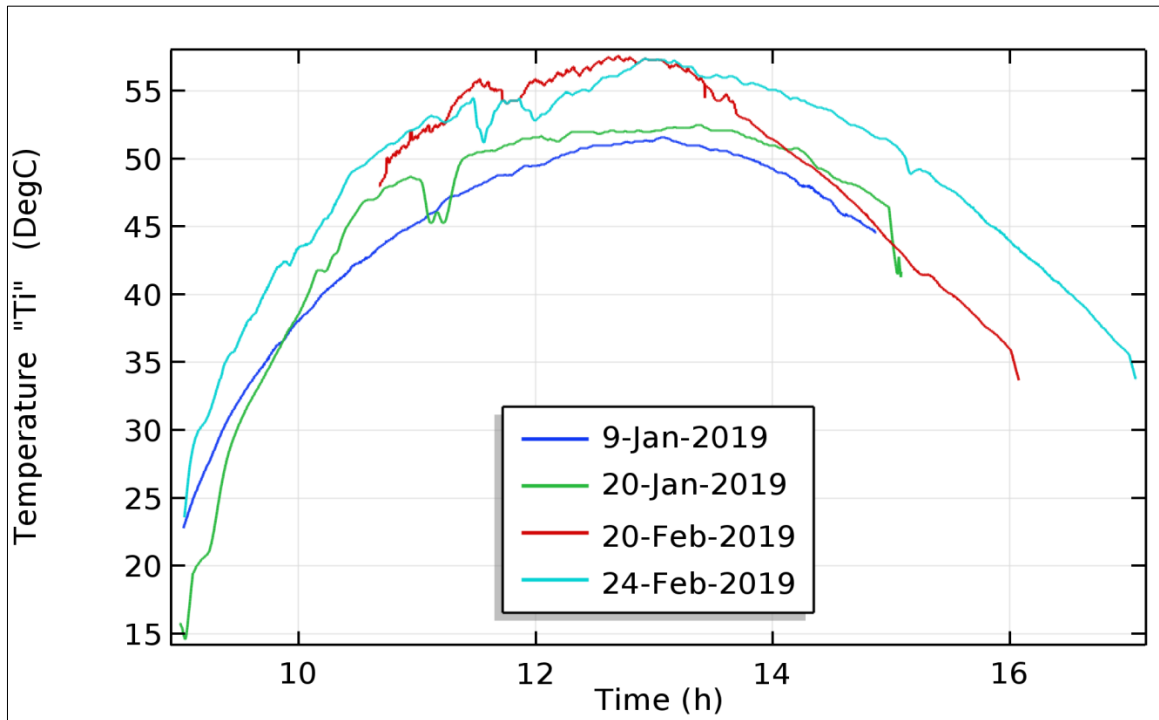
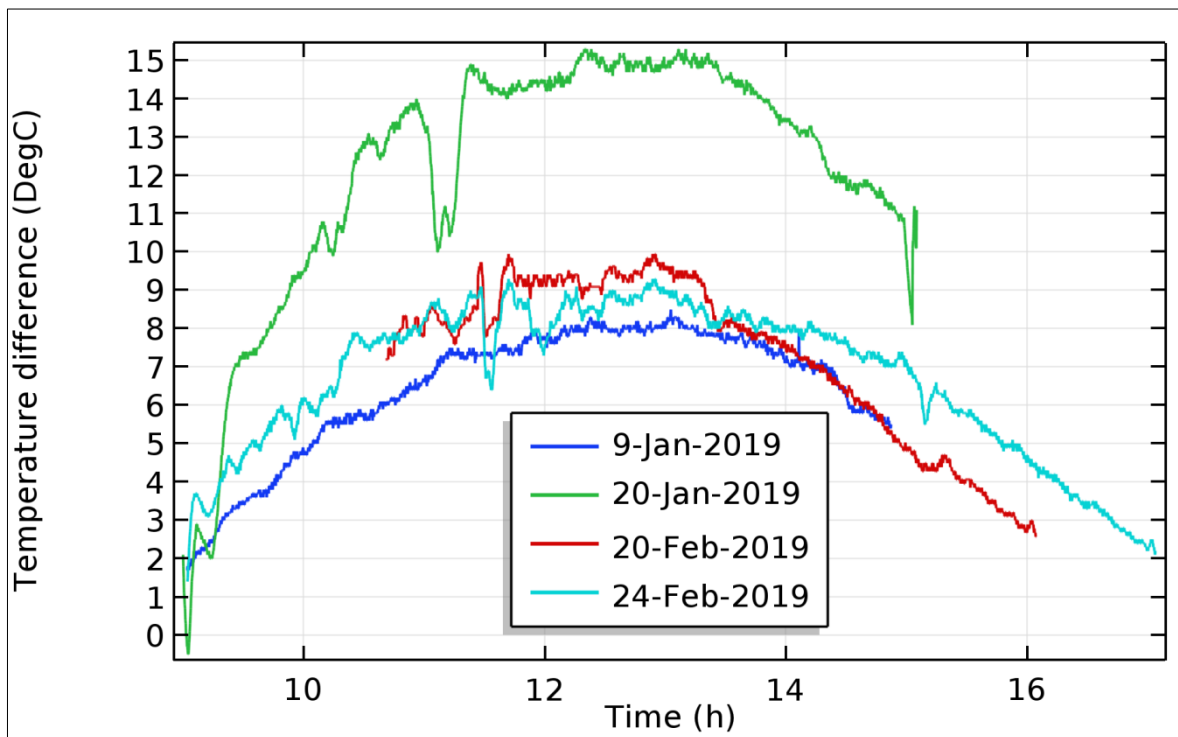Fig. 5.15: shows the inlet water temperature of the radiator during the test days

Fig.5.16: Shows hourly variation of the temperature difference

of the outlet and inlet water of the radiator during testing days.

While on January 20, 2019 the highest ΔT was reached 15.3°C at 12.21pm, The reason that the flow rate of the working fluid was 30L/hr while in other days was 60L/hr, where the slower flow allows for more considerable heat exchange time, which makes the temperature difference for working fluid inlet and outlet is higher and vice versa.

Figure 5.17 shows the useful heat of the radiator during the four test days; Results showed that the useful heat for the test days on January 9,20 and February 20,24, 2019 were somewhat convergent during the day, and the highest values during the days of the test are 593.15 W, 533.84W, 587.3W, 571.33W respectively. It was noted that the useful heat on January 20, 2019 was lower most of the time compared to other days, although the test of this day achieved the highest T_i and ΔT, due to the system operation with volume flow rate of 30 L/hr, which is considered slow relatively. While other days was 60 L/hr in, This significant difference in volume flow rate overcame the increase in temperature to achieve higher useful heat.
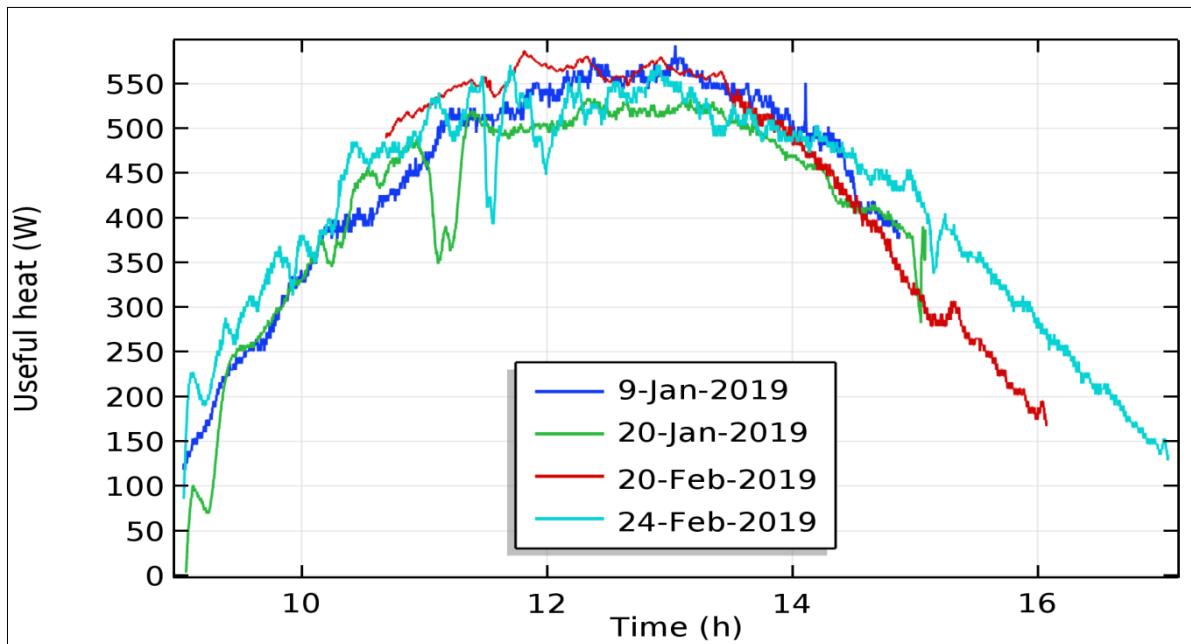

Fig.5.17: Shows hourly variation of the useful heat of the radiator during the test days.

5.3.4 Effect of the weather condition on the heating load of the room

Heating load calculations were carried out for the room to be heated during the four test days. These calculations require knowing the internal conditions of the room as well as weather conditions for all test days. One of the basic parameters for performing heating load calculations is dry bulb temperature and relative humidity or wet bulb temperature inside and outside the room. Internal design conditions should be suitable for the health and comfort of occupants in the room, which has been considered the dry-bulb temperature of 25℃ and relative humidity 50%. As for outside conditions, weather condition parameter is continually changing as they relate to weather changes. Weather condition data were recorded from weather station during the test days, Figure 5.11 showed the hourly variation of ambient air temperatures, which represent dry bulb temperature during testing days. Figure 5.18 shows the hourly variation of outdoor relative humidity values during periods of the test days. The recorded data showed that the relative humidity rates are high at the beginning of the morning and then gradually decrease during daylight hours.
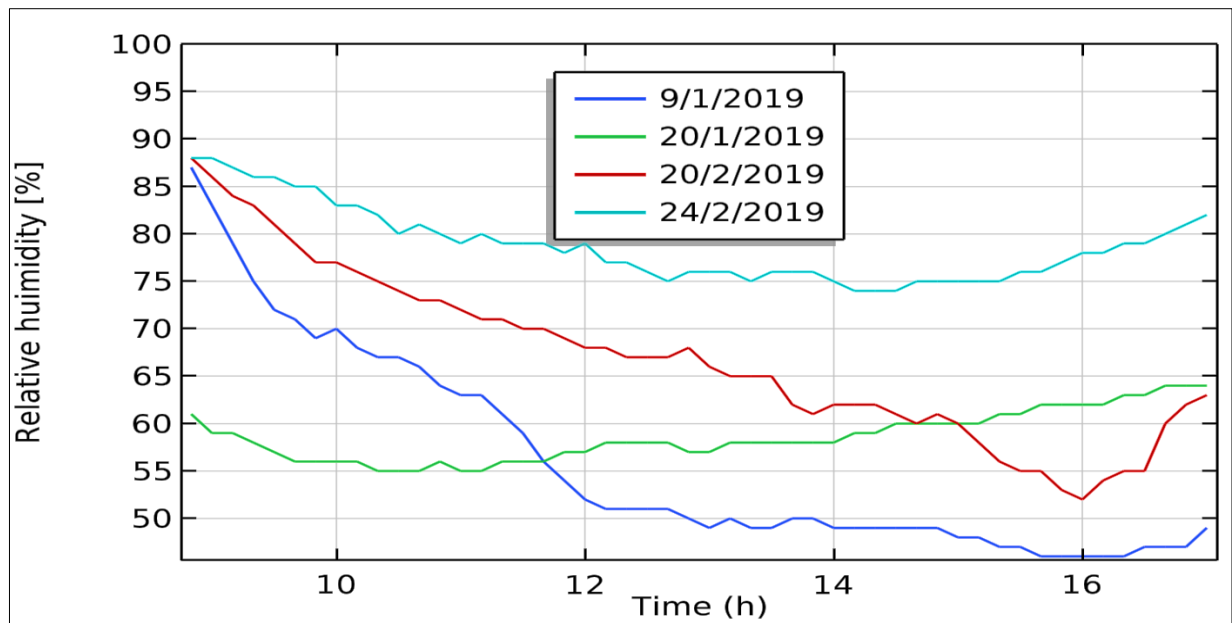

Fig. 5.18 Shows the hourly variation of outdoor relative humidity values during hours for test days.

Relative humidity data is necessary for heating load calculations. They can be used to extract the moisture content values from the psychometric chart in the air and thus calculate the amount of latent heat, which is a component of the heating load, as explained in Chapter three. Increase the amount of relative humidity contributes to increase the amount of latent heat and thus increase the heating load and vice versa. Figure 5.19 shows the time variation of heating load values of the room during the test days. The results showed the most significant values of the heating load on   January 9, 20 and February 20, 24, 2019, was 1718W, 1434W, 1535W, and 1218W respectively at 9:00 am. While the average heating load during the test periods for the above days was 1302W, 1191W, 1158W and 1117W respectively. These results showed that the heating load required for the room is at the highest value in the first morning hours and then decrease gradually until it reaches the lowest value at midday. In afternoon, the heating load begins to escalate slightly. This is because the heating load is directly affected by variation in solar radiation rates during the day, which are weak at sunrise and gradually increase at midday and then decrease to the lowest value at sunset, as shown in Figure5.8.
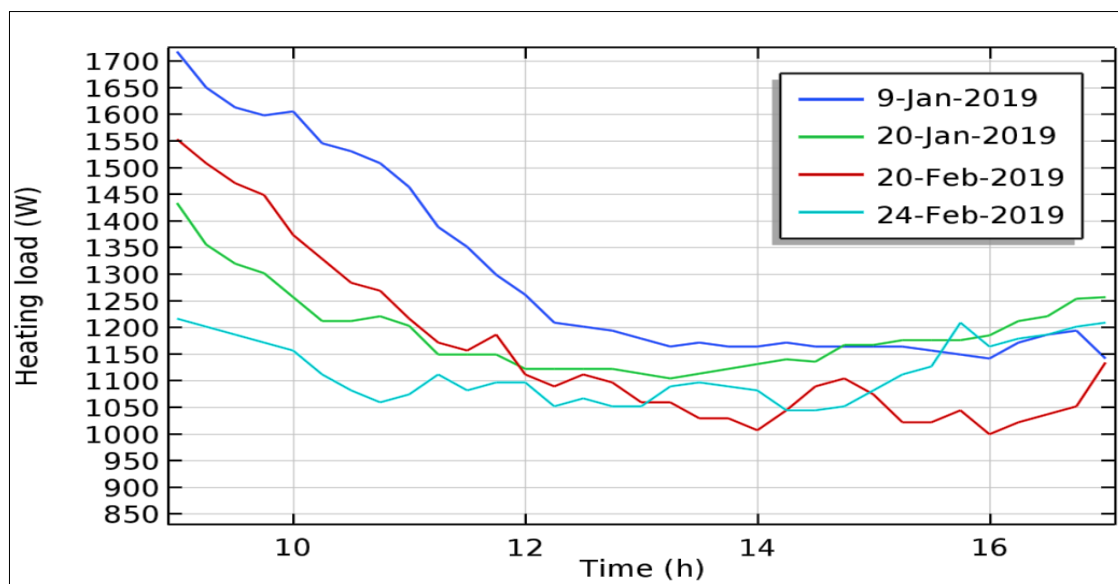

Fig.5.19: Shows hourly variation of the heating load of room during the test days

They are accompanying the heating process, continuously changing the internal conditions of the room, where the heat energy transmitted from the radiator to the room space contribute to raise the air temperature and reduce the relative humidity inside the room. The results showed that the heating process achieved a relatively acceptable result in covering part of the heating load required. Figure 5.20 shows the time variation of the room's internal conditions (room temperature T_{indoor} and relative humidity Rh_{indoor}) as well as ambient temperature T_{amb} during the heating process. During the test days on January 9, 20 and February 20, 24, 2019. The results indicate the similarity in a variation of room temperature and ambient air temperature. Recorded data showed that the relative humidity decreases between 44% and 32% in most days. Any increase in room air temperature was accompanied by a decrease in relative humidity in the heating process. As for highest room temperatures during the test hours were 21.19 °C, 22.9 °C, 23.04 °C, and 23.86 °C, respectively. It was found that the last three days of the test achieved the highest temperature of the room is about 23°C, which means the system produced thermal energy near the required heating load in the midday period. While on January 9, 2019, the room temperature reached the highest value of 21.19 °C. Because the weather was cold compared to the other days, and the solar radiation rates were lower, in general, it had been observed that the heating system warm the space weakly at the beginning of the morning and near sunset and does not provide the minimum required design conditions in these periods. Because the solar heating system gives useful heat less more from required due to weak solar radiation in sunrise and sunset times. while it reaches peak value in the middle of the day, although the solar heating system did not give heat energy equal to the load required during the four days of tests, it contributed to increasing the room temperature within acceptable limits in some times. Based on the above, In the period time between 11:00 am, and 4:00 pm, The solar heating system can work at

the highest possible performance and cover an essential part of the desired heating load.
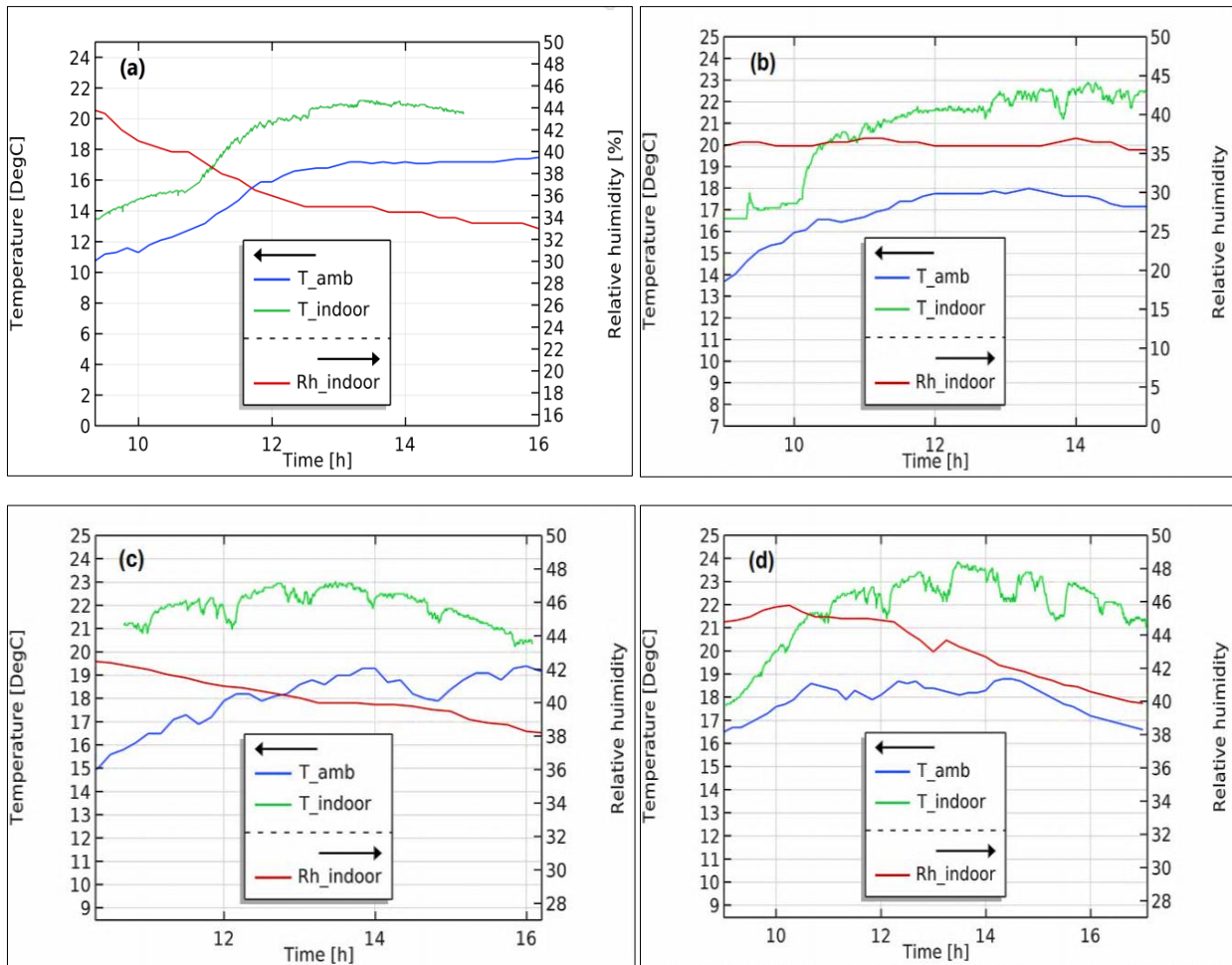

Fig.5.20: Hourly variation of T_{indoor}, $T_{amb,}$ and Rh_{indoor} during the testing day

(a) on 9/1/2019 (b) on 20/1/2019 (c) on 20/2/2019 (d) on 24/2/2019

5.3.5 Effect of using different working fluids on the performance of the flat plate solar collector

The thermal efficiency of the solar collector can be improved through several variables, including the geometric shape, type of material, and the working fluid type. Working fluid has an important role in improving thermal efficiency. The

amount of heat transferred in the solar collector varies from fluid to another because they have different thermal properties.

Three types of working fluids were tested in three different days. The water was tested on January 9, 2019 and the Ethylene glycol-Water mixture (50%-50%) on February 28, 2019 and oil engine grade (10W-30) on March 19, 2019. Tests of ethylene glycol-Water and water were performed at a volume flow rate of 60 L/hr, while the engine oil test conducted at 120L/hr.

In the beginning, we must clarify the weather conditions during the test days. Figure 5.5 show time variation of solar radiation, ambient air temperatures, and wind speed during days test. Figure 5.21 shows the time variation of outlet fluid temperatures of collector T_{out} during testing different working fluid in different days. The results showed that the experimentally recorded data of T_{out} to use water, ethylene-glycol-water, and engine oil which have different physical properties they gave significant differences in the outlet fluid temperature of collector. The highest T_{out} was recorded by using engine oil reached of 75.5°C at 12:03 pm on March 19, 2109. As for the test of Ethylene glycol-Water mixture, the highest temperature reached 64.8°C at 12:38 pm on February 28, 2019. Finally, the water test showed that the lowest fluid temperature, which reached highest temperature of 57.1°C at 12:58 pm on January 9, 2019. There is a clear difference in temperatures of different fluids, Although the tests was done on different days. The working fluid has an important effect in the performance of the solar heater collector, and the engine oil has the highest ability to heat transfer from the collector then coming ethylene glycol-water mixture and at last water. Figure5.22 Shows hourly variation of temperature difference of outlet and inlet fluid of collector ΔT during testing different working fluids in different days.
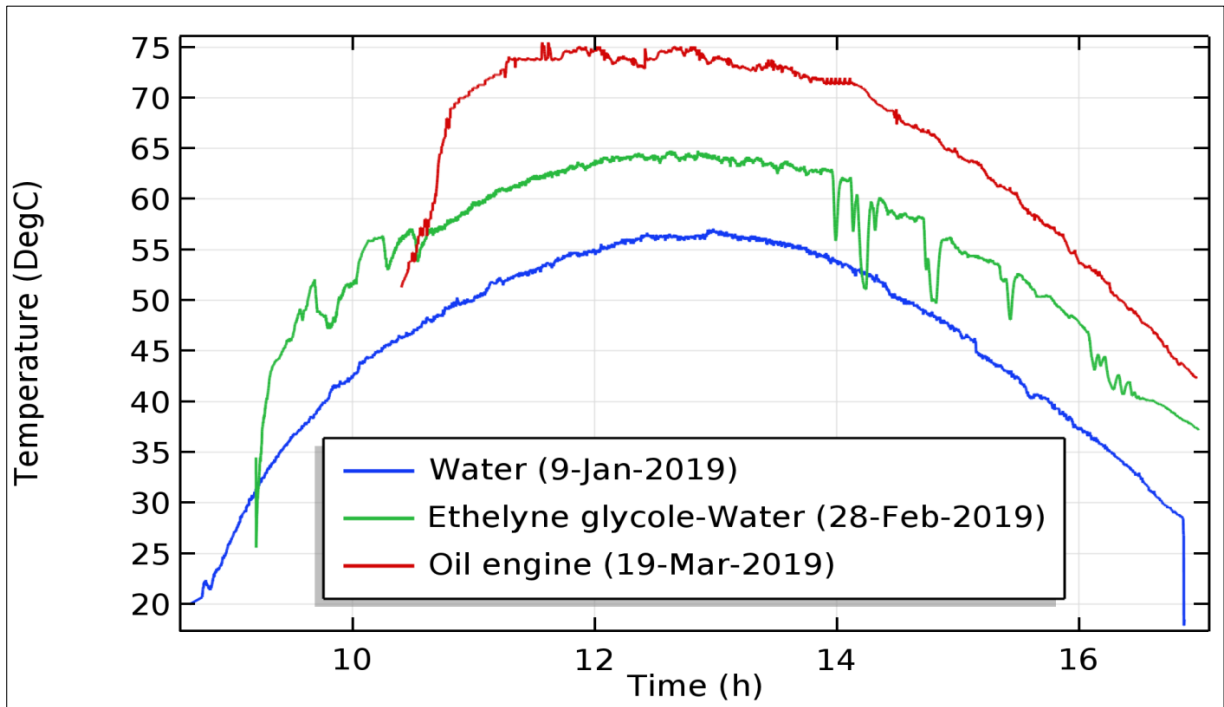
Fig.5.21: Hourly variation of the outlet fluid temperatures of the
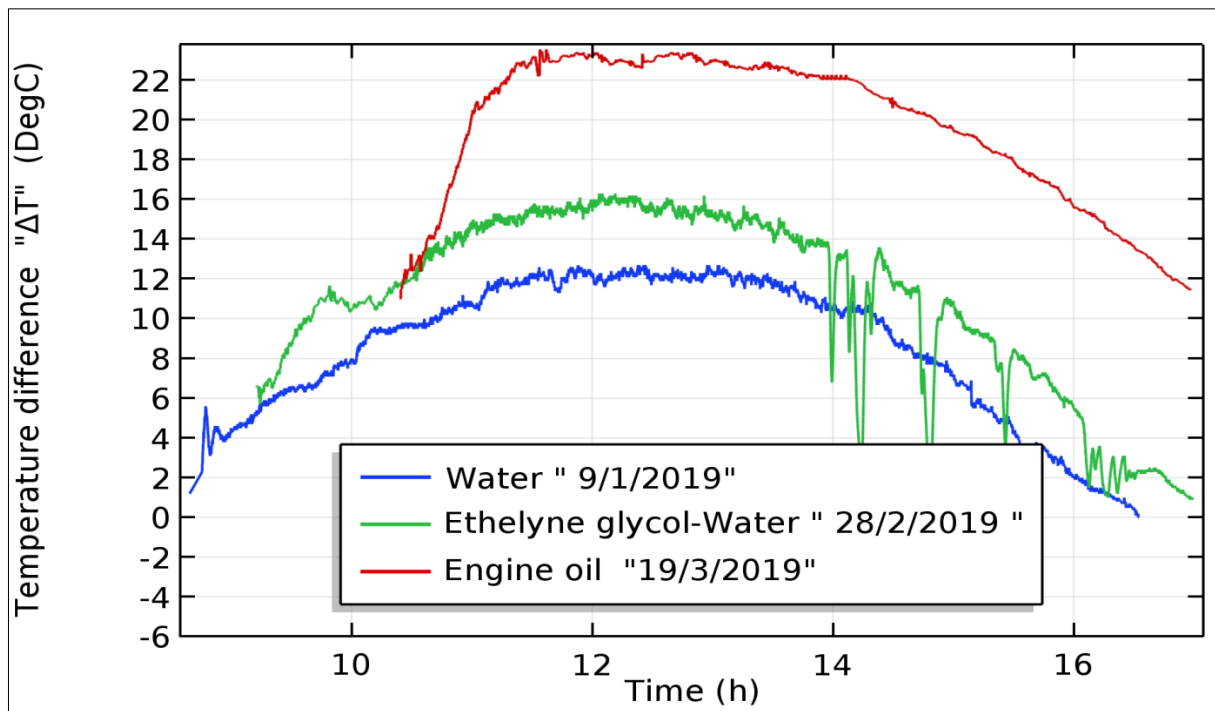
solar collector during testing days

Fig.5.22: Shows an hourly variation of temperature difference of outlet and

inlet fluid of collector during testing days

The engine oil showed a high ability to transfer heat from the collector and reached the highest value of ΔT to 23.5℃ at 11:40 am on March 19, 2019, while the ethylene glycol-Water mixture test showed that the highest temperature difference was 16.3℃ on February 28, 2019 at 12:02 pm. Finally, water was less fluid that gave the ability to transfer thermal energy, where the highest temperature difference was 12.7 on January 9, 2019 at 11:53 am.

Figure 5.23 shows the time variation of useful heat of the solar collector during the use of different working fluids on different days. The results showed that the engine oil gave the highest value of useful heat from other fluids, which reached 1562.6W at 11:39 am on March 19, 2019. For Ethylene glycol-water mixture, the highest useful heat was 1001.3W at 12:04 pm on February 28, 2019. As for water, the highest useful heat was 886.24W at 11:53 am on January 9, 2019. The variation of useful heat for working fluids tests of a solar collector is due to different physical properties such as density, viscosity, thermal conductivity, and specific heat. However, the most important characteristics of the increase the heat exchange is the specific heat, The engine oil, has the lowest specific heat of 1.99[kJ/kg.c] at 50 ℃, while the specific heat of ethylene-glycol-water mixture and water were 3.686[kJ/kg.c] and 4180[kJ/kg.c] respectively,. Heat transfer increases as the specific heat of the working fluid are low and vice versa, This gives preference to engine oil in the increasing of heat exchange and extract as much useful heat as possible from collector.
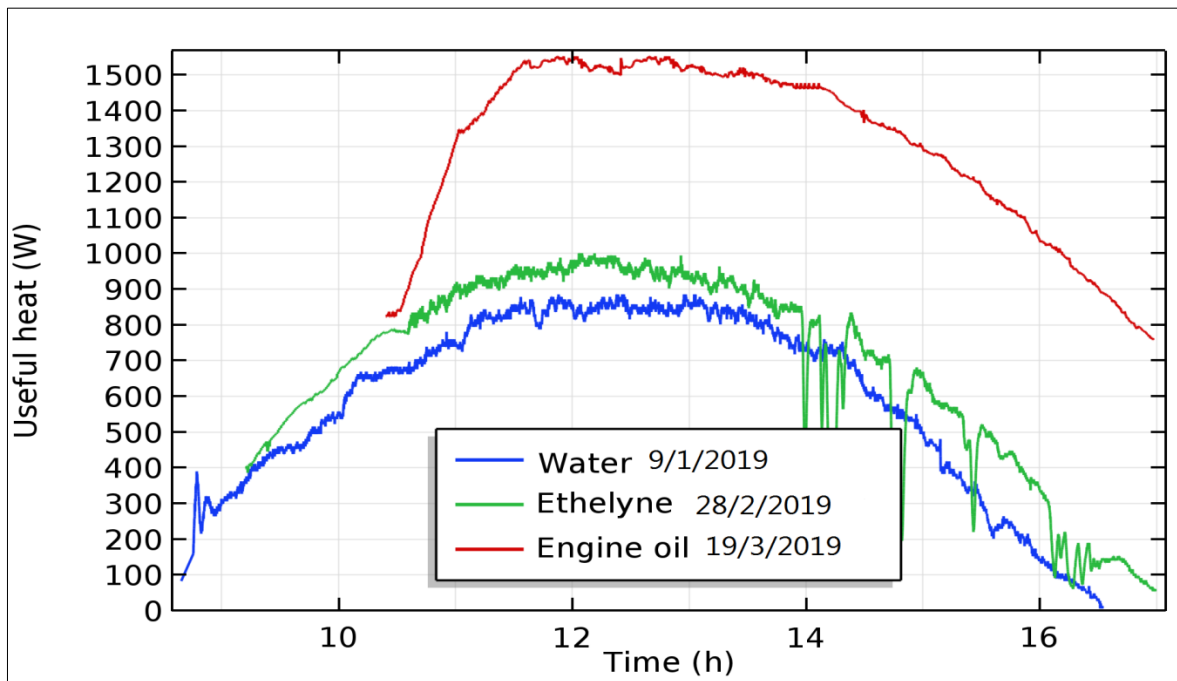
Fig.5.23: Shows an hourly variation of the useful heat of collector during testing different working fluids in different days.

Figure 5.24 shows the time variation of the thermal efficiency of a flat plate solar collector during testing different working fluids in different days. Where the results showed that the solar collector achieve the highest efficiency when the working fluid used is engine oil which reached of 66% on March 19, 2019. When Ethylene glycol-water tested the efficiency of the solar collector reached 58% on February 28, 2019. The water test recorded the lowest efficiency of the solar collector, reaching 50.5% on January 9, 2019. There is a clear difference in thermal efficiencies of the solar collector when testing different working fluids. The reason of difference in thermal efficiencies because each fluid has a certain heat transferability. Whenever the fluid contributes to transfer more amount of useful heat, this reduces the amount of losses and vice versa. This different behavior leads to different thermal efficiencies. From above, it is concluded that the engine oil achieved better possesses a high capacity in the transfer of thermal energy and was utilized from its thermal properties in the possibility of increasing the volume of

flow rate by twice compared to other fluids. This feature gives it an advantage in increasing the amount of useful heat and efficiency of the solar collector.
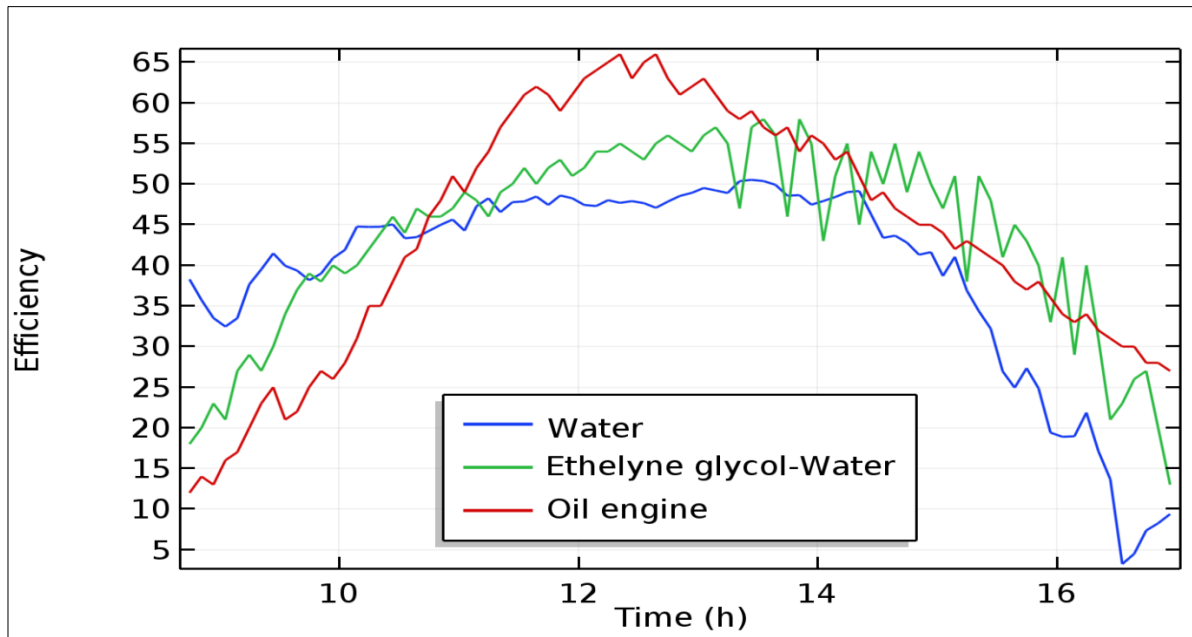

Fig.5.24: shows the thermal efficiency of the flat plate solar collector during testing different working fluids in different days.

5.3.6 Effect of using different working fluids on the performance of the indoor radiator

The effect of working fluids on the indoor radiator performance was studied by utilizing its thermal properties in increasing the heat exchange between the fluid and the surface of the radiator and increasing the useful temperature of the radiator. Three types of working fluids were tested in three different days. Figure 5.25 shows time variation of inlet working fluid temperature of radiator T_i during test different working fluid in different days.

Results indicated that the highest T_i during the period test was when using engine oil as the working fluid and reached 63.5˚C. Also, with respect ethylene glycol-Water mixture and water, T_i was 57.8 ˚C and 51.6 ˚C respectively.
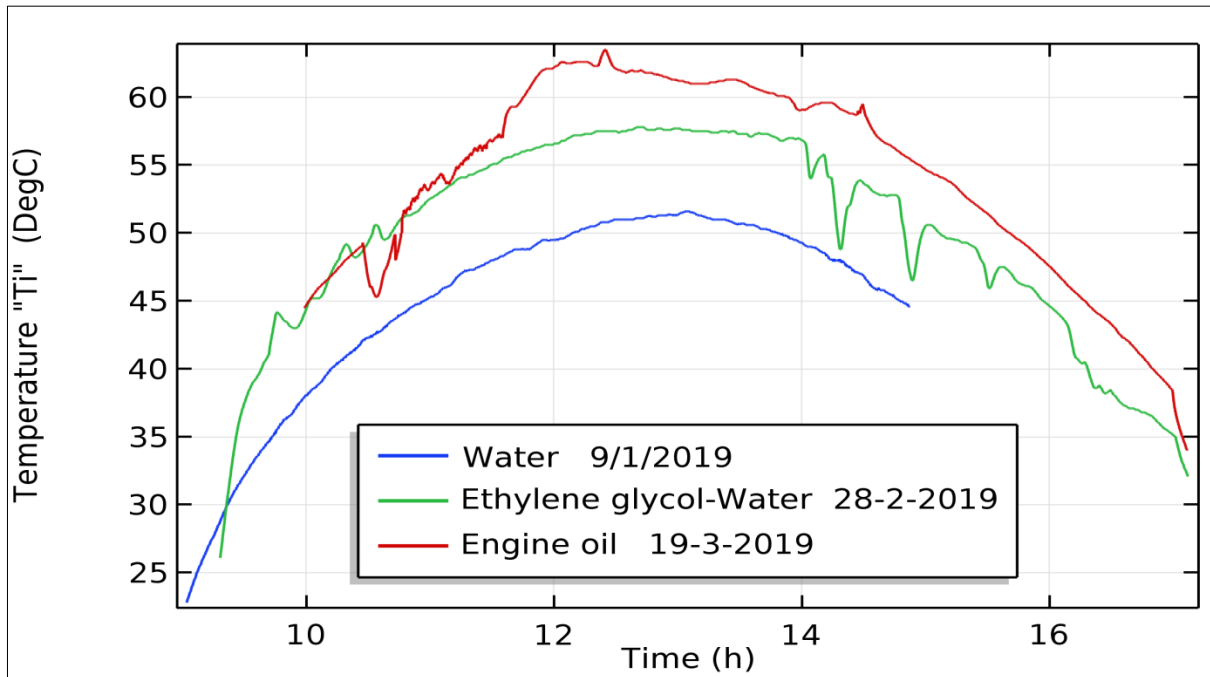
Fig. 5.25: shows time variation of inlet working fluid temperature of the radiator during test different working fluid in different days

Figure 5.26 Shows spectral images taken by a thermal camera showing a temperature distribution in the radiator using different working fluids. Working fluid affects the temperature distribution in the radiator surface. The white areas represent the highest temperatures in the color spectrum and then gradient until they reach the violet color, which represents the lowest amount of temperature. In the oil test, it was observed the high temperatures located in higher radiator surface and take more space compared to the temperatures distribution with other fluid tests. The large area of high temperature gives benefit in increasing the heat transfer from the radiator surface and vice versa. While in ethylene glycol-water mixture and water tests, the high-temperature distribution area in the radiator surface was less than the oil test and its position was concentrated on the side and bottom of the radiator with an advantage of ethylene glycol-water mixture. This difference in temperature distribution is due to the different flow rate of oil was higher than other

fluids in addition to it has better thermal properties relative to other fluids. These advantages of oil make it the best fluid in transferring heat from the radiator surface to room air.

<div align="center">(a)   (b)   (c)</div>
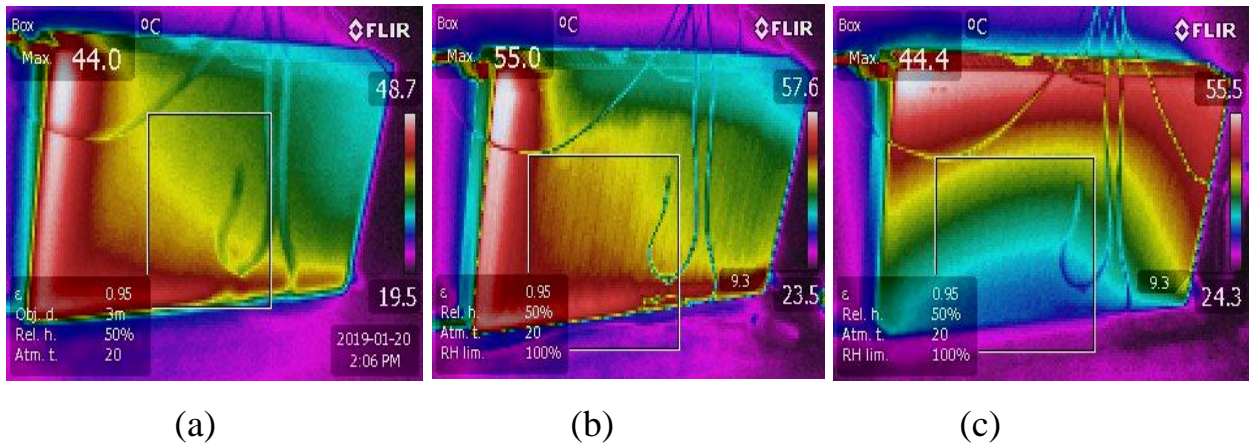
Figure 5.26 Temperature distribution of the radiator surface is constructed by infrared imaging using various working fluids (a) water (b) Ethylene glycol-Water mixture (c) Engine oil

Figure 5.27 shows time variation of temperatures difference between inlet and outlet fluid of radiator ΔT. It is noted that the engine oil test gave the highest ΔT and reached a maximum value of 16.85 $^{\circ}$C at 11:27 am on March 19, 2019. While the highest value when using ethylene glycol-Water was 10.4 $^{\circ}$C at 12:21 pm on February 28, 2019. Finally, its highest value when using water was 8.5 $^{\circ}$C at 1:03 pm on January, 2019.

Figure 5.28 shows the useful heat of the radiator using various working fluids during different days. The results indicated that the highest value of useful heat of the radiator when the engine oil was used as working fluid which reached 1031W. At 11:14 am on March 19, 2019. For ethylene glycol-Water mixture was the highest value of useful heat 639W at 12:19 pm on February 28, 2018. Finally,

water gave the lowest value of the useful heat of the radiator, which reached 593W at 1:02 pm on January 9, 2019. It is noted that testing the engine oil in the heating system achieved an amount of useful heat more higher than the other fluids, for two reasons, the first reason because the engine oil has a better thermal properties of water and ethylene glycol-water mixture especially the property of the specific heat, which is less than other fluids, This gives it a preference in the process of heat exchange. The second reason is that the oil tested at a volume flow rate of 120L/hr while the other fluids were tested at a volume flow rate of 60 L/hr. The engine oil tested at high volume flow rate due to it has ability to increase the heat exchange process in high volume flow rate. Also high solar radiation rates allow it to raise the volume flow rate with increasing the heat transfer. Finally, the high viscosity of the oil requires pumping it at a high flow rate to overcome flow losses and pressure drop.
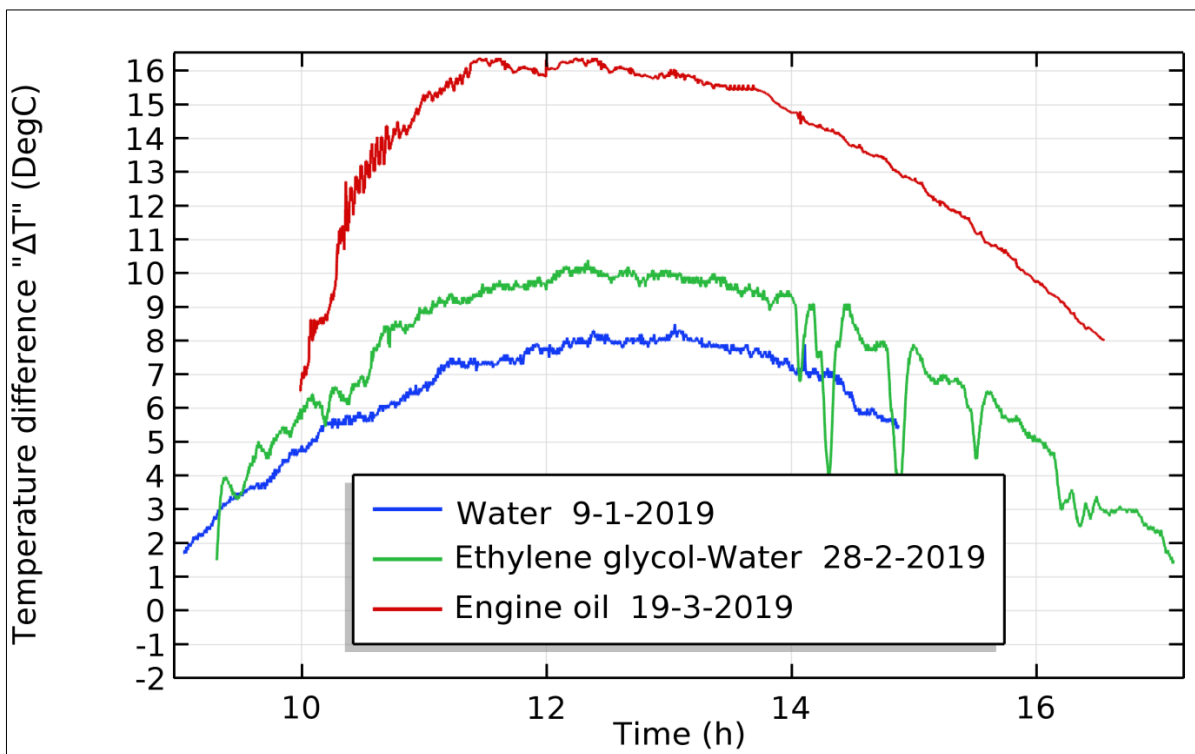

Fig.5. 27 shows time variation temperatures difference between inlet and outlet fluid of radiator during test different working fluid in different days.
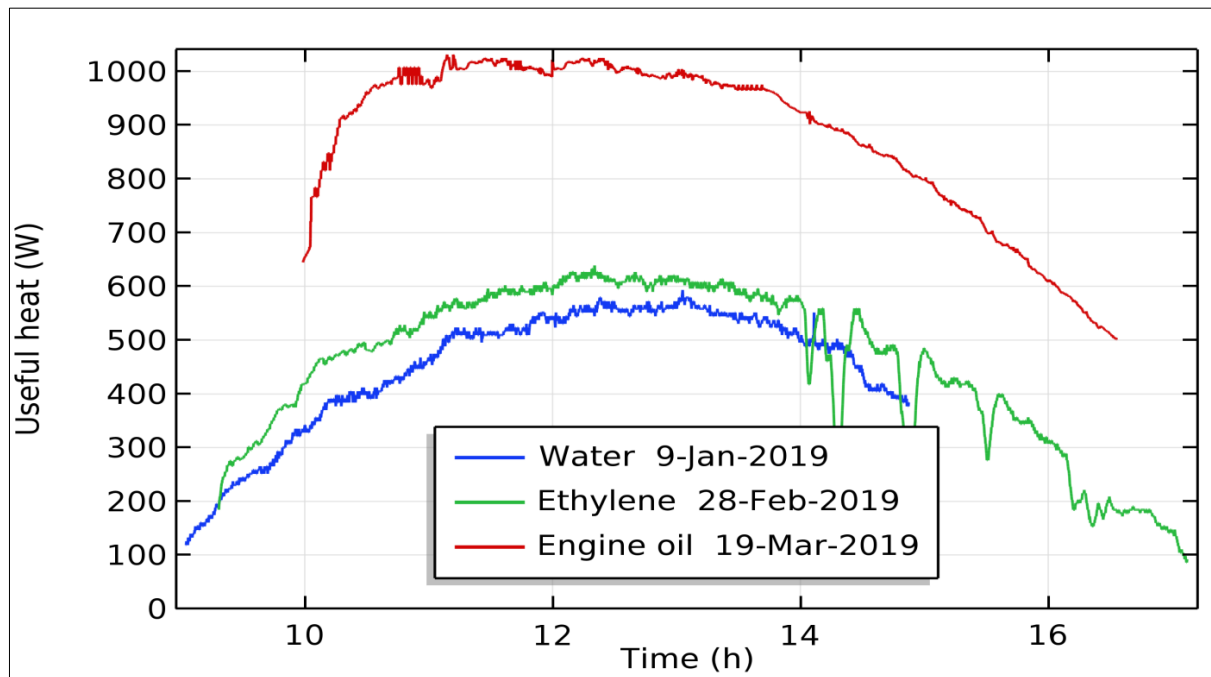
Figure 5.28 shows the useful heat of the radiator using various working fluids during different days

5.3.7 Effect of using different working fluids in the solar heating system on the room heating

The effect of the use of different working fluids in different days on enhancement heating system was examined, and utilized from the thermal characteristics of some working fluids were used to improve the thermal performance of the heating system. And increase the heat exchange in the solar collector and radiator to determine the best working fluid, which gives the highest useful heat and improves the efficiency of the heating system. Moreover, it makes the most of the useful heat obtained from solar energy to cover as much as possible the amount of heating required or part of it. In the beginning, we should review the calculations of heating loads during the working fluids tests. Figure5.5 showed an hourly variation of ambient air temperatures during testing days, which represent dry bulb temperature during testing days Figure 5.29 shows the hourly variation of relative humidity values during daylight hours for test days.
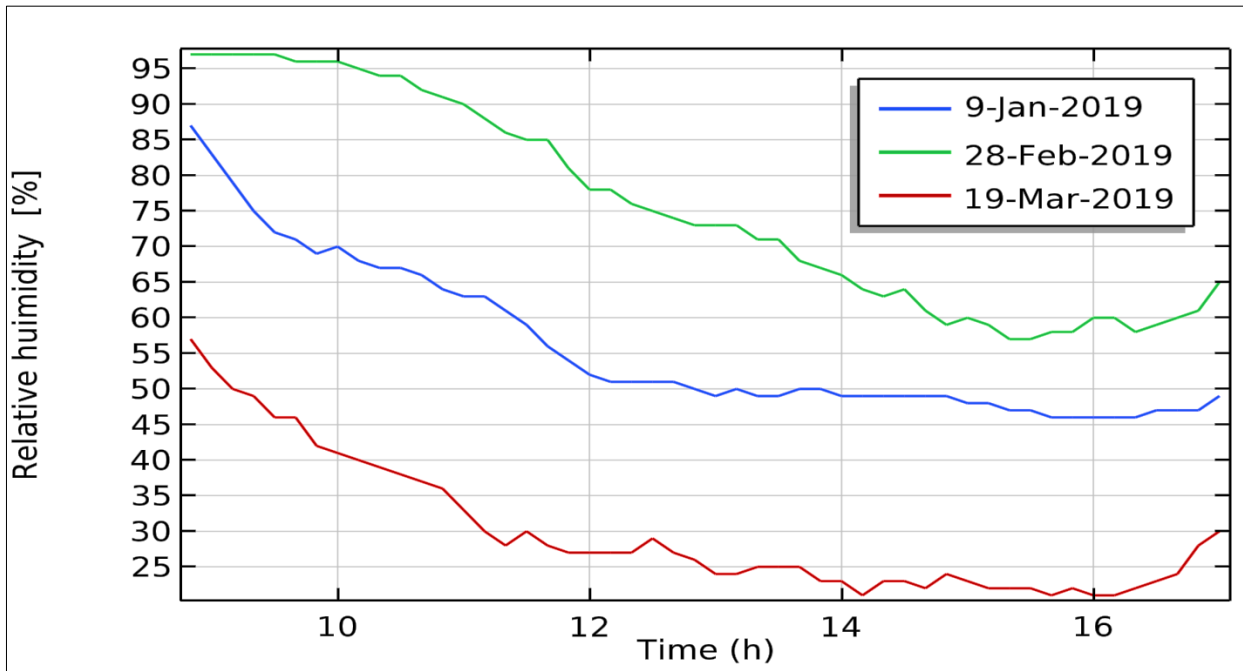
Fig. 5.29 shows the hourly variation of outdoor relative humidity values during test days.

The recorded experimental data showed that the relative humidity rates are high at the beginning of the morning and then gradually decrease during daylight hours. The results showed that there is a sufficient difference in the relative humidity values during the test days and recorded the highest value on 28/2/2019 about 97%. On 9/1/2019, the highest value was 87%, and finally, on 19/3/2019 the value was relatively low and recorded the highest value of 57%, all these results recorded at time 9:00 am.

Figure 5.30 shows the heating load values of the room calculated during the test days. These results showed that the heating load required to warm the room is at the highest value in the first morning hours in all days and then decrease gradually until reaches the lowest value during the midday, after which the value begins to increase relatively little until the time of sunset. This is because the heating load is directly affected by the change in solar radiation rates during the

day. Whose values are weak at sunrise and gradually increase until reach peak level at midday and then decrease to the lowest value at sunset, as shown in Figure5.5.
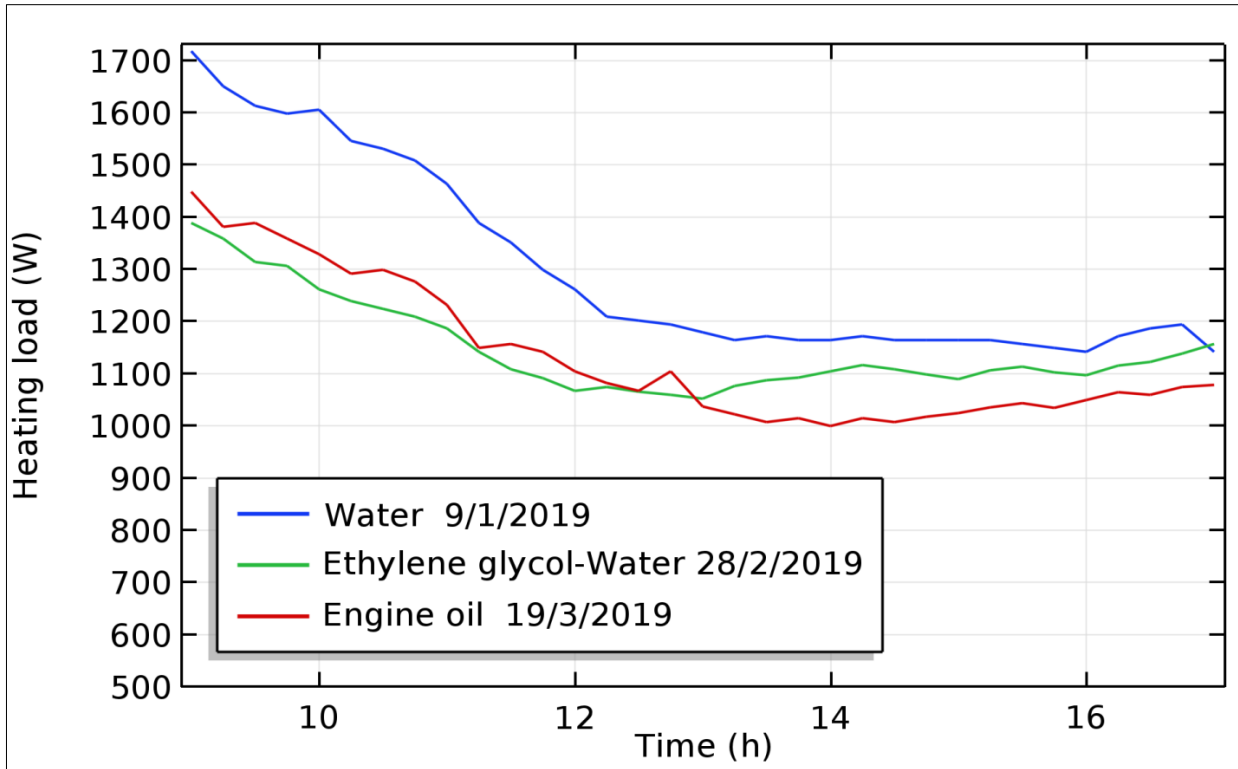

Fig.5.30: Shows hourly variation of the heating load of room during the test days

The results of heating load calculations showed that on January 9, 2019 the heating load reached the highest value of 1718W. While on February 28, 2019 and March 19, 2019, were 1390W and 1449W respectively. All these readings were at 9:00 pm.

The experimental results showed that working fluids could improve the performance of the solar heating system and it contributes to increasing thermal energy provided to heating space by benefit from the advantages of the physical-thermal properties of the working fluids on the one hand. Besides testing these fluids at the optimum volume flow rate in the solar heating system on the other

hand. It is necessary to note testing fluids at different times makes a results comparison inaccurate. To be an accurate and realistic comparison, all fluids must be tested in one day under similar conditions. However, the working fluids can be evaluated and predict the most adequate fluids, even if they were tested on different days, especially after we found some similarities in weather conditions in oil and ethylene glycol-water mixtures tests. In addition to observing significant differences in the improvement of heat exchange, this gives a good impression on the evaluation of different working fluids. Figure 5.28 shows that the oil test gave a useful heat of the radiator more higher than other fluids, taking advantage of its thermal properties and high flow rate and this gives it an advantage on other fluids, despite the disadvantages of high viscosity and freezing. Figure 5.31 shows the time variation of the room's internal conditions (room temperature T_{indoor} and relative humidity Rh_{indoor}) during the heating process as well as ambient temperature T_{amb} during test days. The experimental data showed that the maximum room temperature during days on January 9, 2019, February 28, 2019 and March 19, 2019 was 21.19°C, 22.27°C and 24.4°C, respectively. The relative humidity was reduced during the heating process, and the values ranged during the days of the test between (46%-30%).

It is observed early in the morning and near sunset that the heat energy provided to the room by the solar heating system is weak, and the room temperature is much lower than the indoor design temperature while in the period between 11:00 am and 4:00 pm there is a relative convergence between room temperature and the indoor design temperature. Figure 5.31 shows that the solar heating system in the oil test contributed to the heating space to the limits close of the design conditions and achieved thermal energy close to the required heating load. It also achieved the highest difference between room air temperature and ambient air temperature reached 5.2°C. While in the ethylene-glycol-water mixture

test, the system contributed to heating space to a lesser degree than the oil test and achieved an acceptable amount of thermal energy to heat the room, and the highest difference between room air temperature and the ambient air temperature was 3.95˚C as shown in Figure 5.31 (b). Finally, the system in the test of water achieved the least amount of space heating was the highest difference between room air temperature, and ambient air temperature was 3.5˚C as shown in Figure 5.31 (a).
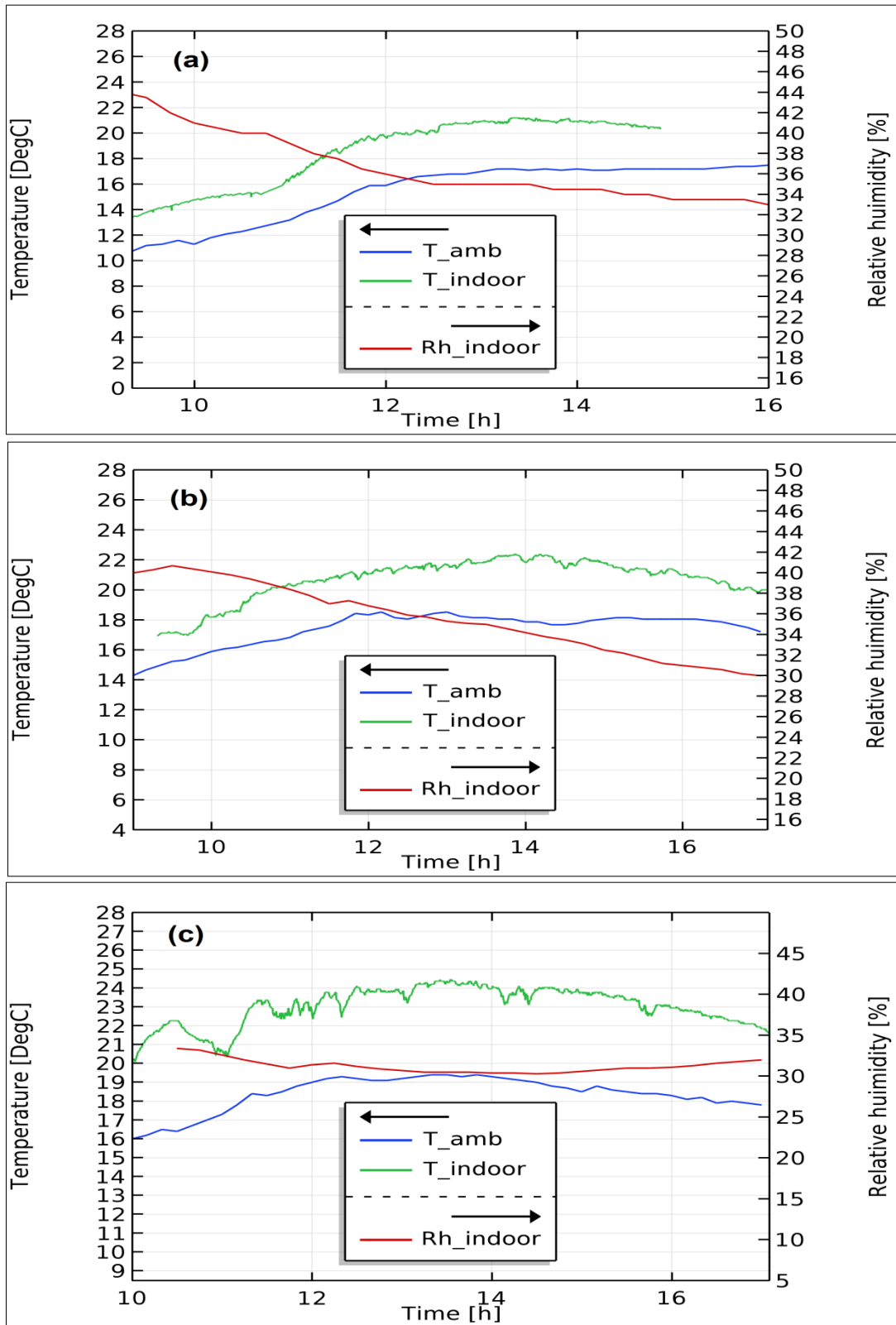
Fig.5.31: Hourly variation of indoor and ambient temperatures and indoor relative humidity on (a) January 9, 2019 (b) February 28, 2019   (c) March 19, 2019

5.3.4 Losses calculation in the pipelines

In each thermal system, thermal losses cannot be eliminated, but the heat lost amount can be reduced by using traditional insulating materials and modern insulation techniques. In our work, there are two types of losses that occur in the solar heating system; the first is the losses in the flat plate collector. These losses occur because of convection and radiation heat transfer from the collector to the surrounding air. The second is the pipeline losses that will be highlighted in our account. The outlet and inlet pipelines to the collector which are connected from the other side to the radiator. It was covered with insulation has a thickness of 0.5 cm and was wrapped from the outside with a thermal tape resistant to weather conditions. Figure 5.32 shows the time variation of the thermal losses in all the pipelines of the system during the four-day test, and the working fluid used was water. The system tested in all days was under a volume flow rate of 60 L/hr, except on January 20, 2019 was 30 L/hr. By observing the results, there was a convergence in the rate of thermal losses on January 9, 2019 and February 24, 2019 and recorded lowest losses which ranged from 150W to 300W in most times. On February 20, 2019, the time variation of the losses was semi identical with the previous two days in the afternoon period and divergence which increased in the afternoon. The losses were volatile, especially in the afternoon and ranged between 100W to 500W. Finally, on 20/1/2019 the losses were high compared to the rest of the days, and the reason was that the volume flow rate it was 30L/hr, which is relatively slow resulting in increased heat exchange time in pipelines resulting raised of fluid temperature to a higher amount than other tests causing an increase in losses. Figure 5.33 shows the time variation of thermal losses by testing various working fluids on different days, Note that there is a convergence in the variation time of losses on January 9, 2019 and February 28, 2019 and reached the highest value of 396W and 357W respectively, with the observation that there is fluctuation

in the value of losses during periods of intermittent time on February 28, 2019 to reach the highest value of more than 450, the reason for this is the appearance of clouds shading on the collector during that period causing increased losses rapidly.
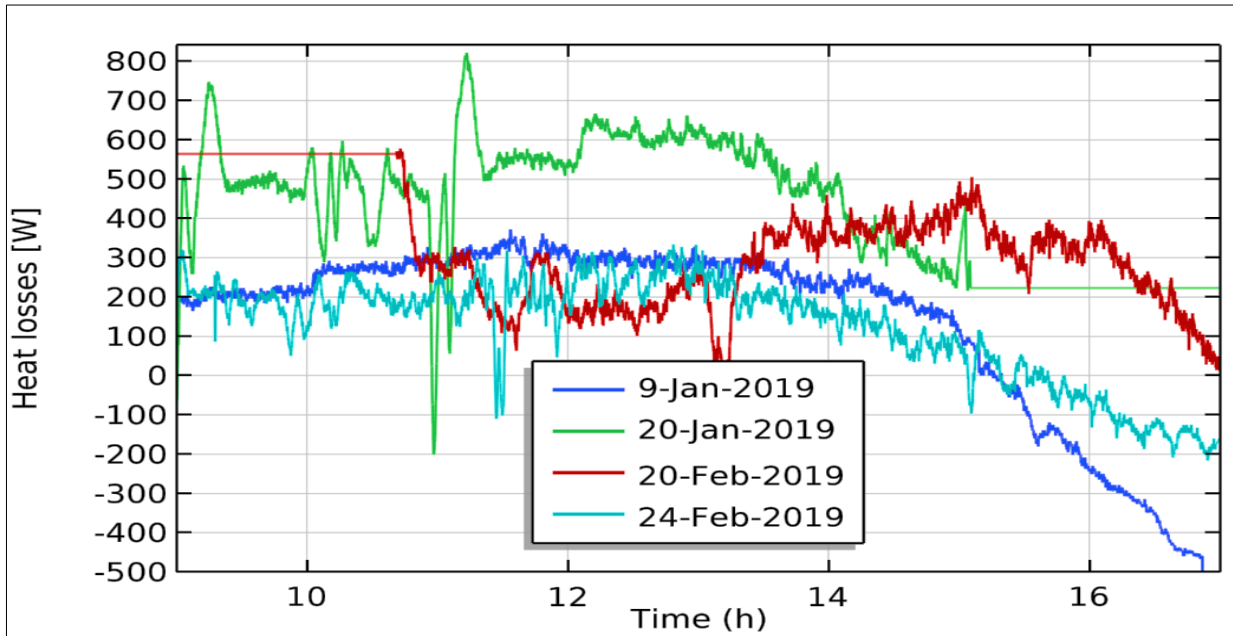

Fig. 5.32: shows the thermal losses in all the pipelines of the system during the four-day test
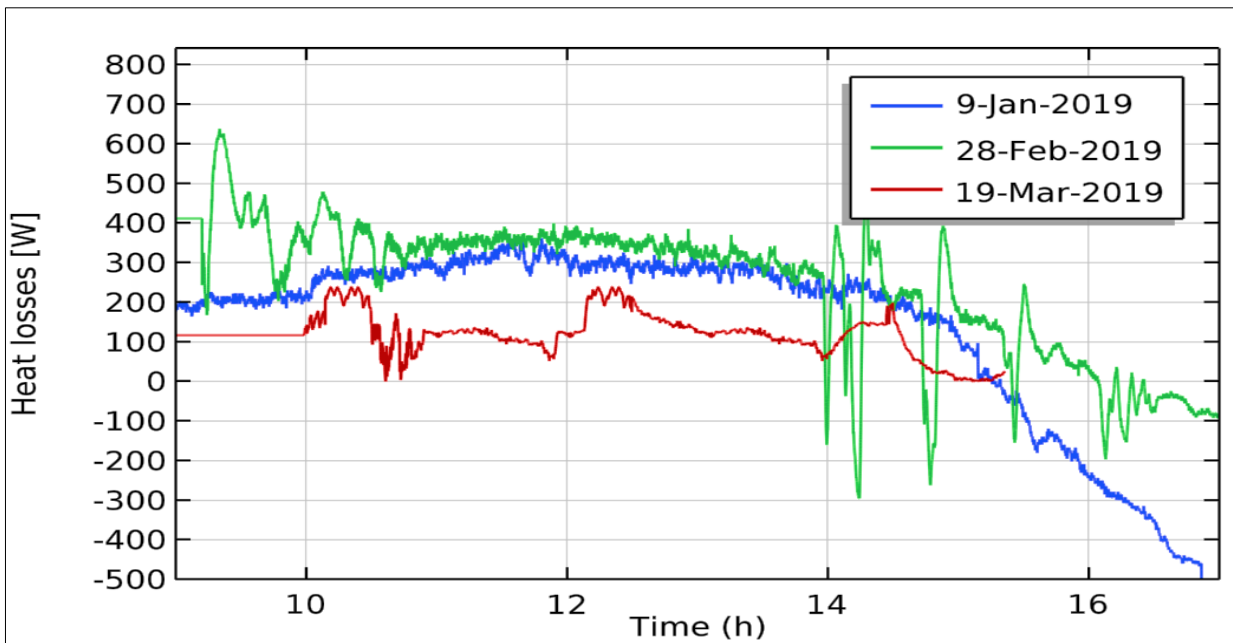

Figure 5.33: shows the time variation of thermal losses by testing various working fluids on different days.

Finally, the heating system achieved fewer losses compared to the previous two days in the test on March 19, 2019 using the working fluid engine oil, and the average value of losses is 124W because the volume flow rate was high in the test of this day and reached 120L/hr, which made the heat exchange time fast, this reduced the losses on the this day. While in the previous two days, it was 60L/hr that led to losses at higher rates.

Figure 5.34 shows the rates of thermal losses in the pipelines compared to the useful heat generated by the collector. The highest losses were observed on January 20, 2019, where the flow of the working fluid was 30L/hr while the lowest losses were on March 19, 2019 where the volume flow rate was 120 L/hr, It is clear that the volume flow rate has an essential impact on pipeline losses.
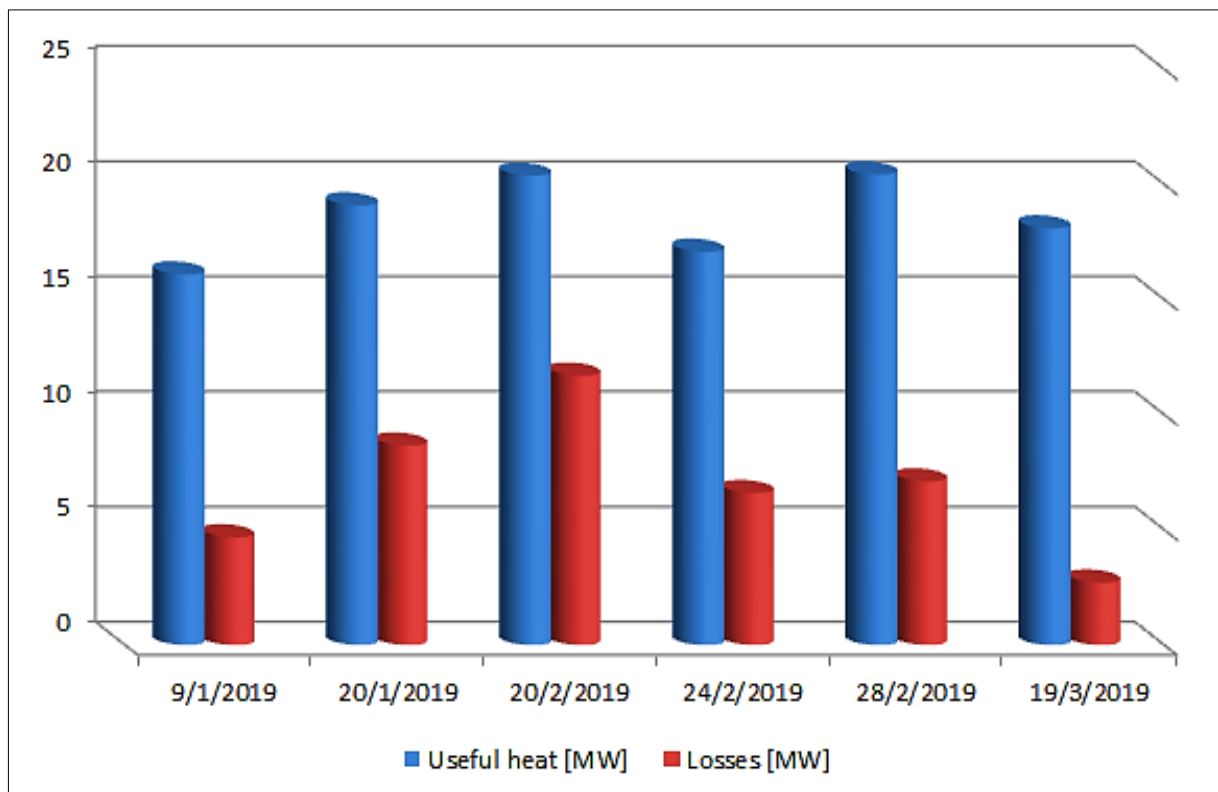

Figure 5.34 shows the ratios of thermal losses in the pipeline compared to the useful heat generated by the collector.

5.4 Energy saving and cost calculations

The cumulative useful heat of the solar system during test days was calculated and compared with the cumulative space heating load for the purpose of economic analysis. The useful heat of the system represents the amount of energy saved. Figure 5.35 shows a comparison of the cumulative quantities of the heating load and useful heat from the solar system for the test days.
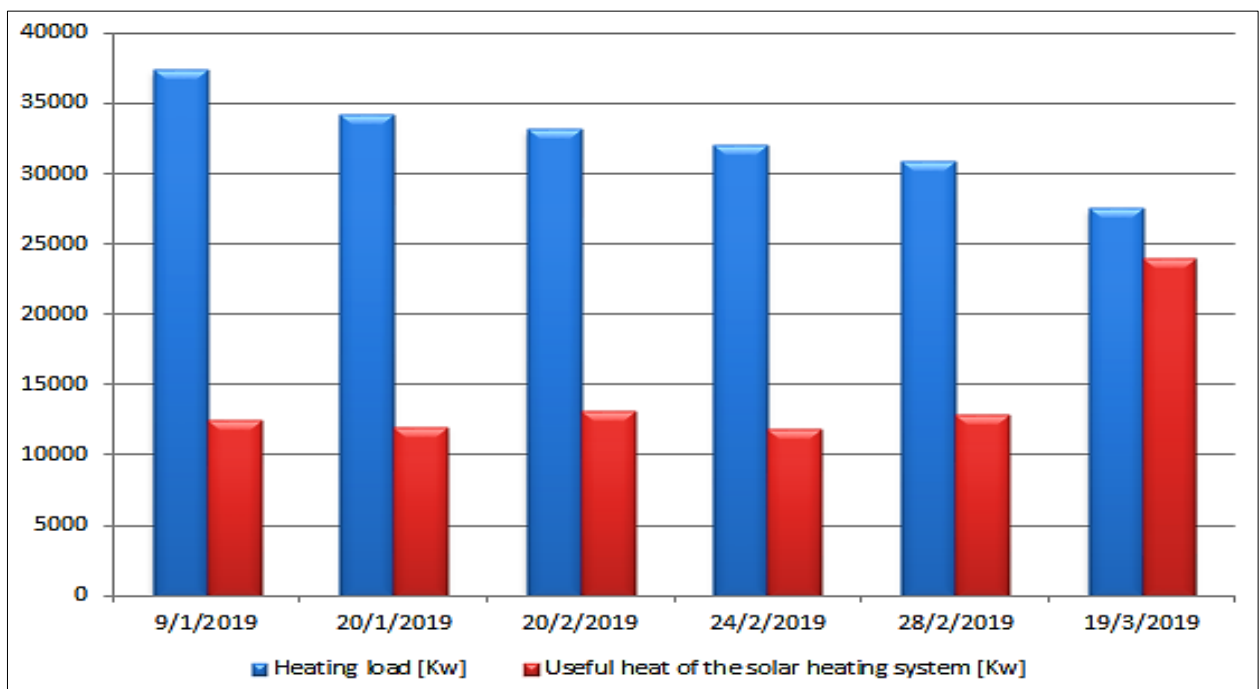
Fig. 5.35: shows a comparison of the cumulative quantities of the useful heating and heating load from the solar heating system for the test days

It is noticeable from the results that the heating load in January is higher than other months where the cumulative load during test hours for January 9, 2019 was 37,383kW and gradually decreased during February and March. The highest heating load recorded on February 20, 2019 was 33,181kW. On March 19, 2019 less heating load was recorded 27,521kW. This difference in the heating load

during the months is due to the different weather conditions during these months, January was the coldest month compared to others in Najaf city. February was also cold in most days, but to lesser extent than January. While in March the weather was cold at the beginning of the month and then the weather seemed to tend to moderate. Useful heat calculations of the solar heating system during the test days showed that there was convergence in the results in January and February, where the average cumulative amount of useful heat was 12,174kW and 12,661kW respectively. While March recorded the highest useful heat on March 19, 2019 was 23,941kW. Figure 5.36 shows the ratio of useful heat of the solar system to the required heating load during the test days. The results indicate that the solar heating system contributed to heating the room with different percentages of the total heating load during the test days. The rate of heating in January was 34% of the total required load, while the rate of heating in February was 39.5%. Finally, in March it was 86%.
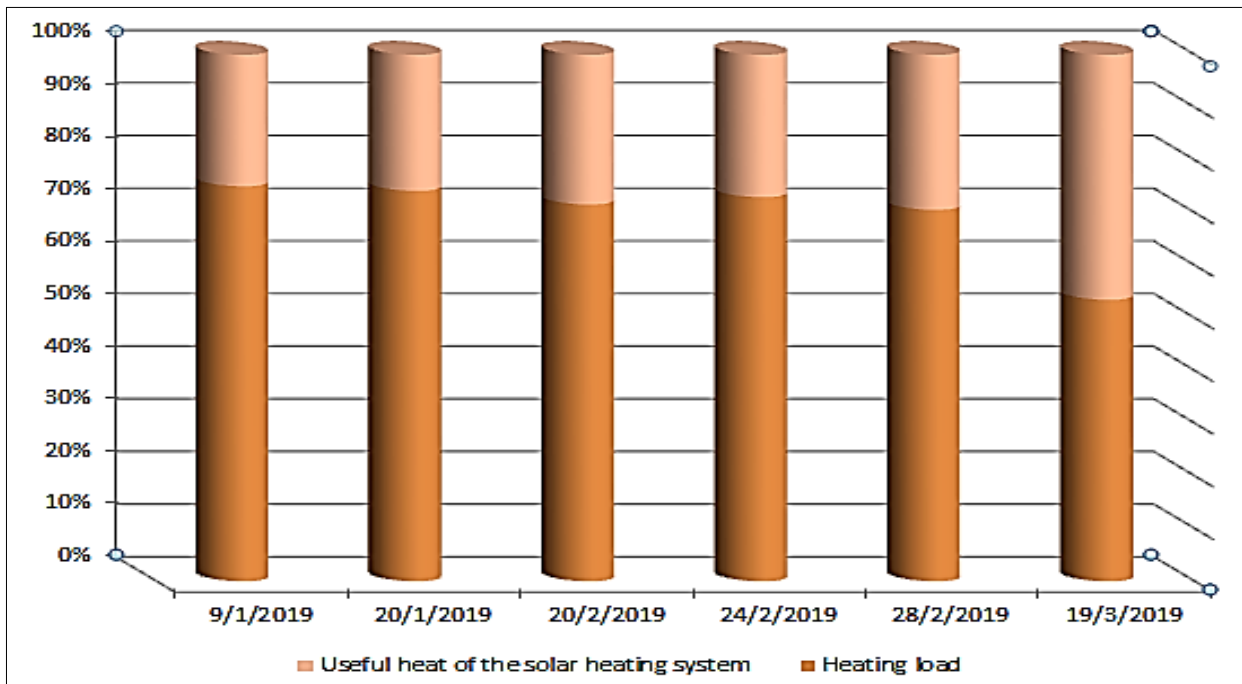

Fig. 5.36: shows the ratio of useful heat to the required heating load

The calculation of the cost of energy saved as a result of the use of the solar heating system is very important to assess the economic feasibility of it and also in calculating the payback period for the cost of the initial investment. Costs were calculated according to the pricing of the Iraqi ministry of electricity and were calculated according to the average category cost of power unit (35 IQD/ unit). It should be a consideration that the calculation of costs must be along the length of the winter months in order to obtain a more realistic economic study. So the average energy saved for test days during each month is assumed to be the amount of energy saved per day during that month. This hypothesis will allow the calculation of costs for each test days as well as for each month as shown in Figure 5.37(a) It was found that the average cost saved during most days about 970 IQD/day, except on 19/3/2019 was the cost saved 1860 IQD/day. The calculation of the cost of energy saved for each month according to the hypothesis of calculating the rate of energy saving for the test days was as shown in Figure 5.38 (b). Where the saving costs were convergence for January and February were 28,400 IQD and 29,550 IQD, respectively, while the cost of March 55,860 IQD. As a result, the period of use of this system during these three months and can add December and part of November to cold months in weather of Iraq; this reduces the payback period of the system after which the cost savings become profits compared to the cost to use of traditional systems. The payback period can be computed, which represents the ratio of the investment cost on energy saved during a year. The cost savings were calculated during the winter season amounting to 114,000 IQD, while the investment cost was 600,000 IQD. The payback period is therefore 5.2 years. Note that the initial cost is not high in these systems types. Many low-income customers can purchase them, although the payback period is relatively medium period. It is concluded that this solar system achieves economic feasibility by relying on a free and available energy source, cheap and easy to install and maintain and provide electricity or fossil fuels by 33% to 45%.
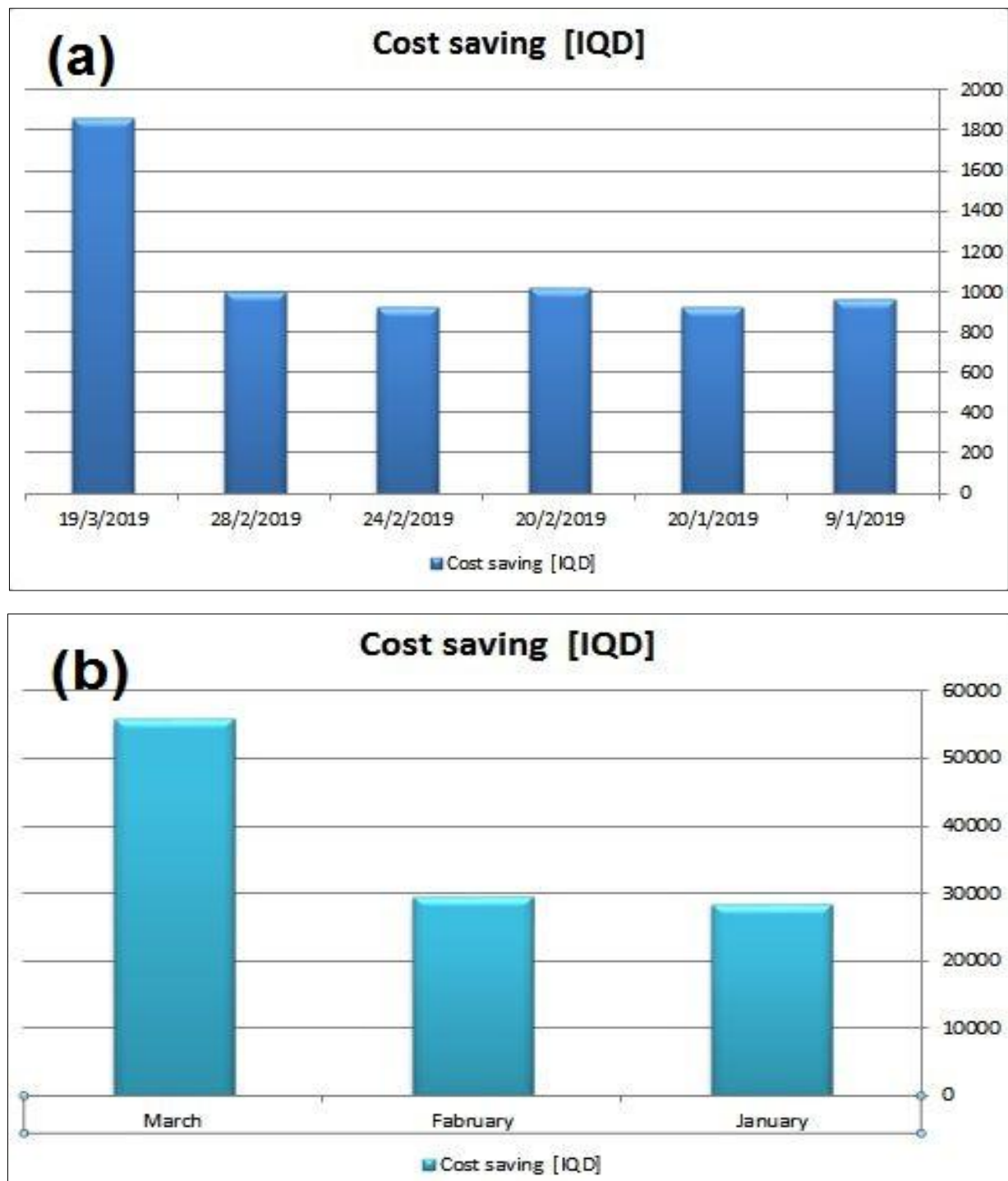
Fig. 5.37 calculates the cost of energy savings (a) during test days (b) during the months

125

CHAPTER SIX

CONCLUSION AND RECOMMENDATIONS

CHAPTER SIX

CONCLUSION AND RECOMMENDATIONS

6.1 Conclusion

The present study aims to evaluate the thermal and economic performance of an active solar heating system for heating space in Najaf, Iraq. A solar system uses flat plate collector solar water heater to provide hot water. The effect of some parameters on the thermal performance of a flat plate collector was studied numerically and experimentally.

The most important conclusions that can be drawn from the present study are as follow:

6.1.1 Numerical study

1. The results showed the optimum value of volume flow rate of the working fluid in solar collector was 40 L/hr.
2. The study effect of the working fluid type used in the solar collector at the same flow rate showed that the engine oil achieved the highest outlet fluid temperature while the ethylene glycol-water mixture achieve highest useful heat and efficiency.
3. Study the effect of climate parameters on the thermal performance of collector showed that increasing the solar radiation rates has a significant impact on increasing the thermal energy of the solar water heater. While the thermal losses of collector are directly proportional to the wind speed and inversely with the ambient air temperature.

6.1.2 Experimental study

1. There was a good agreement between the numerical and experimental results in studying the volume flow rate effect of, working fluid type, and weather conditions.

2. January recorded the highest heating load than February and March.

3. Engine oil achieved the highest amount of useful heat compared to water and ethylene glycol-water mixture, especially when the flow rate was high, but it has some disadvantages in operation such as freezing at low temperature, as well the difficulty of flow within the system because it has a high viscosity.

4. The solar heating system has contributed to saving electric power at a rate of 34% of the total energy required for room heating at the test days in January. Whereas in February, was 39.5%. While in March, the system saved by 86%.

5. The economic study showed that the average saving cost of 38000 IDQ/month while the payback period was 5.2 years.

6.2 Recommendations

The present work can be extended through the development and modification of an experimental rig to improve the thermal performance of the heating system and extend the periods time operation of the system. The following improvements could be performed in four main areas:

1. Studying the thermal and economic performance of a hybrid system by added an auxiliary electric heater to the system to cover the entire required heat load.

2. Study the effect of using a thermal storage tank to the heating system to extend the operation period of the system. The thermal storage capacity can

also be increased by using phase change material PCM to covering the cloudy periods and night.

3. Study the effect of using the active solar system consist from array of solar water heater to cover the entire load required for heating, and connected it with an automatic operating controller.

4. Study the thermal performance of a hybrid domestic heating system consisting of an active solar system that produces hot water and passive system Trombe wall and a direct gain window.

REFERENCE

Reference

[1] E. Dickinson, "LAND SURFACE PROCESSES AND CLIMATE-SURFACE ALBEDOS AND ENERGY BALANCE," vol. 25, 1983.

[2] O. Torres, P. K. Bhartia, J. R. Herman, Z. Ahmad, and J. Gleason, "Derivation of aerosol properties from satellite measurements of backscattered ultraviolet radiation: Theoretical basis," vol. 103, pp. 99–110, 1998.

[3] W. T. Reach, C. Lisse, T. Von Hippel, and F. Mullally, "The Dust and Cloud Around the White Dwarf " G 29-38 . II . SPECTRUM FROM 5 TO 40 μ m AND MID-INFRARED PHOTOMETRIC VARIABILITY," The Astrophysical Journal Letters, 2005, 635.2: L161 pp. 697–712, 2009.

[4] L. Wald and L. Wald, "Basics in Solar Radiation At Earth Surface," Solar energy, 1986, 37.1: 31-39 2018.

[5] T. Kim, "Mitigation of Ecuadorian Earthquake Impact," pp. 195–219, 2018.

[6] H. H. Al-kayiem, "Potential of Renewable Energy Resources with an Emphasis on Solar Power in Iraq : Journal of Earthquake Research, 2018, 7.03: 195 2019.

[7] S. Edition, Solar Energy Engineering Processes and Systems Second Edition. .

[8] J. A. D. Deceased and W. A. Beckman, of Thermal Processes Solar Engineering.

[9]   Muntadher M. Ali, Dhafer Manea Hachim, Hassanain Ghani Hameed, "Numerical Investigation for Single Slope Solar Still Performance with Optimal Amount of Nano-PCM", Journal of Advanced Research in Fluid Mechanics and Thermal Sciences Vol. 63, Issue 2, pp. 302-316, 2019.

[10]   Adel A. Eidan Dhafer Manea Hachim, Assaad Alsahlani, "Measurements of Wind and Solar Energies in Najaf, Iraq", ADVANCES in NATURAL and APPLIED SCIENCES, Vol. 11, Issue 9, pp. 110-116, 2017.

[11]   Dhafer Manea Hachim AL-Hasnawi, Ali Abdulabbas Abdullah, Furkan Kamil, "Novel Technique for Photovoltaic Solar Cell Efficiency Enhancements by Coating with Chlorophyll" Journal of Physics: Conference Series, Vol. 1032, Issue 1, pp. 12-23, 2018.

[12] Hassanain Hammed, Dhafer Manea Hachim, AbdulRasool S. Al-Hilo, Ameer Mazen, Labran Ali, Narjes Maqdad, Zahraa Farhan, "Study the effect of dust

on performance of PV panel and design cleaning system", International Journal of Energy and Environment (IJEE), Vol. 10, Issue 3, pp.119-126, 2019.

[13] Adel A Eidan, Mohamed Al-Fahham, Dhafer Manea Hachim, Assaad Al-Sahlani, "Effect of Enhanced Evaporative Cooling on the Performance of Air-Conditioning in Severe Hot Weather", Journal of Engineering and Applied Sciences, Vol. 13, Issue 6, pp. 6814-6822, 2018.

[14] A. Hobbi and K. Siddiqui, "Optimal design of a forced circulation solar water heating system for a residential unit in cold climate using TRNSYS," Sol. Energy, vol. 83, no. 5, pp. 700–714, 2009.

[15] X. Yang, Y. Wang, and T. Xiong, "Numerical and experimental study on a solar water heating system in lhasa," Energies, vol. 10, no. 7, pp. 1–13, 2017.

[16] Dhakil N.Taha Furkan Kamil, Dhafer Manea Hachim AL-Hasnawi, "IMPROVEMENT THE PERFORMANCE OF POLYCRYSTALLINE SOLAR CELL BY COATING WITH MIXTURE OF POLYMER (NITRO CELLULOSE) AND BLUE VICTORIA DYE", International Journal of Mechanical Engineering and Technology, Vol. 9, Issue 11, pp. 2332-2338, 2018.

[17] Dhafer Manea. H. Al-Shamkhi, "Experimental Study of the Performance of Low Cost Solar Water Heater in Najaf City", International Journal of Mechanical & Mechatronics Engineering IJMME-IJENS, Vol. 16, Issue 1, pp. 109-121, 2018.

[18] Hassanain Hammed, Hayder Aziz Neema, "Experimental Study for Productivity Enhancement of a Parabolic Solar Concentrator System", Al-Qadisiya Journal for Engineering sciences, Vol. 4, No. 2, pp 37-41, 2011.

[19] Hassanain Gh. Hameed1, Ahmed H. Ali2, Zaid M. Al-Dulaimi3, "EXPERIMENTAL INVESTIGATION OF THE ENHANCEMENT PARAMETERS ON THE PERFORMANCE OF SINGLE-SLOPE SOLAR STILL", nternational Journal of Latest Trends in Engineering and Technology Vol.(10)Issue(3), pp.139-145

[20] Hasan S.Khwayyir, Ali Sh. Baqir, Hiba Q.Mohammed, "Effect of Air Bubble Injection on the Thermal Performance of a Flat Plate Solar Collector", Thermal Science and Engineering progress, https://doi.org/10.1016/j.tsep.2019.100476.

[21] Z. Haq, "Outline Grid Connected Solar : Technical and Policy Issues Solar Energy & Grid Connectivity Stand-alone PV Systems World Total Primary

Energy Supply (TPES) Electricity Demand and Electricity Shares by Sector 4 Electricity Generartion by Energy Source Renewable Energy Sources & Technologies," no. November, 2012.

[22] F. Guo, J. Zhang, M. Shan, and X. Yang, "Analysis on the optimum matching of collector and storage size of solar water heating systems in building space heating applications," Tsinghua University Press. p. 549-560, 2010.

[23] EE IIT, Kharagpur " Refrigeration & Air Conditioning " : Lesson," 2008.

[24] G. H. Hundy, A. R. Trott, and T. C. Welch, "Refrigeration and Air-Conditioning," Refrig. Air-Conditioning, 2008.

[25] Ali Sh. Baqir, Hameed B. mahood, "Optimisation and evaluation of NTU and effectiveness of a helical coil tube heat exchanger with air injection", Thermal Science and Engineering ProgressVolume 14, December 2019

[26] Ali Sh. Baqir, Hameed B. Mahood, Alasdair N. Campbell, Anthony J. Griffiths, "Measuring the average volumetric heat transfer coefficient of a liquid–liquid–vapour direct contact heat exchanger," Applied Thermal Engineering, vol. 103, pp.47-55, 2016.

[27] Hameed B. Mahood, A. N. Campbell, Ali Sh. Baqir, A. O. Sharif, R. B. Thorpe, "Convective heat transfer measurements in a vapour-liquidliquid three-phase direct contact heat exchanger, " Heat and Mass Transfer, vol. 54, no. 6, pp. 1697-1705, 2018.

[28] Nawfel M. Baqer, Ali Sh. Baqir, "Numerical Investigation for Enhancement of Heat Transfer in Internally Finned Tubes Using ANSYS CFX Program, " iasj, Basrah journal for engineering sciences, vol. 15, no. 1, pp. 32-42, 2015.

[29] Ali Sh. Baqir,"Theoretical and experimental study of direct-contact evaporation of a volatile drops (N-Pentane) in an immiscible liquid (distilled water),"PhD Thesis, Dep. of Mechanical Engineering, University of Basrah, Iraq, (2010).

[30] G. L. Morrison and J. E. Braun, "System modeling and operation characteristics of thermosyphon solar water heaters," Sol. Energy, vol. 34, no. 4–5, pp. 389–405, 1985.

[31] G. L. Morrison, I. Budihardjo, and M. Behnia, "Measurement and simulation

of flow rate in a water-in-glass evacuated tube solar water heater," Sol. Energy, vol. 78, no. 2, pp. 257–267, 2005.

[32] T. T. Chow, K. F. Fong, A. L. S. Chan, and Z. Lin, "Potential application of a centralized solar water-heating system for a high-rise residential building in Hong Kong," Appl. Energy, vol. 83, no. 1, pp. 42–54, 2006.

[33] A. Ucar and M. Inalli, "Thermal and economic comparisons of solar heating systems with seasonal storage used in building heating," Renew. Energy, vol. 33, no. 12, pp. 2532–2539, 2008.

[34] T. Mateus and A. C. Oliveira, "Energy and economic analysis of an integrated solar absorption cooling and heating system in different building types and climates," Appl. Energy, vol. 86, no. 6, pp. 949–957, 2009.

[35] S. R. Allen, G. P. Hammond, H. A. Harajli, M. C. McManus, and A. B. Winnett, "Integrated appraisal of a Solar Hot Water system," Energy, vol. 35, no. 3, pp. 1351–1362, 2010.

[36] L. M. Ayompe, A. Duffy, S. J. McCormack, and M. Conlon, "Validated TRNSYS model for forced circulation solar water heating systems with flat plate and heat pipe evacuated tube collectors," Appl. Therm. Eng., vol. 31, no. 8–9, pp. 1536–1542, 2011.

37] G. Serale, Y. Cascone, A. Capozzoli, E. Fabrizio, and M. Perino, "Potentialities of a low temperature solar heating system based on slurry phase change materials (PCS)," Energy Procedia, vol. 62, pp. 355–363, 2014.

[38] E. Ekramian, S. G. Etemad, and M. Haghshenasfard, "Numerical Analysis of Heat Transfer Performance of Flat Plate Solar Collectors," Journal of Fluid Flow, Heat and Mass Transfer (JFFHMT), 1, 38-42, 2014.

[39] K. Yao, T. Li, H. Tao, J. Wei, and K. Feng, "Performance Evaluation of All-glass Evacuated Tube Solar Water Heater with Twist Tape Inserts Using CFD," Energy Procedia, vol. 70, pp. 332–339, 2015.

[40] S. Sami, D. Semmar, A. Hamid, R. Mecheri, and M. Yaiche, "Viability of integrating Solar Water Heating systems into High Energy Performance housing in Algeria," Energy, vol. 149, pp. 354–363, 2018.

[41] P. Naphon, P. Assadamongkol, and T. Borirak, "Experimental investigation of titanium nanofluids on the heat pipe thermal efficiency," Int. Commun. Heat Mass Transf., vol. 35, no. 10, pp. 1316–1319, 2008.

[42] D. Reindl, S. K. Kim, Y. T. Kang, and H. Hong, "Experimental verification

of a solar hot water heating system with a spiral-jacketed storage tank," J. Mech. Sci. Technol., vol. 22, no. 11, pp. 2228–2235, 2008.

[43] H. Al-Madani, "The performance of a cylindrical solar water heater," Renew. Energy, vol. 31, no. 11, pp. 1751–1763, 2006.

[44] L. M. Ayompe, A. Duffy, M. M. Keever, M. Conlon, and S. J. Mccormack, "Comparative fi eld performance study of fl at plate and heat pipe evacuated tube collectors (ETCs) for domestic water heating systems in a temperate climate," Energy, vol. 36, no. 5, pp. 3370–3378, 2011.

[45] A. Parida, "Fabrication and Experimental Studies of a Hybrid Flat Plate Solar Collector for Heating Pool Water," National Institute of Technology, Rourkela. PhD Thesis no. 107, 2011.

[46] T. Yousefi, F. Veysi, E. Shojaeizadeh, and S. Zinadini, "An experimental investigation on the effect of Al2O3-H2O nanofluid on the efficiency of flat-plate solar collectors," Renew. Energy, vol. 39, no. 1, pp. 293–298, 2012.

[47] P. Gang, L. Guiqiang, Z. Xi, J. Jie, and S. Yuehong, "Experimental study and exergetic analysis of a CPC-type solar water heater system using higher-temperature circulation in winter," Sol. Energy, vol. 86, no. 5, pp. 1280–1286, 2012.

[48] E. Nouvelles, I. Seminar, and R. Energies, "Estimation of the Direct Solar Radiation on Fixed and Tracking System in Algeria," The 2 nd International Seminar on New and Renewable Energies no. 4, pp. 1–4, 2012.

[49] M. K. Ahmad, "Minimizing the energy consumption for building by using the concentrating water solar collector in hot arid region " Experimental work " Introduction :," vol. 16, no. 3, pp. 50–60, 2012.

[50] G. Pei, G. Li, X. Zhou, J. Ji, and Y. Su, "Comparative experimental analysis of the thermal performance of evacuated tube solar water heater systems with and without a mini-compound parabolic concentrating (CPC) reflector(C < 1)," Energies, vol. 5, no. 4, pp. 911–924, 2012.

[51] F. Wayne, "AC 2012-3019 : SOLAR WATER HEATING SYSTEM EXPERIMENTAL," 2012.

[52] F. Cruz-Peragon, J. M. Palomar, P. J. Casanova, M. P. Dorado, and F. Manzano-Agugliaro, "Characterization of solar flat plate collectors," Renew. Sustain. Energy Rev., vol. 16, no. 3, pp. 1709–1720, 2012.

[53] M. A. Fazilati and A. A. Alemrajabi, "Phase change material for enhancing

solar water heater, an experimental approach," Energy Convers. Manag., vol. 71, pp. 138–145, 2013.

[54] L. M. Ayompe and A. Duffy, "Thermal performance analysis of a solar water heating system with heat pipe evacuated tube collector using data from a field trial," Sol. Energy, vol. 90, pp. 17–28, 2013.

[55] P. K. Mongre, "Experiment study of solar water heater with circulating pump and using of Aluminum tube .," vol. 4, pp. 384–391, 2013.

[56] N. A. Ogie, I. Oghogho, and J. Jesumirewhe, "Design and Construction of a Solar Water Heater Based on the Thermosyphon Principle," J. Fundam. Renew. Energy Appl., vol. 3, pp. 1–8, 2013.

[57] S. K. Sharma and D. Joshi, "Fabrication and Experimental Investigation of V-Through Flat Plate Collector in Hot Climatic Conditions of Rajasthan : A Case Study of Jaipur .," vol. 3, no. 5, 2013.

[58] J. V Madan and O. M. Sirse, "Experimental Study On Efficiency Of Solar Collector At Nagpur (India) During Winter," vol. 4, no. 08, 2015.

[59] A. K. Pandey, V. V. Tyagi, N. A. Rahim, S. C. Kaushik, and S. K. Tyagi, "Thermal performance evaluation of direct flow solar water heating system using exergetic approach," J. Therm. Anal. Calorim., vol. 121, no. 3, pp. 1365–1373, 2015.

[60] X. Luo et al., "Experimental on a novel solar energy heating system for residential buildings in cold zone of China," Procedia Eng., vol. 205, no. December, pp. 3061–3066, 2017.

[61] S. P. Lokhande and H. K. Dubey, "'Experimental Analysis of Solar Water Heater, with Heat Exchanger,'" IOSR J. Mech. Civ. Eng., vol. 14, no. 01, pp. 55–59, 2017.

[62] E. Bellos and C. Tzivanidis, "Development of an analytical model for the daily performance of solar thermal systems with experimental validation," Sustain. Energy Technol. Assessments, vol. 28, no. March, pp. 22–29, 2018.

[63] P. M. E. Koffi, H. Y. Andoh, P. Gbaha, S. Touré, and G. Ado, "Theoretical and experimental study of solar water heater with internal exchanger using thermosiphon system," Energy Convers. Manag., vol. 49, no. 8, pp. 2279–2290, 2008.

[64] I. Budihardjo and G. L. Morrison, "Performance of water-in-glass evacuated tube solar water heaters," Sol. Energy, vol. 83, no. 1, pp. 49–56, 2009.

[65] R. Li, Y. Dai, and R. Wang, "Experimental investigation and simulation analysis of the thermal performance of a balcony wall integrated solar water heating unit," Renew. Energy, vol. 75, pp. 115–122, 2015.

[66] Y. W. Koholé and G. Tchuen, "Experimental and numerical investigation of a thermosyphon solar water heater," Int. J. Ambient Energy, vol. 0750, no. May, pp. 1–11, 2018.

[67] Z. Liu, D. Wu, H. Yu, W. Ma, and G. Jin, "Field measurement and numerical simulation of combined solar heating operation modes for domestic buildings based on the Qinghai–Tibetan plateau case," Energy Build., vol. 167, pp. 312–321, 2018.

[68] M. Potter and D. C. Wiggert, Fluid Mechanics - Schaum's Outlines. 2008.

[69] S. Nicklas, G. Strehlow, S. W. Duda, and P. Simmonds, No Title, no. 28. 2016.

[70] I. Propylene and G. H. Transfer, "Engineering and Operating Guide."

[71] Alghamdi, Integration of Process Modeling, Design, and Optimization with an Experimental Study of a Solar-Driven Humidification and Dehumidification Desalination System. 2018.

Appendix A
Calibration

Appendix A
Calibration

1. Calibration

The relationship between the value of the input to the measurement system and the system's indicated output value is established during the calibration of the measurement system. The wind velocity, the rate of humidity, solar radiation and temperature were measured in this work. In this research, the anemometer is used to measure wind velocity; the digital Pyranometer is used to measure the solar radiation, Thermocouples are used to measure temperatures. Also, the digital hygrometer is used to measure the relative humidity. Since these devises are easy to handle and have acceptable accuracy in measuring. The accurate measurements can be checked by calibrating the equipment at standard conditions or by comparing with other suitable measurement devices. The calibrated gauges must be matched to the correct measuring devices.

2. Thermocouple Calibration

Thermocouples are the most widely used temperature sensors in test and development work. Therefore sometimes will be spent during the following subsection to explain their function and what precautions were undertaken to ensure their accuracy for the experiments carried out for this study. During the experimentation carried, T-type thermocouples were used due to the suitability of temperature range and highest accuracy amongst the different thermocouple types. Thermocouple calibration consists of recording the temperature, measured, and indication by a standardized thermometer, both in a constant temperature bath. For thermocouples with fiberglass insulation, a sample thermocouple is calibrated. All other thermocouples were calibrated combined. Figures (A.1 – A.4) presents the

relation between the thermometer results with standard mercury thermometer (zero degree centigrade of the mixture of ice and water).These results are used to calibrate the thermometer device. Results of the calibration can be found below.
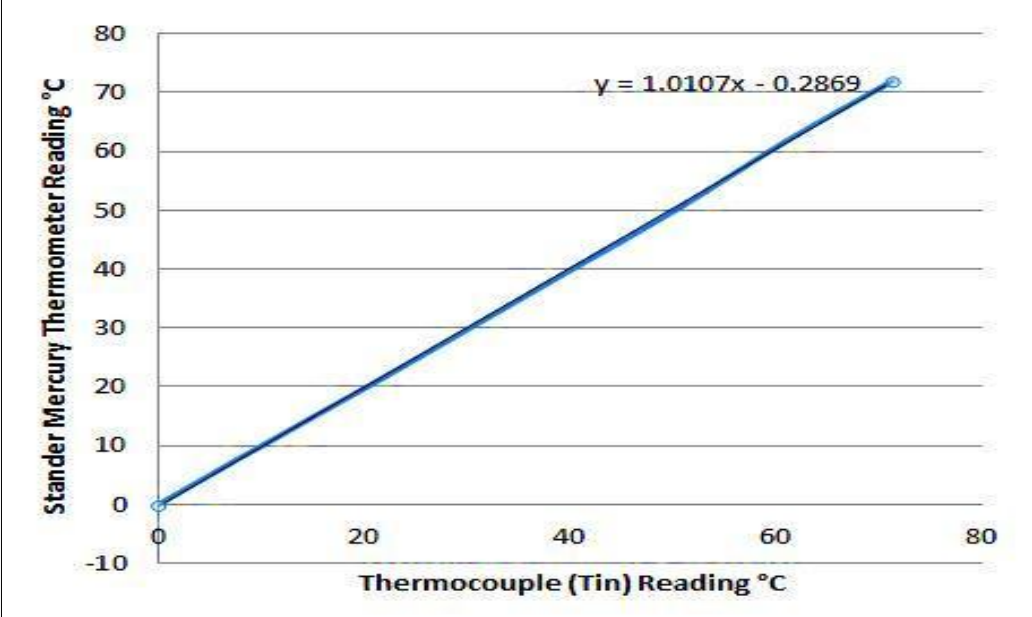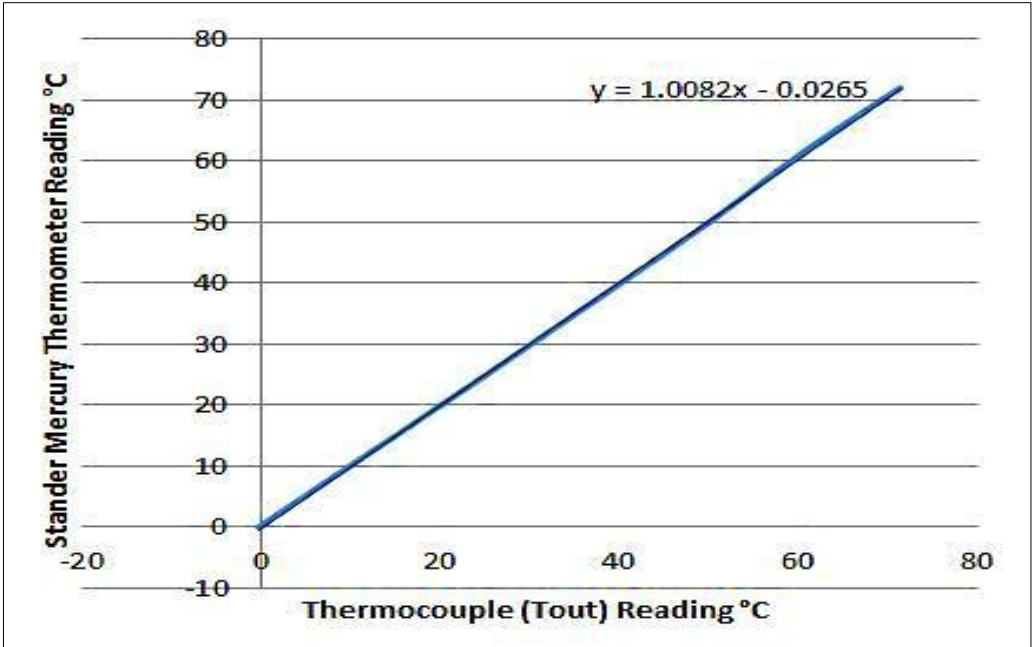

Fig. A.1 Calibration of thermocouple (T_{in})

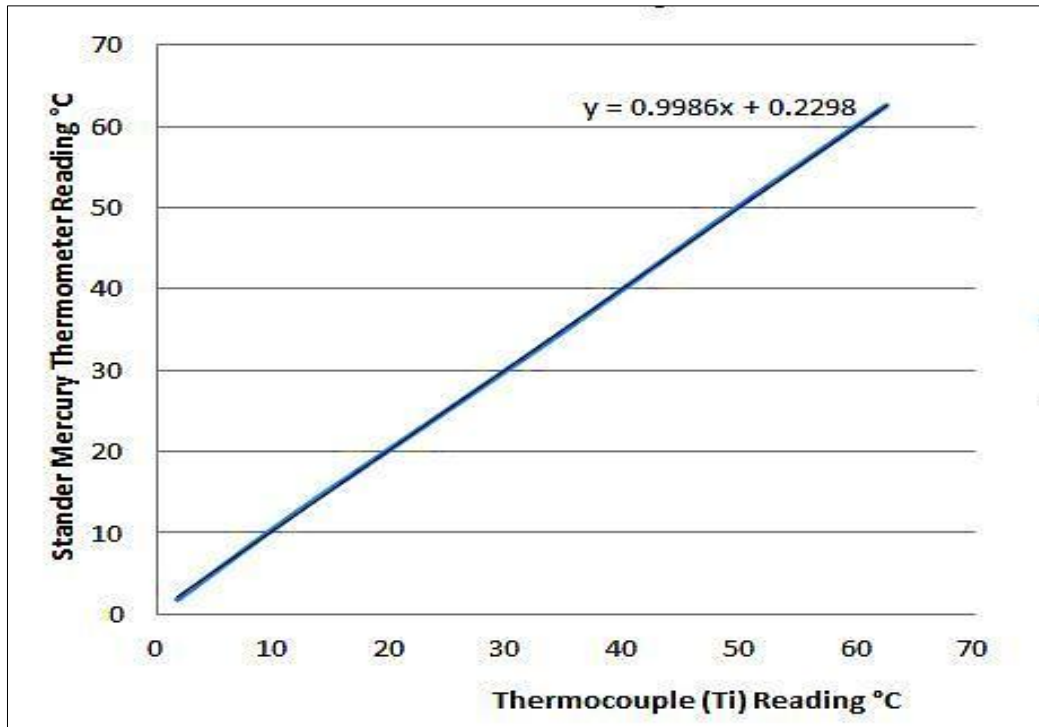

Fig. A.2 Calibration of thermocouple (T_{out})
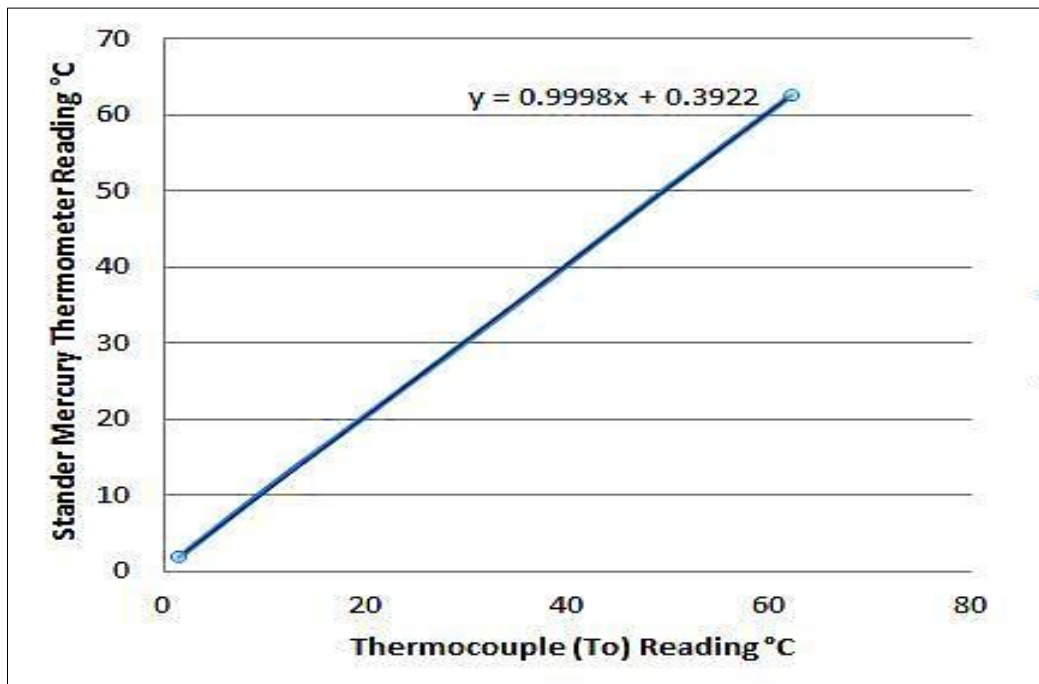
Fig. A.3 Calibration of thermocouple (T_i)

Fig. A.4 Calibration of thermocouple (T_o)

3. Flowmeter calibration
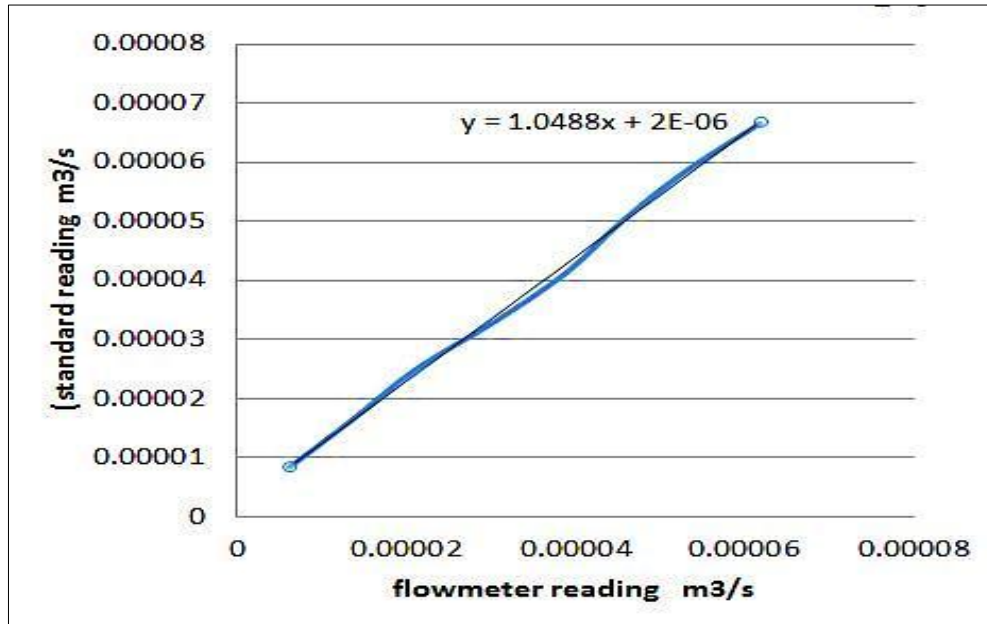
Figure A.18 shows the flowmeter calibration.

Fig. A.5 shows the flowmeter calibration

4. Hygrometers Calibration

Figure A.18 shows the relation between two types of hygrometers.
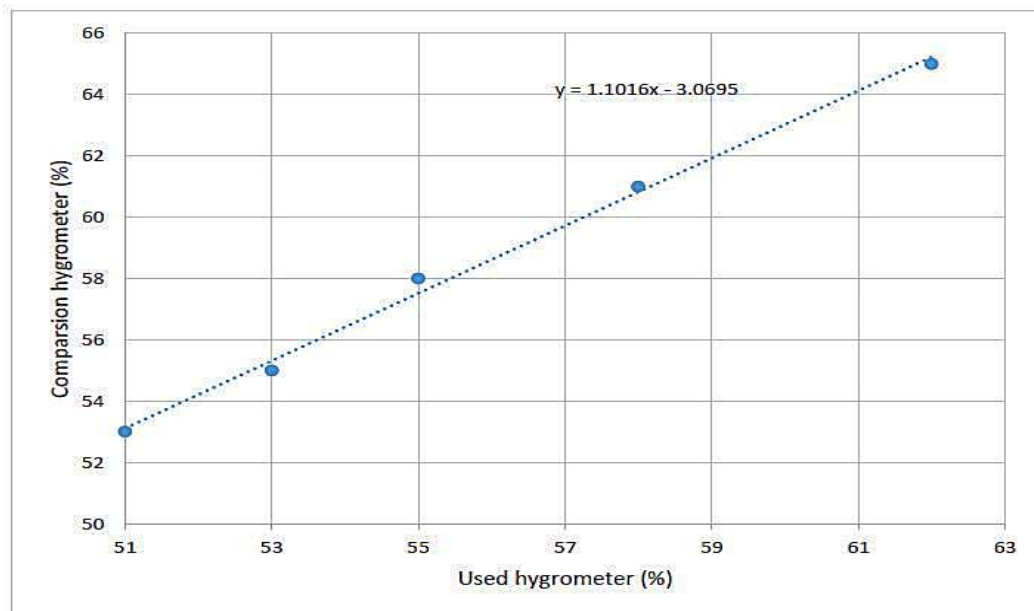Results of the calibration can be found below.

Fig. A.6 Calibration of Hygrometers

Appendix B
Data of Experimental Work

Appendix B
Data of Experimental Work

Table 1-B Data of experimental work of solar radiation, ambient temperature and wind speed for day (9-1-2019).

Time (hr)	Solar radiation (W/m²)	Ambient temperature (°C)	Wind speed (m/s)
09:00	530	9.8	1.8
10:00	752	11.3	2.7
11:00	907	13.2	3.1
12:00	967	15.9	3.6
01:00	961	17	2.7
02:00	839	17.2	3.6
03:00	675	17.2	3.4
04:00	420	17.5	2.7
05:00	95	16.2	2.2

Table 2-B Data of experimental work of solar radiation, ambient temperature and wind speed for day (20-1-2019).

Time (hr)	Solar radiation (W/m²)	Ambient temperature (°C)	Wind speed (m/s)
09:00	500	13.68	4.5
10:00	853	15.96	2.7
11:00	875	16.66	3.6
12:00	985	17.76	2.7
01:00	980	17.82	2.2
02:00	860	17.64	2.4
03:00	684	17.16	2.2

Table 3-B Data of experimental work of solar radiation, ambient temperature and wind speed for day (20-2-2019).

Time (hr)	Solar radiation (W/m²)	Ambient temperature (°C)	Wind speed (m/s)
09:00	720	12	0
10:00	793	14.4	0.4
11:00	1002	16.5	0.45
12:00	1103	17.9	0
01:00	1071	18.6	0.4
02:00	967	19.3	1.3
03:00	767	18.4	1.8
04:00	517	19.4	0.9
05:00	159	17.6	0.75

Table 4-B Data of experimental work of solar radiation, ambient temperature and
wind speed for day (24-2-2019).

Time (hr)	Solar radiation (W/m^2)	Ambient temperature (^{o}C)	Wind speed (m/s)
09:00	591	16.5	3.1
10:00	722	17.6	2.2
11:00	999	18.4	2.7
12:00	1080	18.1	2.2
01:00	1095	18.4	1.8
02:00	966	18.3	1.3
03:00	745	18.3	1.4
04:00	506	17.4	0.9
05:00	186	16.6	0.4

Table 5-B Data of experimental work of solar radiation, ambient temperature and
wind speed for day (28-2-2019).

Time (hr)	Solar radiation (W/m^2)	Ambient temperature (^{o}C)	Wind speed (m/s)
09:00	688	14.63	0
10:00	840	15.26	0
11:00	1051	16.16	0.4
12:00	1177	17.61	0.5
01:00	1162	17.79	0.9
02:00	1077	17.85	0.4
03:00	887	17.16	0.9
04:00	601	17.34	1.3
05:00	246	16.52	0.9

Table 6-B Data of experimental work of solar radiation, ambient temperature and
wind speed for day (19-3-2019).

Time (hr)	Solar radiation (W/m^2)	Ambient temperature (^{o}C)	Wind speed (m/s)
10:00	1015	16	0.4
11:00	1175	17.3	0.45
12:00	1224	19	0.4
01:00	1206	19.4	0.5
02:00	1083	19.3	0.9
03:00	901	18.5	0.4
04:00	619	18.3	0.4
05:00	271	17.8	1.3

Appendix C
Publish Papers from Thesis

Experimental Study of the Performance of A Flat Plate Solar Water Heater

Mohammed Jasim O. alghurabe

Construction committee-Najaf Governorate

Najaf city, Iraq

Mohammadjasim25@gmail.com

Dhafer Manea H. Al-Shamkhee, Assaad Alsahlani
Engineering Technical College / Najaf, Al-Furat Al-Awsat Technical University
Najaf city, Iraq
dhafeer_manee@yahoo.com
alsahlan@msu.edu

Abstract__ **Flat Plate collector is the most common type of solar water heater, due to its low price, easy installation, and long life. The efficiency of a solar collector is key to evaluating its performance in thermal facilities, especially applications requiring low or medium temperatures. The most important factors affecting the efficiency of the solar collector are the weather conditions, the design of the collector, the type of work fluid used. A Flat plate collector tested experimentally in solar heating system worked by direct flow and closed system to heating space in Najaf, Iraq (32° 1' N / 44° 19' E). Experimental results showed that the overall daily efficiency of the collector reached 37.16%. Moreover, the maximum temperature of hot water for collector reached 57.1oC**

Keywords: flat plate collector, an experimental test, solar radiation

Nomenclature

Q_u *useful work*   *(W/m^2)*

I_T *solar irradiation (W/m^2)*

η *efficiency of the collector*

A_c *collector area (m$^{2)}$)*

T_{in} *inlet water temperature (℃)*

T_{out} *outlet water temperature (℃)*

S *absorbed solar radiation (W/m^2)*

U_L *overall heat loss coefficient based on (W/m^2 K)*

T_{pm} *plate temperature (℃)*

T_a *ambient temperature (℃)*

T_m *Average temperature of the water inside and outside of the collector*

I. INTRODUCTION

The economic growth in countries and the increase in population have led to increasing the demand for energy. Currently, the need for energy is primarily met by fossil fuels, which it source of toxic gases that pollute the environment, So that could run out shortly. Leading to a threat to energy availability in countries around the world. This has made many countries to diversify energy sources. The most important of these sources are renewable energy because it is sustainable, clean, and can contribute to reducing environmental pollution. A large amount of energy is used for heating in buildings and produce hot water for household use. Solar water heaters can supply much of the heat energy required especially in-home uses. One of the most important types of solar water heaters is flat plate collectors because they are characterized to be easy in manufacturing, cheap costs, easy installation, and low maintenance costs. The researchers have developed flat plate collectors to improve their performance and efficiency through the geometrical design of the collector, enhancement of the thermal properties of working fluid and studied the impact of weather changes on its performance. Solar water heaters convert solar radiation falling on the absorber into thermal energy and then the heat is transferred to the working fluid inside the tubes then hot water is kept in the thermal storage tank. With flat-plate collectors are extensively studied theoretically and experimentally over the past several decades. For instance:

(Morrison and Braun 1985) Studied the performance of the thermosyphon approach of solar water heaters for the model of two type tank: horizontal and vertical numerically. Numerical results showed a discrepancy in the results obtained from two locations. They noticed that when the thermosyphon operates at its best performance, it can provide enough hot water for daily use. Moreover, the horizontal tank system is better than the vertical tank system in the same operating conditions.

(Chow et al. 2006) Evaluated the daily production of domestic hot water DHW in high- rise virtual building in Hong Kong by fixing central solar water heaters SWH in the south and west vertical facades of the building. The economic feasibility study was carried out in terms of technical and cost aspects. The results of the numerical model reported that the evaluated annual thermal energy produced was 904GJ, and the

thermal efficiency of solar water heater collector was 38.4% and average annual hot water temperature achieved was 41.4C .payback period was 9.2 years and this period can be less if energy saving for air cooling is taken into consideration contribute solar collector by blocking the solar radiation on building facades.

(Hobbi and Siddiqui 2009) studied the performance of solar water heaters with an indirect forced flow rate to provided domestic hot water for a single-family house in Montreal, Canada using flat plate collector and evaluated by simulation using TRNSYS software tool to analysis all main design parameters for system and collector and determined the optimum value for its. Moreover, consider the solar fraction was the optimization parameter. The simulation results explained that the rapid increases of solar fraction and collector efficiency when circulation rate increases. Moreover, the system can produce 83–97% in summer and 30–62% in winter from hot water needs. Moreover, found the collector non-selective coated locally made can provide 54% from annual water heating demands which obtained by solar energy.

(Serale et al. 2014) Proposed an enhancement for thermal performance of flat plate collector which produce limited temperature. Thermal enhancement can be achieved by using latent heat. Which can be obtained by fitted slurry phase change material PCS with water and surfactants and heat carried the fluid are evaluated. This study suggested that conceptual proposals to an integrated solar thermal system with slurry PCMs were presented, and a prototypal system based on n-eicosane PCS was developed. This leads to giving the system thermo-physical and rheological properties and material behavior that interest flat-plate solar thermal collectors. To interface possible problems to use of PCSs as HTF such as clogging in pipes, high-pressure drop, some sedimentation in the storage tank and capsule rupture as a result to pumping work, suitable design solution was taken.

(Sami et al. 2018) Investigated the energetic and economic possibility of the integration of flat plate collector solar water heaters system with high energy performance housing. They choose four houses in different locations to have a distinct climatic zone in Algeria to study this case. The evaluation of this study based on calculations depending on using the F-Chart method with monthly weather station data characterizing each region. The study focused on finding the optimum solar collector area, which minimized the cost of installation in versus economic and energetic aspects. The results showed that the SWH contributed to saving the traditional energy reach to 46% and 57% in northern and southern regions respectively and in the same time-saving in the annual operating cost of the solar system reached 51% and 69% respectively.

(Yousefi et al. 2012) Evaluated the effect of nanofluid (Al2O3-water) as an absorbing medium to enhance the thermal efficiency of a flat plate collector. Nanofluid tested with a mass concentration of 0.2% and 0.4 %, With or without used surfactant Triton X-100, Nanoparticle has diameter 15 nm and circulation rate varied (1-3) L/min. Experiments showed that the thermal efficiency of FPC system enhancement reached 28.3% by using nanofluid 0.2 wt% Al2O3 in comparison with water base fluid and maximum improvement efficiency by use surfactant was 15.63%.

Based on previous studies, The research aims to study the thermal performance of flat solar collector experimentally in Najaf, Iraq, and to calculate the useful energy and efficiency of solar collector.

The collector efficiency is defined as the ratio of the useful energy delivered to the energy incident on the collector aperture area as shown in equation (1). The incident solar flux consists of direct and diffuse radiation. While flat-plate collectors can collect both as following.

$$\eta = \frac{Q_u}{I_T A_c} \qquad (1)$$

While the heat energy extracted from the collector or the useful heat can be calculated from equation (2).

$$Q_u = A_c[S - U_L(T_{pm} - T_a)] \qquad (2)$$

The overall daily efficiency of the collector can be calculated from the equation (3)

$$\eta = \frac{\sum Q_u}{A_c \sum I_T} \qquad (3)$$

II. Validation works

E. Ekramian[7] presented his work numerically and compared the work with experimental results presented by Cruz-Peragon[8] for identical parameters and conditions. Where in this study, the flat plate solar collector contains 15 riser tubes. Solar incident irradiation was 936.8 W/m2. Water inlet temperature, ambient temperature, and water flow rate are 31°C, 23.2 °C and 6.42 kg/h. Respectively. The thickness of the glass cover and absorber are 4mm and 2mm, respectively. The inner diameter of risers was 10 mm, and the distance between risers was 30 mm with riser's length of 450 mm. Numerical results of E. Ekramian. The study showed that the average relative error between the experimental and numerical results is about 5.5%. In our work, a numerical study was conducted on the solar collector and operation condition used by Cruz-Peragon et al. [8]. Where the numerical results were obtained more accurate and approximate to the experimental results, and the average relative error ratio of experimental data to numerical results is about 0.062%. as shown in Figure (1)
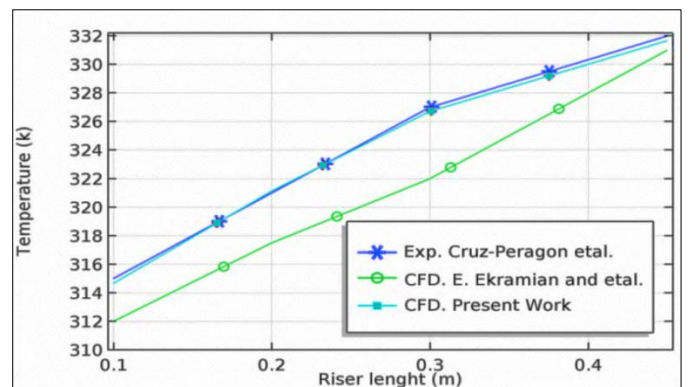

Fig. (1) Comparison between experimental and numerical temperature

Fig. (3) Flat plate collector

III. Experimental work

A. System Description

The experimental work consists of several parts, as shown in Figure (2). The central part is the solar water heater flat plate collector which is installed at the roof of the college building as shown in Figure (3). The specifications of the flat-plate solar collector indicated in table I. Parts of the collector surrounded by an aluminum structure. This system is working by forced convection by circulation working fluid in the system by using electrical 0.5 hp bump. Flowmeter installed before the collector to measure water flow rate input to the
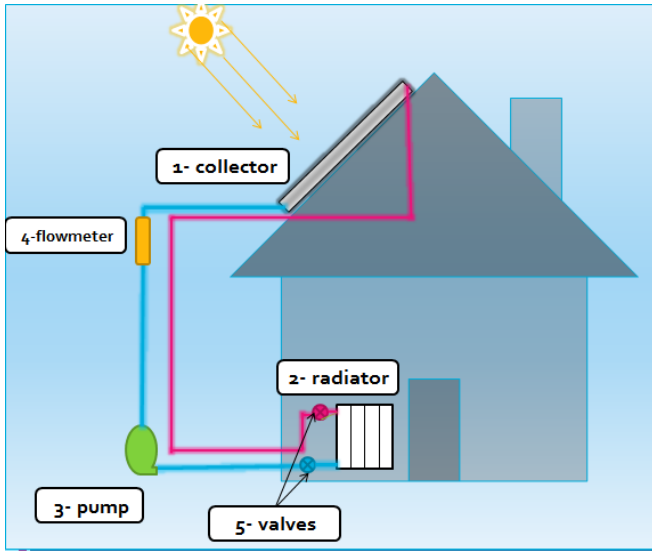
.collector. The last part is the radiator with dimensions (100x60) cm, which is placed inside the laboratory as shown in Figure (4). Hot water is transferred between the collector and the radiator by polyethylene pipes surrounded by insulating material, and valves control flow rate inside the system.
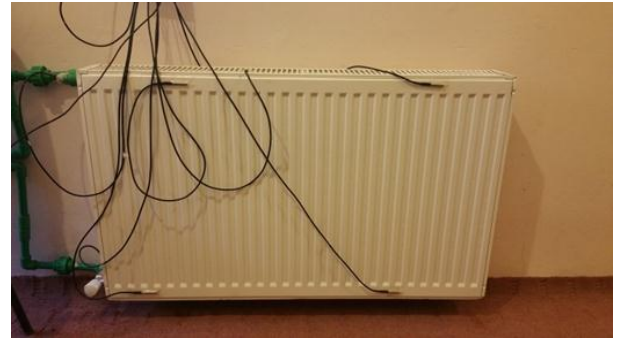

Fig. (4) Indoor radiator

A data logger as shown in figure (5) with seven thermocouples type (T) is connected to different locations in the collector to record temperatures of inlet and outlet water by two thermocouples fixed inside pipes, three thermocouples fixed in the top, bottom and centre of glass, two thermocouples for edge and back of collector. The ambient temperature recorded from the weather station of laboratory and Solar irradiation measured by the solar radiation sensor.

Fig. (2) scheme of the experimental rig

Table I. The Specifications of the Flat-Plate Solar Collector

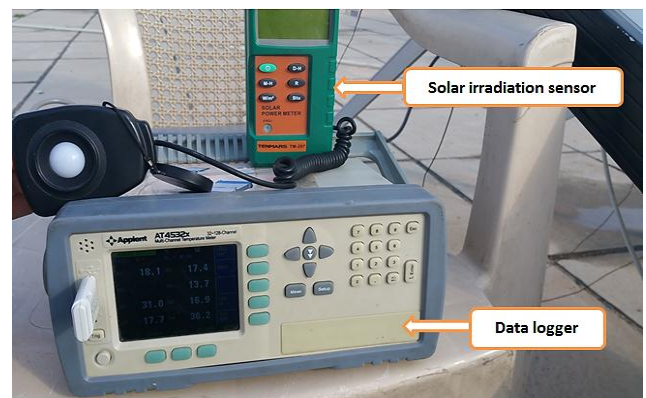| Specification	details
Dimension of collector	(2000x1000x80)mm
Glass cover thickness	3.2 mm
Aluminum Absorber plate thickness	0.7 mm
Header tube diameter	22mm / 2 headers
Riser tube diameter	8mm / 7 risers
glass wool insulation thickness	30 mm

Fig. (5) Show data logger and solar irradiation sensor

3

B. Testing method

The solar collector is experimentally investigated at AL-Furat AL-Awsat University/ Engineering Technical College in Najaf, Iraq (32° 1' N / 44° 19' E). The collator is installed facing the south with a Tilt angle of 32^0. Experiments are conducted on 9 January 2019 from 9:00 am to 5:00 pm. During this period, solar radiation falls on the solar heater collector, where solar radiation was passed through the glass cover and falls on the absorber plate, which it converts the solar radiation into thermal energy causing temperature rise. Conductive heat transfer occurs between absorber plate and tubes, and heat transfer from tubes to working fluid by convection. Hot water comes out of the collector and passes through the pipelines to input indoor radiator. The heat is transferred from the hot radiator surface to the indoor room by the convection and radiation causing indoor temperature rise and heating the room. The electric pump then pumps the outlet water from the radiator into flow meter then return to the solar collector. System tested underflow rate 60L/hr. Several factors affect the efficiency of the collector such as the ambient temperature, wind speed and the intensity of solar radiation which can study their effect on performance of collector.

IV. Results and discussions

The experiments are performed from 9:00 am to 5:00 pm on 9 Jan 2019 in Najaf city. At first, we review the weather conditions on this day. Figure (6) showed time variation of solar radiation and ambient temperature during test period where the maximum solar irradiance reach of $987W/m^{2,}$ as for the ambient temperature was low at the first time and reached $9.8C^o$ then it increased until it reached 17.5The highest temperature difference was recorded at 12.5 . Figure (7) showed time variation of the wind speed which ranged from (1.8 to 4) m/s.
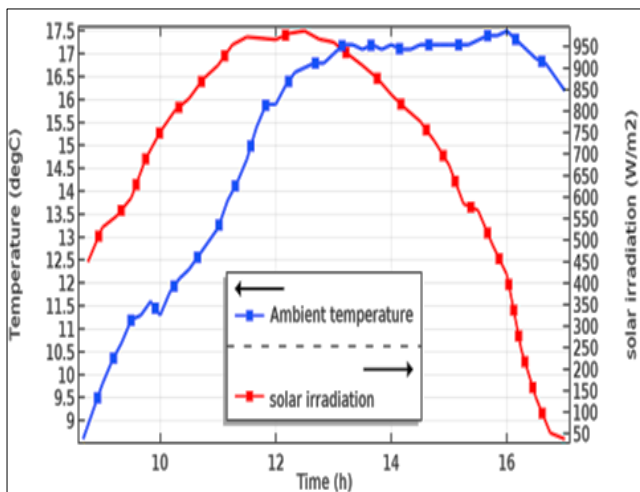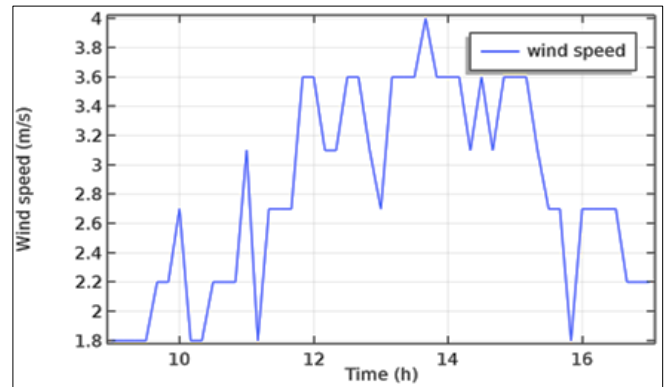

Fig. (7)Hourly variation of the wind speed on 9/1/2019

Flat plate collector tested experimentally under variable climatic parameters, and also the inlet water temperature of collector was continuously changing because the working fluid in the system flows in a closed system. The outlet water of the collector comes out at high temperature and then returns to it at a lower temperature. Due to the loss of part of its thermal energy in space heating. By repeating this process the inlet water temperature of the collector will change continuously. The system tested with the mass flow rate of water of 60L/hr. The performance of flat plate collector depends mainly on solar radiation absorbed by the collector. On the contrary, an increase in wind speed causes an increase in heat losses by convection and reduces the efficiency of the collector. Figure (8) show the time variation in the inlet and outlet water temperature of the collector through from 9:00 am to 5:00 pm, The outlet temperature of collector increase when solar irradiance increase and vice versa. It has been noted that increasing wind speed contributes to increased thermal losses and reduces the outlet water temperature of the collector. The maximum temperature recorded was 57.1^oC at 12:58 pm., Figure (9) shows the time variation of the temperature difference between the outlet and inlet of the collector, The highest temperature difference recorded was 12.5The highest temperature difference was recorded at $12.5\ ^oC$.

Fig. (6)Hourly variation in solar irradiance and ambient temperature on 9/1/2019
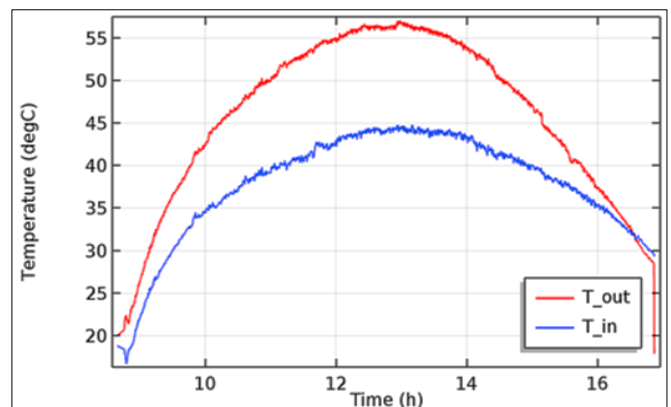

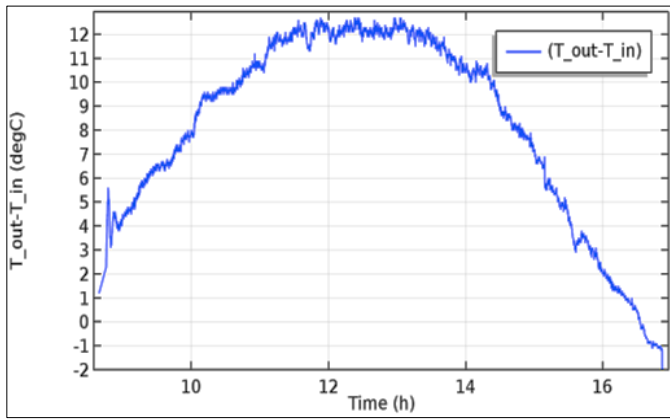Fig. (8) hourly variation of inlet and outlet temperature of collector

4

Fig. (9) Hourly variation for the difference between outlet and inlet temperature of the collector

Figure (10) showed the time variation of useful heat of collector which represents the generated heat in absorber as a result of falling solar radiation minus heat loss by convection and radiation form collector. Useful heat can be calculated from the recorded temperature of the water inside and out from a collector at each specific time. Maximum instantly value of useful heat was 886W.
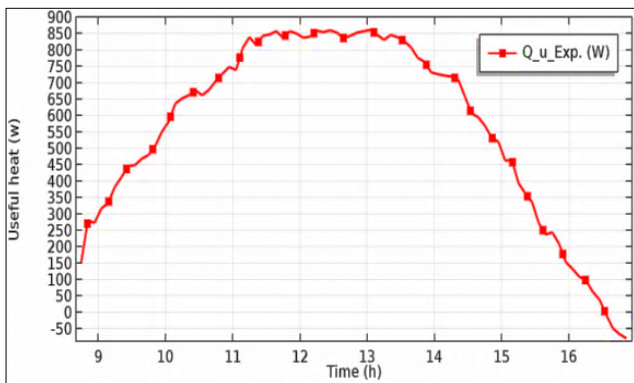

Fig. (10) hourly variation of useful heat of collector from 9:00 am to 5:00 pm on 1 January 2019

Figure (11) showed the time variation of the efficiency of collector which represents the ratio of useful heat of collector to solar irradiance falling on the area of the collector in the specified time. The maximum value of instantly efficiency reached 50.44% at 1:27 pm.
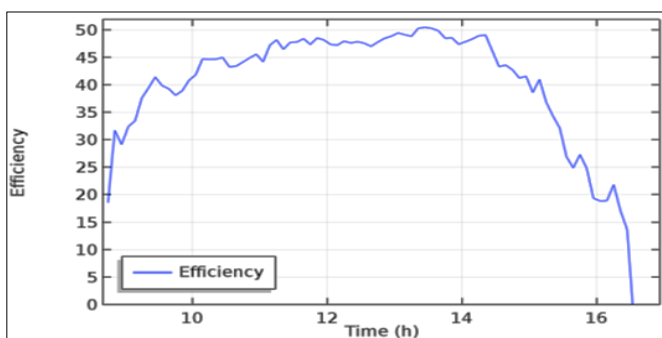

Fig. (12) Show a typical collector efficiency curve

Fig. (11) Hourly variation of efficiency of the collector from 9:00 am to5:00 pm on 1 Jan 2019

Collector efficiency is not always a good indicator of overall collector performance. On any given day, a solar collector can operate over a wide range of efficiencies as solar radiation, ambient temperature, and heat transfer fluid temperature change. Figure (12) showed an efficiency curve between the instantaneous efficiency and the temperature difference between the average water temperature and the ambient temperature divided on solar irradiance.
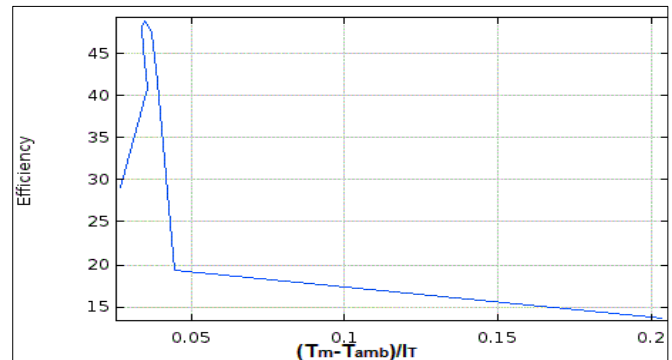
V.   Conclusion

The thermal performance of the flat plate solar collector is studied experimentally under weather conditions of Najaf, Iraq. During cold weather conditions on 9/1/2019. The thermal energy extracted from the solar collector has been used for space heating. This study focused on the effect of climate parameters changes on the efficiency of the collector and concluded the study to the following:
• Najaf city characterized by its geographical location with high solar radiation rates, which encourages the use of solar water heaters for household use and heating space.
• The maximum temperature of hot water for collector reached 57.1^{o}C.
• The overall daily efficiency of the collector reached 37.16%, While the highest value for instant efficiency was 50.44%.
• The maximum value of instantly useful heat of solar collector was 886W and the daily amount of useful heat reached 3355.734KW, This amount of energy contributes to saving of electricity consumption and achieves the economic feasibility of the use of flat plate solar water heaters.

References

References

[1]   G. L. Morrison and J. E. Braun, "System modelling and operation characteristics of thermosyphon solar water heaters," Sol. Energy, vol. 34, no. 4–5, pp. 389–405, 1985.

[2]   T. T. Chow, K. F. Fong, A. L. S. Chan, and Z. Lin, "Potential application of a centralized solar water-heating system for a high-rise residential building in Hong Kong," Appl. Energy, vol. 83, no. 1, pp. 42–54, 2006.

[3]   A. Hobbi and K. Siddiqui, "Optimal design of a forced circulation solar water heating system for a residential unit in cold climate using TRNSYS," Sol. Energy, vol. 83, no. 5, pp. 700–714, 2009.

[4]   G. Serale, Y. Cascone, A. Capozzoli, E. Fabrizio, and M. Perino, "Potentialities of a low temperature solar heating system based on slurry phase change materials (PCS)," Energy Procedia, vol. 62, pp. 355–363, 2014.

[5]   S. Sami, D. Semmar, A. Hamid, R. Mecheri, and M. Yaiche, "Viability of integrating Solar Water Heating systems into High Energy Performance housing in Algeria," Energy, vol. 149, pp. 354–363, 2018.

[6]   T. Yousefi, F. Veysi, E. Shojaeizadeh, and S. Zinadini, "An experimental investigation on the effect of Al2O3-H2O nanofluid

on the efficiency of flat-plate solar collectors," Renew. Energy, vol. 39, no. 1, pp. 293–298, 2012.

[7]   E. Ekramian, S.Gh. Etemad, M. Haghshenasfard,   " Numerical Analysis of Heat Transfer Performance of Flat Plate Solar Collectors", Journal of Fluid Flow, Heat and Mass Transfer Volume 1, Year 2014

[8]   Cruz-Peragon, F., Palomar, J.M., Casanovab, P.J., Dorado, M.P., Manzano-Agugliaro, F., (2012). Characterisation of solar flat plate collectors .Renewable and Sustainable Energy Reviews 16, 1709– 1720

الملخص

في هذا العمل ، تم استخدام سخانات المياه بالطاقة الشمسية لتدفئة حيز الغرفة عن طريق تمرير السائل الساخن من مجمع الطاقة الشمسية إلى الراديتر داخل الغرفة. يهدف هذا العمل إلى توفير الطاقة الكهربائية وتوفير الكلف المالية وتقليل التلوث البيئي . أجريت دراسة عددية وتجريبية لتقييم الأداء الحراري لنظام التدفئة الشمسية. أجريت اختبارات تجريبية لتدفئة غرفة مساحتها 10م^2 باستخدام سخانات المياه بالطاقة الشمسية المسطحة (FPC) في الكلية التقنية الهندسية / جامعة الفرات الاوسط التقنية في وحدة أبحاث الطاقة البديلة والمتجددة في النجف / العراق (31.59^0 شمالاً ، طول 44.19^0 شرقًا) في غضون ثلاثة أشهر (كانون الثاني، شباط، اذار) 2019. العوامل التي تمت دراسة تأثيرها هي (الأحوال الجوية ، ونوع مائع العمل ، والتحليل الاقتصادي للنظام). الدراسات العددية تمت بواسطة برنامج المحاكاة COMSOL 5.3 لتحليل الأداء الحراري لسخان المياه بالطاقة الشمسية المسطح ، حيث تمت دراسة تأثير (معدل تدفق الحجمي، نوع السائل العمل، وظروف الطقس). أظهرت النتائج العددية أن معدل التدفق الحجمي الأمثل كان 40 لتر/ساعة. وحقق خليط الإيثلين كليكول-الماء أعلى كمية من الطاقة الحرارية والكفاءة بالمقارنة مع الموائع الأخرى بنفس معدل التدفق الحجمي. أظهرت النتائج التجريبية أن استخدام زيت المحرك نوع (10W-30) كمائع عمل يعطي أعلى كمية من الطاقة الحرارية والكفاءة عند معدل التدفق الحجمي العالي مقارنة بالسوائل الأخرى. ساهم نظام التسخين الشمسي في توفير الطاقة الكهربائية بمعدل 34٪ من إجمالي الطاقة اللازمة لتسخين الغرفة في أيام الاختبار في كانون الاول. اما في شباط واذار فكانت 39.5 ٪ و 86 ٪ على التوالي. أظهر التحليل الاقتصادي لاستخدام أنظمة التدفئة أن متوسط الكلفة المدخرة كانت 38000 دينار عراقي/الشهر. في حين أن فترة استرداد كلفة الاستثمار الاولي لمنظومة التدفئة الشمسية كانت 5.2 سنة. النتائج العددية كانت متوافقة مع النتائج التجريبية وكان نسبة الخطأ الأقصى لا تتجاوز(8٪) بين النتائج النظرية والتجريبية.

دراسة عددية وتجريبية لاستخدام سخان الماء بالطاقة الشمسية في تدفئة الحيز

رسالة

مقدمة الى قسم هندسة تقنيات ميكانيك القوى

كجزء من متطلبات نيل درجة الماجستير في تقنيات الحراريات

في هندسة تقنيات ميكانيك القوى

تقدم بها

محمـــد جاســـم عبـــيد

اشراف

الدكتور ظافر مانع الشمخي   الدكتور اسعد عواد السهلاني

كانون الثاني 2020